NAVAL POSTGRADUATE SCHOOL
Monterey, California

19980121 115

THESIS

SYSTEM IDENTIFICATION
OF AN
ULTRA-QUIET VIBRATION ISOLATION PLATFORM

by

George D. Beavers

June, 1997

Thesis Advisor: Brij Agrawal
Second Reader: Gangbing Song

Approved for public release; distribution is unlimited.

DTIC QUALITY INSPECTED 3

REPORT DOCUMENTATION PAGE			Form Approved OMB No. 0704-0188

Public reporting burden for this collection of information is estimated to average 1 hour per response, including the time for reviewing instruction, searching existing data sources, gathering and maintaining the data needed, and completing and reviewing the collection of information. Send comments regarding this burden estimate or any other aspect of this collection of information, including suggestions for reducing this burden, to Washington headquarters Services, Directorate for Information Operations and Reports, 1215 Jefferson Davis Highway, Suite 1204, Arlington, VA 22202-4302, and to the Office of Management and Budget, Paperwork Reduction Project (0704-0188) Washington DC 20503.

1. AGENCY USE ONLY *(Leave blank)*	2. REPORT DATE June 1997	3. REPORT TYPE AND DATES COVERED Master's Thesis

4. TITLE AND SUBTITLE SYSTEM IDENTIFICATION OF AN ULTRA-QUIET VIBRATION ISOLATION PLATFORM	5. FUNDING NUMBERS
6. AUTHOR(S) Beavers, George D.	

7. PERFORMING ORGANIZATION NAME(S) AND ADDRESS(ES) Naval Postgraduate School Monterey, CA 93943-5000	8. PERFORMING ORGANIZATION REPORT NUMBER

9. SPONSORING / MONITORING AGENCY NAME(S) AND ADDRESS(ES)	10. SPONSORING / MONITORING AGENCY REPORT NUMBER

11. SUPPLEMENTARY NOTES

The views expressed in this thesis are those of the author and do not reflect the official policy or position of the Department of Defense or the U.S. Government.

12a. DISTRIBUTION / AVAILABILITY STATEMENT Approved for public release; distribution unlimited.	12b. DISTRIBUTION CODE

This thesis details the system identification and initial system validation of the an Ultra-Quiet Vibration Isolation Platform (UQP). With the move toward lighter and more flexible spacecraft, the effects of vibration are of immense concern. As natural or passive damping becomes less effective in controlling undesired vibrations, active vibration control becomes essential. The UQP uses a special configuration of the six degree of freedom Stewart Platform with piezoceramic strut actuators and geophone sensors. This combination gives an extremely sensitive and responsive six degree-of-freedom active vibration control system. Each actuator was designed to be controlled independently without coupling with other actuators. In order to develop control laws, the plant must be identified in terms of system zeros and poles and the uncoupled design validated. Dynamic modeling using parametric estimation methods can accurately describe a complex system. Using parameter estimation methods, models of the actuator system dynamics were obtained. A simple lead-lag controller was applied to individual actuators then all six actuators acting simultaneously to verify system coupling. Significant interaction between base adjoining actuators was discovered.

14. SUBJECT TERMS	15. NUMBER OF PAGES 172
	16. PRICE CODE

17. SECURITY CLASSIFICATION OF REPORT Unclassified	18. SECURITY CLASSIFICATION OF THIS PAGE Unclassified	19. SECURITY CLASSIFI- CATION OF ABSTRACT Unclassified	20. LIMITATION OF ABSTRACT UL

NSN 7540-01-280-5500

Standard Form 298 (Rev. 2-89)
Prescribed by ANSI Std. 239-18

SYSTEM IDENTIFICATION
OF AN
ULTRA-QUIET VIBRATION ISOLATION PLATFORM

George D. Beavers
Lieutenant Commander, United States Navy
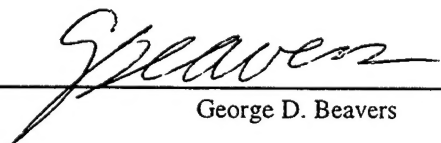B.S., Boston University, 1987

Submitted in partial fulfillment of the
requirements for the degree of
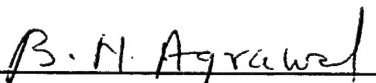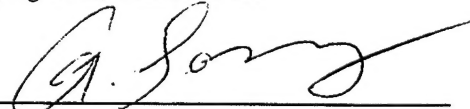
MASTER OF SCIENCE IN ASTRONAUTICAL ENGINEERING
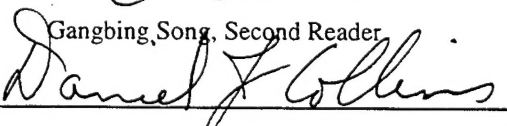
from the

NAVAL POSTGRADUATE SCHOOL
June 1997

Author: _____
George D. Beavers

Approved by: _____
Brij Agrawal, Thesis Advisor

_____
Gangbing Song, Second Reader

_____
Daniel Collins, Chairman
Department of Aeronautical and Astronautical
Engineering

ABSTRACT

This thesis details the system identification and initial system validation of the an Ultra-Quiet Vibration Isolation Platform (UQP). With the move toward lighter and more flexible spacecraft, the effects of vibration are of immense concern. As natural or passive damping becomes less effective in controlling undesired vibrations, active vibration control becomes essential. The UQP uses a special configuration of the six degree of freedom Stewart Platform with piezoceramic strut actuators and geophone sensors. This combination gives an extremely sensitive and responsive six degree-of-freedom active vibration control system. Each actuator was designed to be controlled independently without coupling with other actuators. In order to develop control laws, the plant must be identified in terms of system zeros and poles and the uncoupled design validated. Dynamic modeling using parametric estimation methods can accurately describe a complex system. Using parameter estimation methods, models of the actuator system dynamics were obtained. A simple lead-lag controller was applied to individual actuators then all six actuators acting simultaneously to verify system coupling. Significant interaction between base adjoining actuators was discovered.

v

TABLE OF CONTENTS

ACKNOWLEDGEMENTS

There are many people who have provided invaluable assistance in the writing of this thesis. Dr. Eric Anderson of CSA Engineering who installed and shared his time and knowledge of the platform. Many thanks to Dr. Gangbing Song who re-directed my research at a critical time and provided a tremendous amount of assistance in both the experimental and writing stages of this thesis. Dr. Brij Agrawal whose knowledge, advice, and encouragement both as an instructor and thesis advisor well served the author throughout this entire process.

Most importantly, my family. To my parents, for their prayers and support. To Christopher and Sarah, their unconditional and unwavering love, patience and understanding kept me strong through the tough times. A special thanks to my wife, Denise. Her support and countless sacrifices over the past ten years made this all possible. The author is forever in her debt.

I. INTRODUCTION

A. PURPOSE FOR RESEARCH

With increased use of lightweight materials, spacecraft will become more flexible and susceptible to excitation from sources of vibration. With loss of stiffness and rigidity, passive damping alone may be insufficient to attenuate disturbances to an acceptable level. Active Vibration Control (AVC) is rapdily emerging as a method of eliminating or reducing unwanted vibration. The purpose of this thesis is to provide a detailed description and system identification of the Ultra Quiet Vibration Isolation Platform (UQP). It will be the basis for future research in the area of AVC. The UQP is an excellent sytem for AVC and can be applied to a broad range of disturbances. A disadvantage of the UQP is the complexity of the plant dynamics and kinematics. Accordingly the complexity of the control system design is increased. This thesis will charaterize the plant for future control design on the UQP.

B. SCOPE

The "plant" is the UQP which consists of six piezoceramic control actuators. This thesis will use parameter estimation methods to create a dynamic model of the UQP control actuators with the ultimate goal of extracting actuator zeros, poles and transfer functions. These actuators are designed to operate independently. Theoretically, each actuator can be controlled without coupling or interaction with the other actuators. This assumption is of extreme importance as it critically impacts upon the performance of the system and control system design. This assumption will be checked for validity by applying a lead-lag feedback compensator to an actuator and then to all six actuators simultaneously.

1

II.   EXPERIMENTAL SETUP

A.   BACKGROUND

In many spaceborne applications the dynamics and control of vibrations must be addressed as a multiple degree-of-freedom (DOF) problem. Translations and rotations about all three axis must be considered. The Stewart Platform is the ideal mechanism for multiple DOF vibration control applications.

1.   The Stewart Platform

The original motivation put forth by Stewart [Ref. 1] was to design a mechanism capable of simulating flight conditions to train pilots. In order to be realistic it had to be capable of translating and rotating in three directions just as a real aircraft. The original configuration consisted of a triangular plate and a rigid parallel base connected by six legs in a "linear coordinate" leg system. At each triangle vertex two legs were attached in a three DOF joint mechanism. These legs, with hydraulic actuators, were mounted to two DOF joints at the base. The advantages of choosing this configuration were inherent rigidity and absence of bending moments. Additionally with this configuration the only forces present were in the plane of the leg. A similiar six leg arrangement had also been used by a machine designed to study tire to ground forces [Ref 2].   In this system computer controlled jacks were used as actuators.   A cubic arrangement was devised such that the relationship of one actuator to any other is the same (see Figure 2.1). This arrangement showed inherent stability and the capability for accepting large moments.
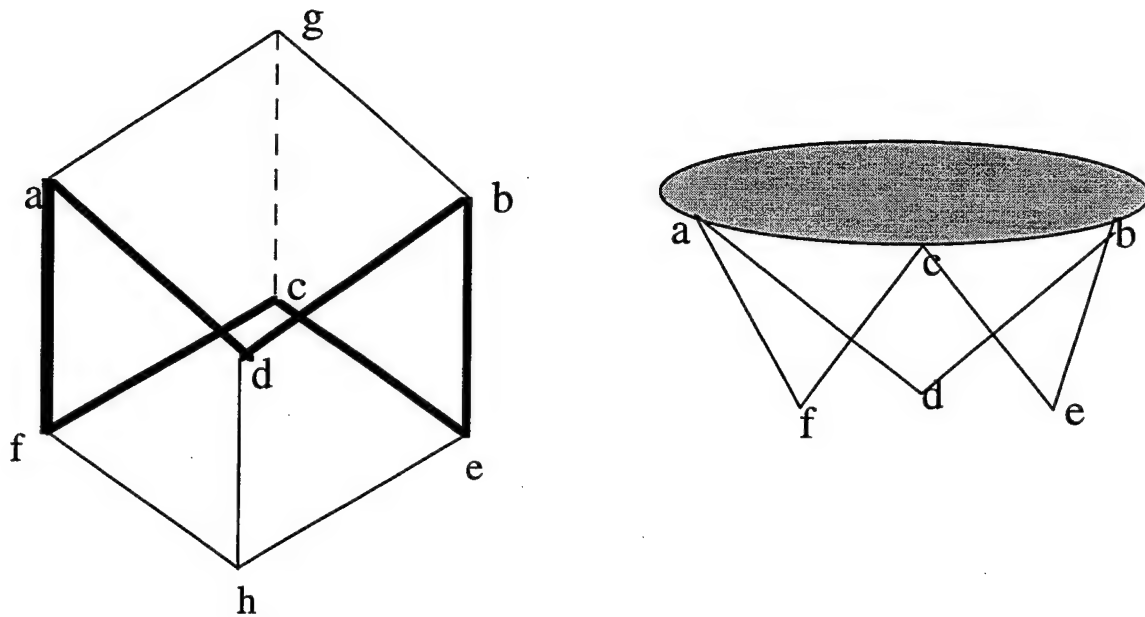
3

Figure 2.1

Cubic Arrangement

Stewart Platform mechanisms have been the subject of studies as multiple DOF parallel systems [Ref. 3 and Ref. 4:p 46]. The Stewart Platform configuration has shown wide applicability from motion simulators to robotics and now Active Vibration Control. The UQP employs the cubic configuration of the Stewart Platform which has an extremely important property with respect to AVC. With the exception of inertial loads and gravity forces, all other forces are carried axially. The significance is that if axial forces due to vibration can be eliminated the vibration is eliminated [Ref. 4:p. 46].

B.   HARDWARE CONFIGURATION

The experimental hardware is divided into two sections: the UQP and the Power, Control and Analysis Hardware.

1. Ultra-Quiet Vibration Isolation Platform (UQP)

The UQP is an adaptation of the Stewart Platform for AVC designed and built by CSA Engineering INC. It consists of a circular plate attached to a rigid base by six variable length actuators (see Figure 2.2).
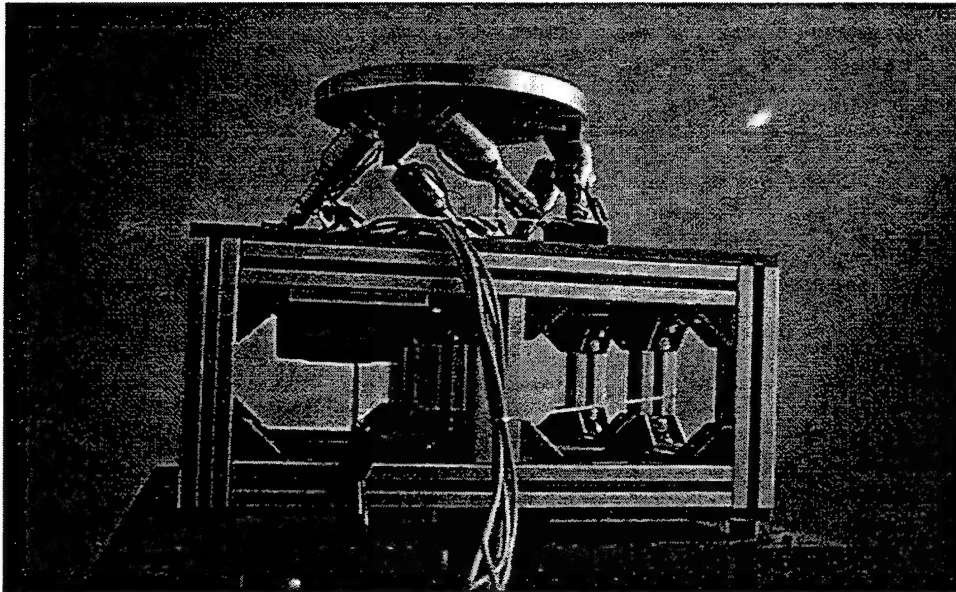

Figure 2.2

Ultra-Quiet Vibration Isolation Platform

The base consists of an aluminum plate supported by aluminum stringers and longerons. The base is used to simulate a rigid spacecraft. Mounted inside one of the "spacecraft" bays is an AURA Bass Shaker which is used as a known disturbance source. The entire aparatus is bolted to a 3800lb NEWPORT optical table.

a) Control Actuator Struts

The UQP uses six mutually orthoganol struts to provide control over six degrees of freedom. Each strut consists of a piezoceramic actuator and a geophone sensor. The use of piezoceramics for shape and vibration control is becoming

increasingly widespread. For interested readers, further information on piezoceramics and their applications in vibration control can be found in Reference 8. By taking advantage of the cubic configuration, all six struts can be considered linear motion actuators [Ref 1]. Stewart Platform based AVC mechanisms using the same cubic configuration with Terfanol-D actuators [Ref. 4] and voice coil actuators [Ref. 5] have also been developed. These platforms displayed significant reduction of vibration over passive means alone. Figure 2.3 is a basic diagram of each actuator. The actuator stroke is approximately 50 microns. In the passive (open loop) mode it provides moderate damping to low frequency vibrations. In the active (closed loop) mode it provides damping to higher frequency vibrations. Passive damping is provided by a flexure with damping material. An extremly sensitive geophone measures velocity. This velocity is the error signal fed into the control law.
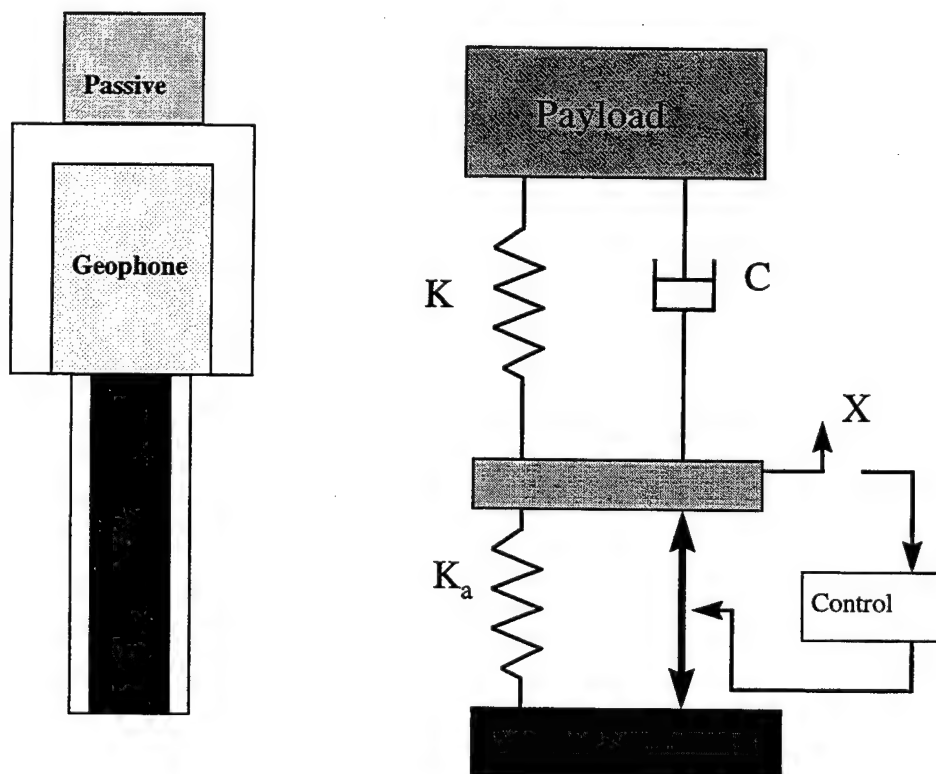

Figure 2.3
Actuator

6

In general applications, geophones consist of wire coils supported by soft springs under the influence of a magnetic field. Vibrations cause movement of the magnet relative to the stationary coil inducing a voltage proportional to velocity [Ref. 6:p 449]. The stiffness K refers to the stiffness of the passive stage. The stiffness K_a corresponds to the piezoceramic stack actuator (PZT).

b)   Disturbance Shaker

To create a disturbance source against which the performance of the UQP and applied control can be measured, a known disturbance source was mounted to the base. A sinusoidal waveform from a signal generator is amplified and input to a AURA Bass Shaker (see Figure 2.4). This simulates a cyclic disturbance. It has a resonant frequency at 42 Hz which is used as the disturbance frequency in initial experiments.
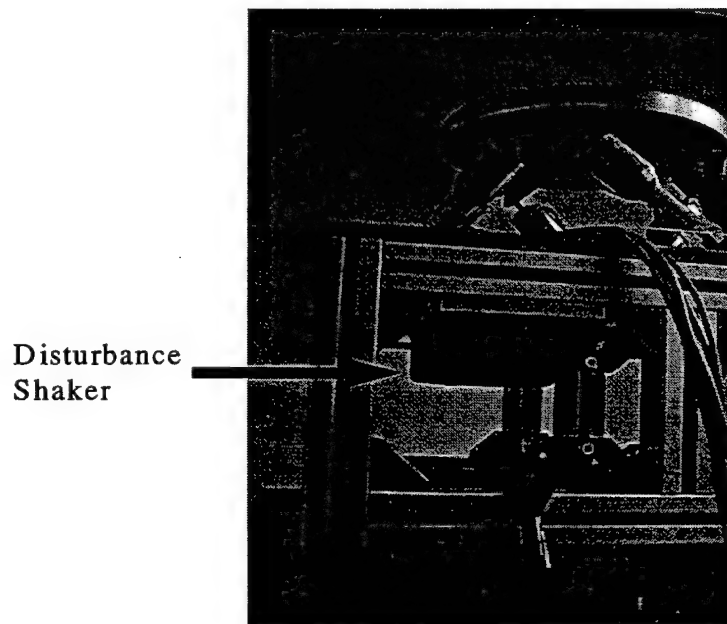
Disturbance
Shaker

Figure 2.4
Disturbance Shaker

2. Power, Control and Analysis

To operate the UQP and extract meaningful experimental data requires several important components (see Figures 2.5 & 2.6).

Control Input-Sensor Output

Sensor Output- Channel of Interest

PWR Supply

AVCS

HP 35665A
ch1 ch2

Disturbance Shaker

KEPCO Operational
Amp. & Pwr. Supply

HP 33120A Function/
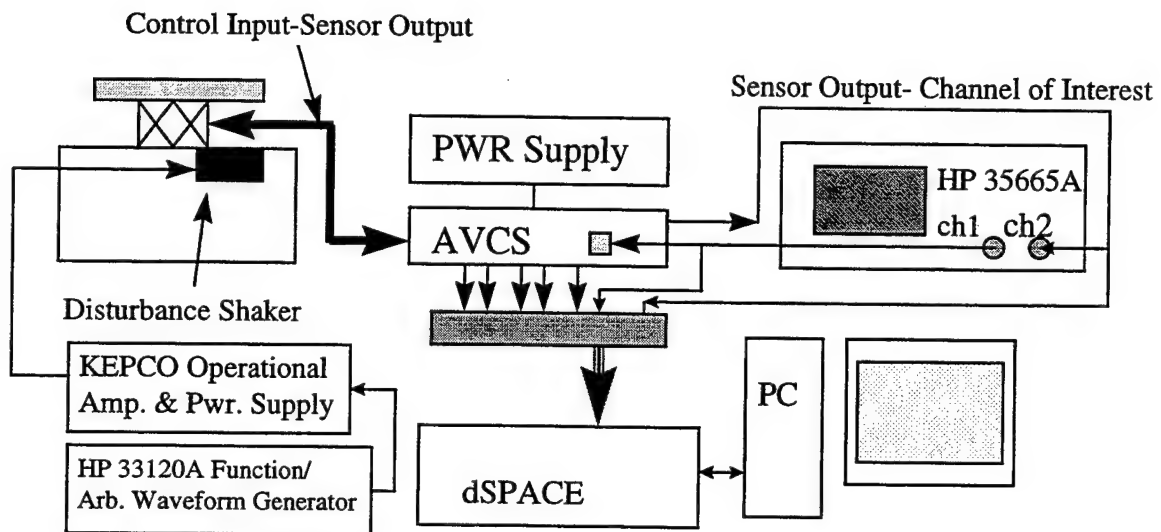Arb. Waveform Generator

dSPACE

PC

Figure 2.5.
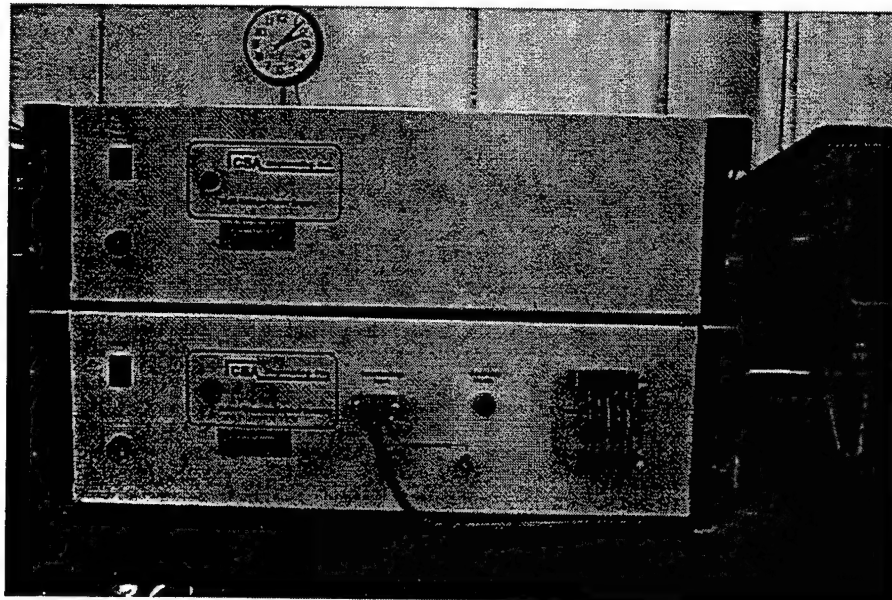Power, Control and Analysis Hardware Configuration

Figure 2.6
High Voltage Power Supply (HVPS)(top) and Active Vibration Control System (AVCS)

The current configuration requires a MATLAB capable PC with an RS232 I/O port. The control design is done in MATLAB. Once the design is completed, the MATLAB code is translated into C code. The C code is converted to machine language and down loaded via the I/O port to the CSA Active Vibration Control System (AVCS) (see Figure 2.6). It provides the interface for control implementation and geophone sensor output. Its main component is a digital signal processor (DSP). Once the machine code has been loaded the AVCS applies the control to the actuators. It receives the feedback signal from the geophones, processes and feeds it into the control algorithm. The output is sent to a HP 35665A Dynamic Signal Analyzer for analysis. The CSA High Voltage Power Supply (Figure 2.6) supports the power equirements of the piezoceramic actuators and is not required for use in the open loop mode.

III.   SYSTEM IDENTIFICATION

In order to design an effective compensator or controller for a dynamic system the plant must be well known or characterized.   By the use of system identification techniques a plant model can be obtained. The use of a model is extremely beneficial in cases when the dynamics of a plant are not well known or complex. Although articles have been written investigating the dynamic and kinematic complexities of Stewart type platforms [Ref. 3.], active vibration control using Stewart Platform based mechanisms is a relatively new field.   Experimental dynamic modeling can be used to bypass the need for a complete theoretic dynamic analysis of the UQP. The goal of identifying the UQP plant was to obtain an accurate plant transfer function which can assist control design. Of particular interest were system modes or resonances and interaction or couplings among actuators. An initial key assumption on the actuators is that they each act independently (uncoupled) and can be controlled as such. Validation of this assumption is one of the goals of identification of each plant.

A.   DYNAMIC MODELING

There are two categories of system identification used in dynamic modeling: Non-parametric and Parametric.   Non-parametric methods are used to estimate transient response, spectra and frequency functions in order to gain basic knowledge of the system. Parametric methods are used to obtain the mathematical parameters or elements used by well know system modeling algorithms.   These models are broken down into two subcatagories. "Tailor Made" models are built based on physical principles (i.e. the parameters have some type of physical interpretation). "Ready Made" or "Black Box" models are general in nature and use parameters that have no direct physical interpretation.   They are used to characterize the relationship of output to input of a system.   By treating the UQP as a "Black Box" and analyzing the input-output relationship it is possible to obtain an accurate model of the system by using a Ready Made model. [Ref. 10]

1. Background

The concept behind the use of transfer functions is to describe the relationship between the input and output of a system and can be expressed in terms of either continuous or discrete time. The use of discrete time representations are preferable when the data is sampled in nature.

$$u(t) \longrightarrow \boxed{\begin{array}{c}\text{Transfer} \\ \text{Function}\end{array}} \longrightarrow y(t)$$
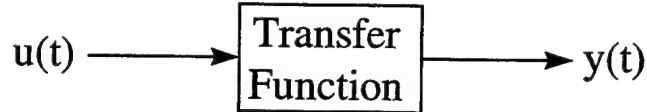
Figure 3.1
Input-Output Relationship

One of the most important tools used to gain an understanding of the behavior of a system is by looking at its impulse response. For a linear system (plant) the impulse response is the output when the applied input is an impulse at t=0.

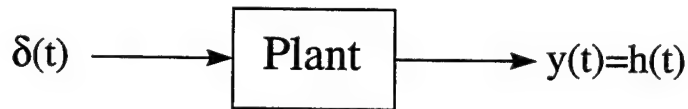$$\delta(t) \longrightarrow \boxed{\text{Plant}} \longrightarrow y(t)=h(t)$$

Figure 3.2
Impulse Response Relationship

If the impulse response h(t) of a system is known, the output to a given input can readily be determined by convolution of the input with the impulse response:
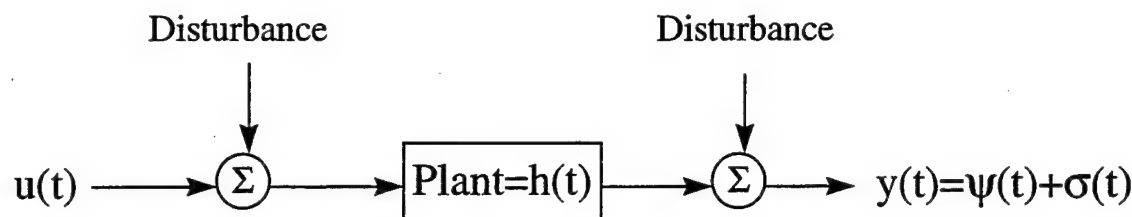
$$y(t) = u(t)*h(t) \tag{3.1}$$

or:

$$y(t) = \sum_{m=-\infty}^{+\infty} h(t) \bullet u(t-m) \tag{3.2}$$

The impulse response is a key element of non-parametric system identification.

An essential element of system identification is characterizing the output. In an ideal system the output would simply be the input modified by the system transfer function. In physical systems however, the output also contains elements resulting from internal and external disturbances (see Figure 3.3).

12

Disturbance   Disturbance

$$u(t) \longrightarrow \Sigma \longrightarrow \boxed{\text{Plant=h(t)}} \longrightarrow \Sigma \longrightarrow y(t)=\psi(t)+\sigma(t)$$

Where:

y(t)=Total Output
ψ(t)=*Undisturbed* Output
σ(t)=*Disturbance* term

Figure 3.3

In order to develop a model of the input output relationship, define:

$$y(t) = \psi(t) + \sigma(t)$$

$$\psi(t) = G(q,\rho)u(t)$$ (3.3 a,b,c)

$$\sigma(t) = H(q,\rho)\varepsilon(t)$$

where $\varepsilon(t)$ is white noise, ρ is the parameter vector:

$$\rho = \begin{pmatrix} \rho_1 \\ \vdots \\ \rho_n \end{pmatrix}$$ (3.4)

and q_T is the shift operator based on sampling interval T:

$$q_T y(t) = y(t+T)$$
$$q_T^{-1} y(t) = y(t-T)$$ (3.5 a,b)

Introduce the general difference equation:

$$y(t) + a_1 y(t-1T) + a_2 y(t-2T) + \ldots + a_N y(t-NT) = b_0 u(t) + b_1 u(t-1T) + \ldots + b_L u(t-LT)$$

(3.6)

where T is the sampling interval of the discrete time representation. This standard expression is a specialized geometric series that relates input and output of a system using past values of input, output and a set of parameters a_i and b_i. By applying the shift operator q_T equation (3.6) becomes:

13

$$y(t)\left[1+a_1q_T^{-1}+a_2q_T^{-2}+\cdots+a_nq_T^{-n}\right]=u(t)\left[b_0+b_1q_T^{-1}+b_2q_T^{-2}+\cdots+b_nq_T^{-n}\right]$$

$$\frac{y(t)}{u(t)}=\frac{\left[b_0+b_1q_T^{-1}+b_2q_T^{-2}+\cdots+b_nq_T^{-n}\right]}{\left[1+a_1q_T^{-1}+a_2q_T^{-2}+\cdots+a_nq_T^{-n}\right]} \qquad (3.7)$$

Define:

$$G(q,\rho)=\frac{y(t)}{u(t)} \qquad (3.8)$$

and introduce a time delay of nk samples on the input:

$$G(q,\rho)=\frac{B(q)}{A(q)}=\frac{\left[b_0q_T^{-nk}+b_1q_T^{(-nk-1)}+b_2q_T^{(-nk-2)}+\cdots+b_nq_T^{(-nk-nb)}\right]}{\left[1+a_1q_T^{-1}+a_2q_T^{-2}+\cdots+a_{na}q_T^{-na}\right]} \qquad (3.9)$$

Changing variables to be consistent with the notation used by Ljung and Glad [ref. 11] and the MATLAB System Identification Toolbox (SITB) [Ref. 12]:

$$G(q,\rho)=\frac{B(q)}{F(q)}=\frac{\left[b_0q_T^{-nk}+b_1q_T^{(-nk-1)}+b_2q_T^{(-nk-2)}+\cdots+b_nq_T^{(-nk-nb)}\right]}{\left[1+f_1q_T^{-1}+f_2q_T^{-2}+\cdots+f_{nf}q_T^{-nf}\right]} \qquad (3.10)$$

Applying to equation (3.3b) and equation (3.6):

$$\psi(t)+f_1\psi(t-T)+\cdots+f_{nf}\psi(t-nfT)=b_0u(t-nkT)+\cdots+b_{nb}u(t-(nb+nk)T) \quad (3.11)$$

Similarly the disturbance term becomes:

$$H(q,\rho)=\frac{C(q)}{D(q)}=\frac{\left[1+c_1q_T^{-1}+c_2q_T^{-2}+\cdots+c_{nc}q_T^{-nc}\right]}{\left[1+d_1q_T^{-1}+d_2q_T^{-2}+\cdots+d_{nd}q_T^{-nd}\right]} \qquad (3.12)$$

The coefficients b_i, c_i, d_i and f_i comprise the parameter vector ρ. These coefficients represent the unknown system parameters. Essentially they approximate a complex system's physical parameters but have no direct correlation to any specific physical quantity. The parameters nb, nc, nd and nf characterize the order and type of ready made model. The model constructed by equations (3.3) through (3.12) is shown in equation (3.13). It represents the Box-Jenkins model[1] [Ref. 10].

$$y(t)=G(q,\rho)u(t)+H(q,\rho)\varepsilon(t) \qquad (3.13)$$

---

[1] Named after the statisticians G.E.P. Box and G. M. Jenkins

The following models are variations of the Box-Jenkins model. The most simple one is the case where the disturbance is not modeled.

$$y(t) = G(q, \rho)u(t) + \varepsilon(t) \qquad (3.14)$$

Equation (3.14) is known as the *Output Error* method. The difference between the actual output and undisturbed output is manifested in the white noise term $\varepsilon(t)$. The next model utilizes the same poles for the input and disturbance (noise) models defined as:

$$F(q) = D(q) = A(q) = 1 + a_1 q_T^{-1} + \cdots a_{na} q_T^{-na} \qquad (3.15)$$

Applied to equations (3.10), (3.12) and (3.13) yields:

$$y(t) = \frac{B(q)}{A(q)} u(t) + \frac{C(q)}{A(q)} \varepsilon(t) \qquad (3.16)$$

or:

$$A(q)y(t) = B(q)u(t) + C(q)\varepsilon(t) \qquad (3.17)$$

This is known as the ARMAX (AutoRegression Moving Average eXtra input) model. The final model that will be described is the AutoRegression eXtra input(ARX) model (equation 3.18). [Ref. 10]

$$A(q)y(t) = B(q)u(t) + \varepsilon(t) \qquad (3.18)$$

The next step is to describe how these ready made techniques model a system based on past values of output and input. Essentially these algorithms attempt to predict the output based on a given set of input-output data. Introduce the concept of One-Step-Ahead prediction of output. From equations (3.6) and (3.14), we have:

$$y(t) = -a_1 y(t-1) - \ldots - a_{na} y(t-na) + b_1 u(t-nk) + \ldots + b_{nb} u(t-nk-nb+1) + \varepsilon(t) \quad (3.19)$$

Since $\varepsilon(t)$ is white noise and cannot be predicted, the prediction becomes:

$$\tilde{y}(t, \rho) = -a_1 y(t-1) - \ldots - a_{na} y(t-na) + b_1 u(t-nk) + \ldots + b_{nb} u(t-nk-nb+1) \qquad (3.20)$$

Expanding to the general case of equation (3.13) and dividing out the noise transfer function:

$$H^{-1}(q, \rho)y(t) = H^{-1}(q, \rho)G(q, \rho)u(t) + \varepsilon(t) \qquad (3.21)$$

$$y(t) - y(t) + H^{-1}(q, \rho)y(t) = H^{-1}(q, \rho)G(q, \rho)u(t) + \varepsilon(t) \qquad (3.22)$$

$$y(t) + [-1 + H^{-1}(q, \rho)]y(t) = H^{-1}(q, \rho)G(q, \rho)u(t) + \varepsilon(t) \qquad (3.23)$$

$$y(t) = [1 - H^{-1}(q, \rho)]y(t) + H^{-1}(q, \rho)G(q, \rho)u(t) + \varepsilon(t) \qquad (3.24)$$

15

the prediction becomes:

$$\tilde{y}(t,\rho) = [1 - H^{-1}(q,\rho)]y(t) + H^{-1}(q,\rho)G(q,\rho)u(t) \qquad (3.25)$$

Since equation (3.25) only contains past values of the output $y(t)$ and input $u(t)$ the difference between the prediction and the output (the prediction error) is:

$$E(t,\rho) = y(t) - \tilde{y}(t,\rho) = \varepsilon(t) \qquad (3.26)$$

where $\varepsilon(t)$ is white noise. [Ref. 9: p. 56 and Ref. 10: p.235]

B.   FREQUENCY RESPONSE OF ACTUATORS

The diagram in Figure 3.4 is a modification of the experimental set up in Figure 2.5 used to extract the input-output data.
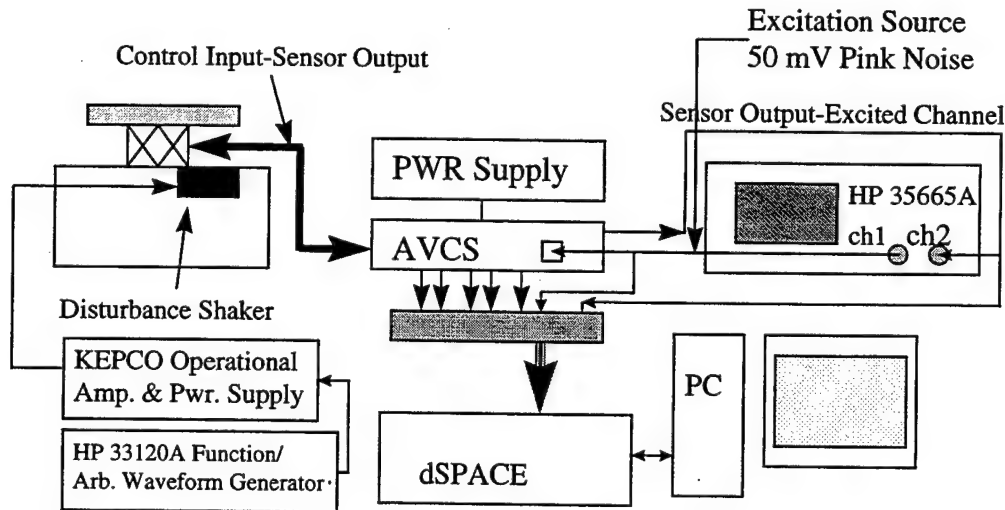

Figure 3.4
Experimental Setup

The purpose behind measuring the frequency response of each actuator is to obtain both basic insight into the plant and a model verification baseline. Each actuator was excited by a 50 mV "pink noise" source provided by the HP Dynamic Signal Analyzer (HPDSA). The "pink noise" is random noise which provides 3dB roll off per octave. The motivation to use pink noise is to place an equal amount of energy in each octave band. The response is sensed by the geophone of the excited channel (actuator) and fed into the

16

HPDSA. The HPDSA computes and plots the time averaged frequency response which are shown in Figures 3.5 through 3.10.
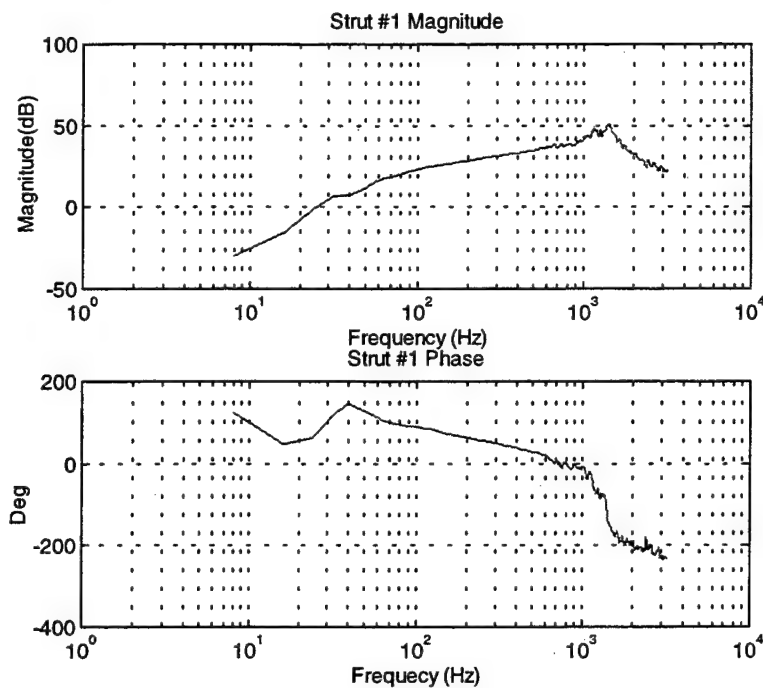

Figure 3.5
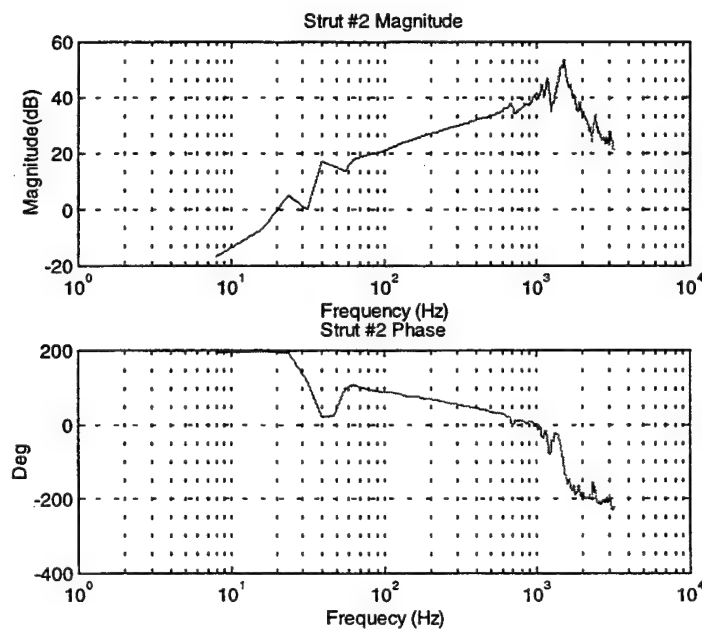Frequency Response of Actuator #1

Figure 3.6
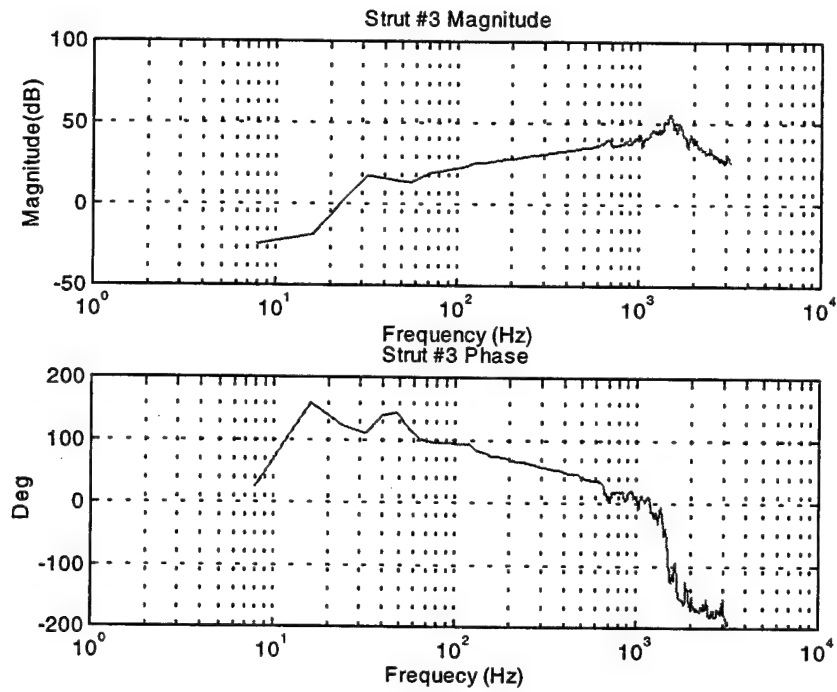Frequency Response of Actuator #2

Figure 3.7
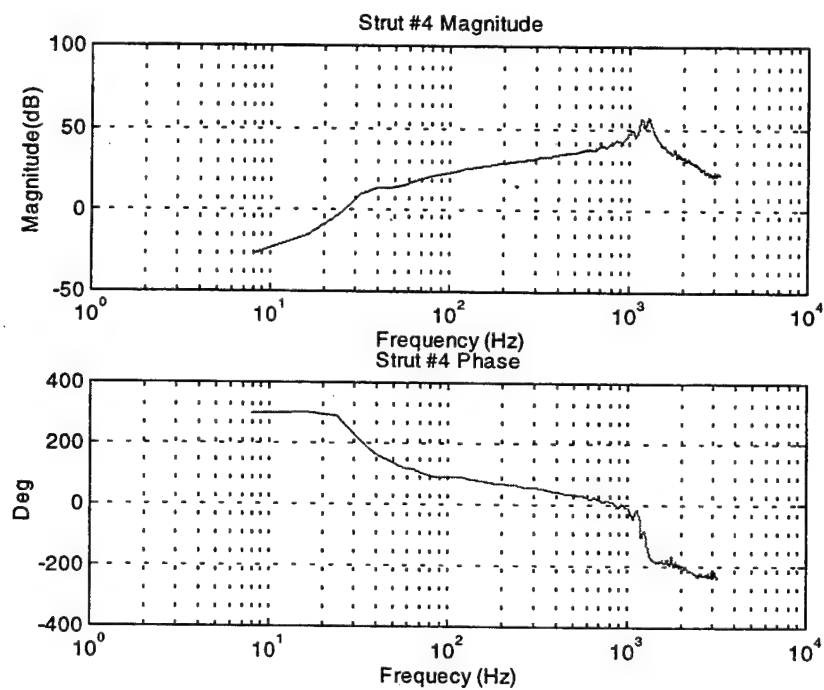Frequency Response of Actuator #3

Figure 3.8
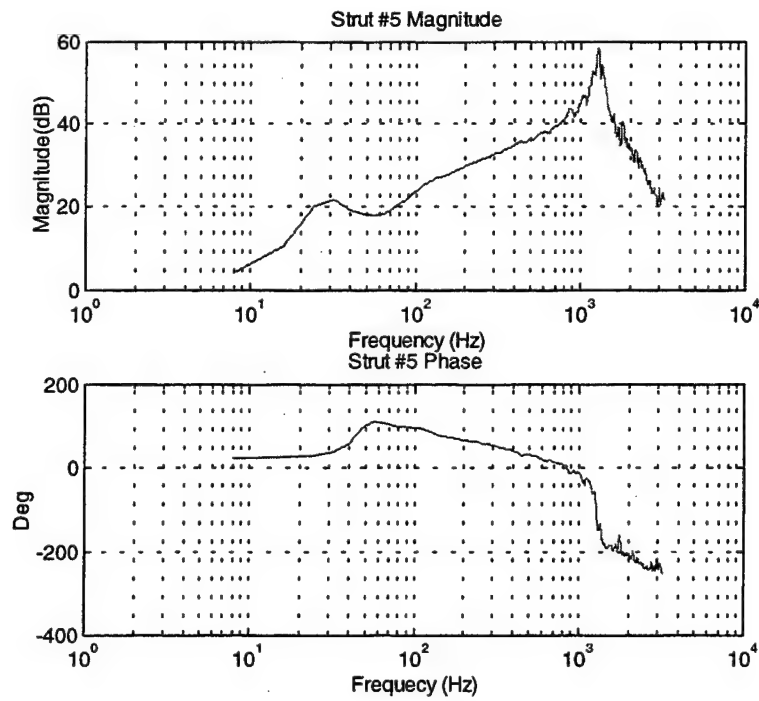Frequency Response of Actuator #4
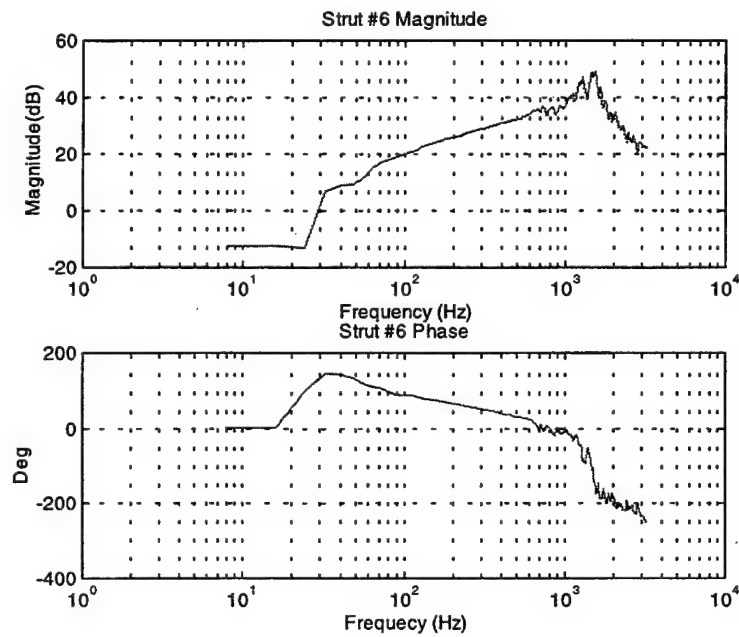
Figure 3.9
Frequency Response of Actuator #5

Figure 3.10
Frequency Response of Actuator #6

The plots show that the plant transfer functions for the actuators are basically the same. The resonant dynamics of the struts are readily discernible, specifically the actuator natural frequency at 1.4 kHz.

C.   MODEL STRUCTURE SELECTION

The type of system and method of data collection are major factors determining a suitable model type for a given application. For example, the Output Error, OE, would be best applied when the disturbances (which are not modeled) are small. The ARX is the most widely used because it is the simplest and serves as a good baseline to select a model. However, it uses the same poles to model noise as those used to model the system. This can create problems in system identification requiring the use of higher order models than would otherwise be necessary. The Box-Jenkins method models the system dynamics and disturbances separately with no common parameters. The ARMAX also models the disturbance but uses the same poles as the system dynamic model. It differs from the ARX by the addition of the C(q) polynomial. The Box-Jenkins and ARMAX both provide detailed system models and can be extremely accurate. The decision on which to use is based on the nature of the disturbance. If "noise" enters the process in the early stages or is carried through the plant (see Figure 3.3) the ARMAX is preferable over the Box-Jenkins model which is more adept to characterizing noises that enter later in the system. In the case of the UQP, the ARMAX would appear to be the preferred method if there is interaction between actuators because the resulting disturbances would enter into the process early on. Additionally the disturbance caused by another actuator should show similar dynamics as the plant under experimentation. The flow chart in Figure 3.11 represents the process used in building a model of each actuator. As Figure 3.11 shows, the process of system identification and modeling is a step-by-step iterative process. The basic idea was to develop and validate a basic ARX model structure (i.e. *na*, *nb* and *nk*) for all six actuators and then apply it to the more complex ARMAX and Box-Jenkins methods and determine the best model. The application of this process on actuator number one will be detailed in the following sections. [Ref. 10]
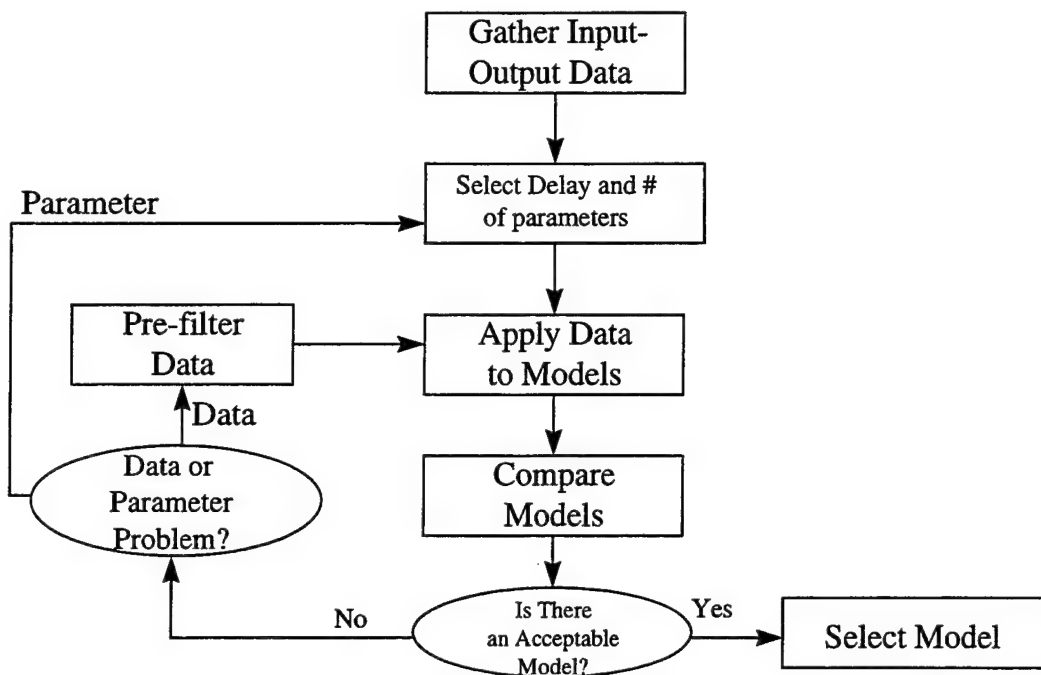
20

Figure 3.11
Model Selection Flow Chart

The computer program used to accomplish this can be found in appendix A.

1. Data Collection

The process of system identification and dynamic modeling relies on a set of plant input-output data. For the UQP each actuator was provided an excitation and the response of all six actuators (as measured by each respective geophone) recorded (see Figure 3.4). Using the HPDSA as the excitation source, 50mVRMS "Pink Noise" was applied to the actuator via the 25 pin connection on the front of the AVCS (see Figures 2.6 and 3.3). Under normal operation the ribbon cable on the front of the AVCS is connected to close the control loop. By disconnecting the cable, each actuator can be accessed individually. The geophone sensor output was connected via a BNC interface box to a dSPACE system. The dSPACE was used to gather, display and save all six channels of data simultaneously. For comparison purposes the active channel sensor output (actuator under excitation) and excitation source was also input to the HPDSA. For each actuator the output corresponding to the excitation source was measured at a

sampling frequency of 10 kHz for two seconds. This gave 20,000 input/output sample points. The choice of sampling frequency was based on the desire to obtain a sufficient number of sample points from which to construct and validate a model. The first 10,000 (input and output) sample points are used by the parameter estimation algorithms to build the model. The last 10,000 points (of input) are used in model validation. If the sample points used to build the model are also used in validation, the true accuracy and validity of the model will be corrupted.

a)   Data Preparation

Prior to using the data to build a model it is necessary to pre-treat the data. The most common factors adversely affecting collected data are:

1. Drift, offset, trends and low frequency and/or periodic disturbances.
2. Outliers or faulty data points.
3. High frequency disturbances.

Before treating for these possible problems the data is given a preliminary analysis to see if they do in fact exist or could be the possible source of erroneous results [Ref. 9:p 386].

External sources are the main cause of drifts, trends and low frequency disturbances that are either impossible or undesirable to model. This can be remedied by removing external disturbances, using the noise model to account for the disturbances and/or using an algorithm to de-trend the data. Due to the extreme sensitivity of the geophone sensors it is impossible to remove all the external disturbances. The latter two options were selected. It is assumed that the external disturbances received by the geophones are relatively small compared to those entering into the process early on and will be adequately addressed by the noise model. The offset problem is a result of the failure of input-output data to correspond in a consistent manner. This causes the model to waste parameters in attempt to adjust these levels. This is compensated by a MATLAB function included in the computer code (see appendix A.). [Ref. 12:p1-63]

In any data collection effort there are obviously erroneous values. However, removal of these "outliers" requires caution. Removal can either be manual (i.e. selecting bad values by hand) or by some type of automatic algorithm. The best way to determine if outliers are problematic is to check the model residuals for excessively large values that stand out. This method was chosen due to the vast amounts of sampled data used. [Ref. 12:p1-63]

The final source of data deficiency is the presence of high frequency disturbances outside the region of interest. In this case the primary concern is the performance of the actuators up to and including the resonance frequency. A 10th order Butterworth filter with a pass band below approximately 1.5kHz was used to eliminate disturbances outside the range of interest [Ref. 11: p 272].

2. Delay and Parameter Number/Structure Selection

Prior to applying one of the aforementioned parametric models to the gathered data, the input delay nk, and the structural elements na, nb, nc, nd and nf must be determined. This was done using the Model Structure Selection functions in the MATLAB SITB. The SITB has functions to calculate ARX-based and OE-based structures. Figure 3.12 represents a flow chart of the algorithm used to select the delay and structure. Since the assumption was that the ARMAX model would provide the best model for the UQP, an ARX-based structure selection algorithm was applied (see appendix A).
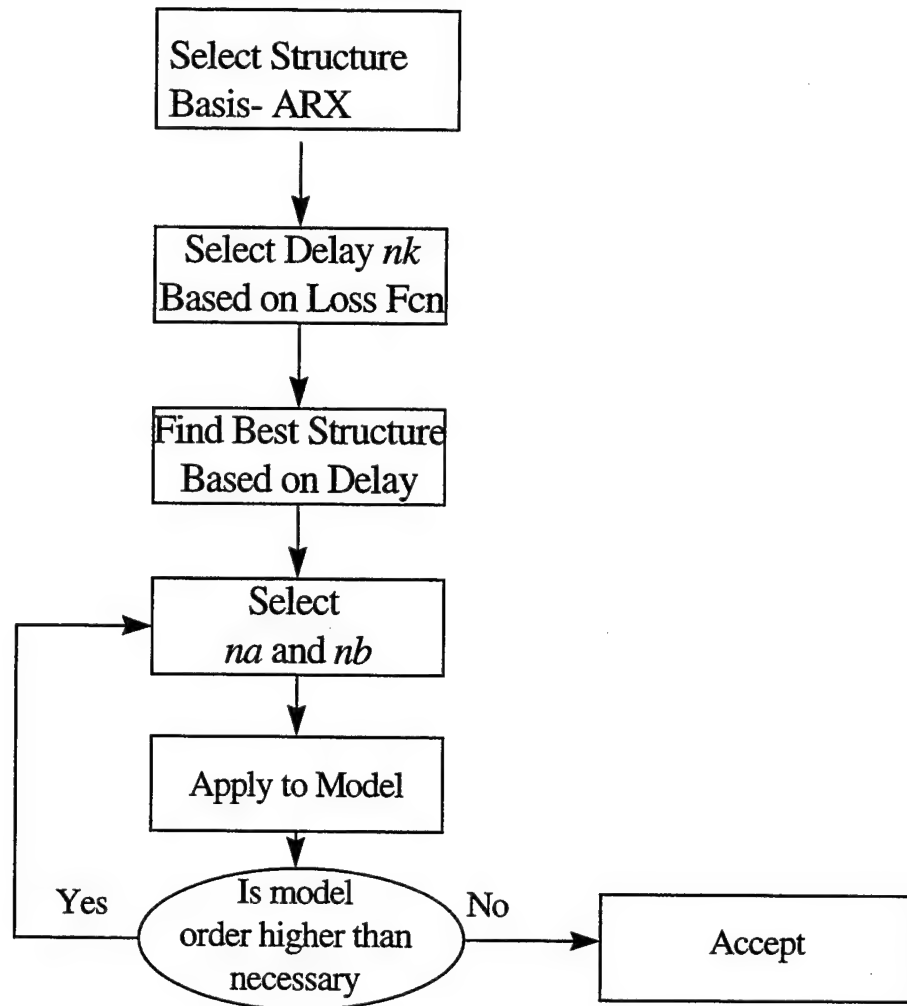
```
            ┌─────────────────┐
            │ Select Structure│
            │ Basis- ARX      │
            └────────┬────────┘
                     │
                     ▼
            ┌─────────────────┐
            │ Select Delay nk │
            │ Based on Loss Fcn│
            └────────┬────────┘
                     │
                     ▼
            ┌─────────────────┐
            │Find Best Structure│
            │ Based on Delay  │
            └────────┬────────┘
                     │
                     ▼
            ┌─────────────────┐
     ┌─────►│    Select       │
     │      │  na and nb      │
     │      └────────┬────────┘
     │               │
     │               ▼
     │      ┌─────────────────┐
     │      │  Apply to Model │
     │      └────────┬────────┘
     │               │
     │               ▼
     │         ╱───────────╲
 Yes │        │  Is model   │  No      ┌──────────────┐
     └────────┤ order higher ├────────►│    Accept    │
              │ than        │          └──────────────┘
               ╲ necessary ╱
                ╲─────────╱
```

Figure 3.12
Structure Selection Algorithm

The process of selecting *na* and *nb* as well as the number of total parameters from which they are derived is an iterative process. Since the input delay should be the same no matter what the order of the model is, a second order ARX model will serve as the foundation of this process. Table 3.1 shows the results of *nk* values ranging from 1 to 10 applied to a second order ARX model.

24

Act.	nk=1	nk=2	nk=3	nk=4	nk=5	nk=6	nk=7	nk=8	nk=9	nk=10
1	-5.5975	-5.6122	-5.4704	-5.4708	-5.4659	-5.4686	-5.4755	-5.5046	-5.5184	-5.5077
2	-5.3380	-5.3175	-5.2293	-5.2301	-5.2297	-5.2375	-5.2463	-5.2602	-5.2596	-5.2426
3	-4.6214	-4.4221	-4.4132	-4.4391	-4.4432	-4.4293	-4.4357	-4.4282	-4.4252	-4.4256
4	-5.5237	-5.5711	-5.3791	-5.3872	-5.3928	-5.3946	-5.4007	-5.4106	-5.4054	-5.3905
5	-5.0731	-5.1164	-5.0082	-5.0077	-5.0044	-5.0028	-5.0089	-5.0239	-5.0259	-5.0130
6	-5.8464	-5.8072	-5.7362	-5.7301	-5.7204	-5.7390	-5.7443	-5.7598	-5.7747	-5.7610

Table 3.1
Input Delays

The numbers represent the logarithms of a quadratic loss function based on the selected *nk* for *na=nb=*2 (second order model). Once an input delay has been selected a plot of the number of parameters used versus loss function is produced. Based on the results in Table 3.1, the best choice for an input delay for actuator number one appears to be *nk=*2. Figure 3.13. is the resulting plot.
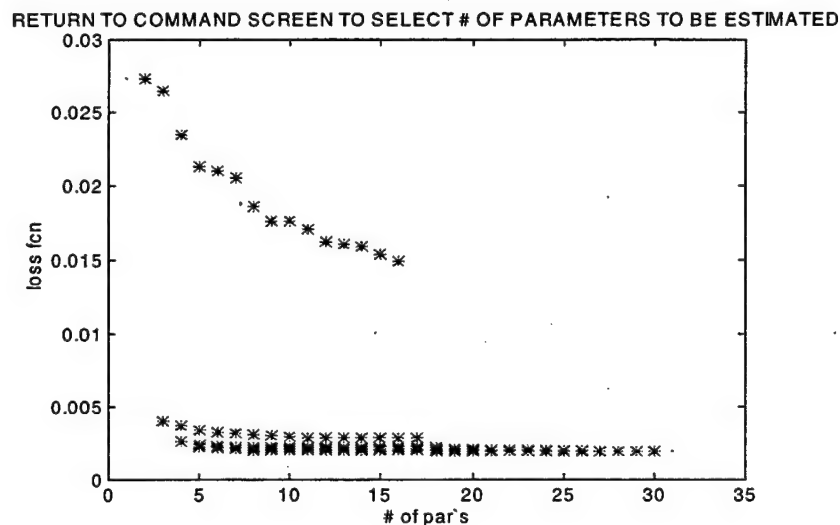
Figure 3.13
Parameters Vs. Loss Function for Actuator #1 *nk=*2

The multiple results for a given number of parameters is due to the fact that there can be several different structures (i.e. combinations of *na* and *nb*). The SITB has functions that

automatically compute the structures based on the minimization of Akaike's Information Theoretic Criterion (AIC) and Rissanen's Minimum Description Length (MDL)[Ref. 11]. After a structure has been selected it can be applied to a parametric estimation method to develop a model. Even with the availability of functions capable of selecting the optimum number of parameters based on minimization techniques, it can be seen in Figure 3.13 that there is a point of diminishing returns beyond which the addition of more parameters is of little benefit. Further, the addition of more parameters than necessary will actually cause a loss in model accuracy. Referring to Figure 3.13 the structures chosen are listed in table 3.2.

Number of Parameters	Structure [*na nb nk*]	Notes
30	15 15 2	AIC Based
22	14 8 2	MDL Based
18	14 4 2	Automatic

Table 3.2
Structures For Actuator #1 Input Delay *nk*=2

The notes column provides information on how the structure was obtained. AIC and MDL based structures were automatically generated along with the plot in Figure 3.13. The term "Automatic" means the number of parameters in the first column were manually extracted from the plot in Figure 3.13 and entered in to an SITB function that "Automatically" selects the structure. The term "Manual" refers to the complete structure being manually selected.

3. Model Structure Application and Evaluation

After determining the ARX model structure for actuator number one, a model was computed using the algorithm in appendix A. There are numerous methods for measuring the accuracy and validity of a model. The ones utilized to validate the actuator models are described as they were applied to the ARX model of actuator number one using the structure [na=15 nb=15 nk=2].

models are described as they were applied to the ARX model of actuator number one using the structure [na=15 nb=15 nk=2].

a) Frequency Response

One of the quickest ways to determine a model's validity is to compare the Bode plot of the system to that of the model.

Blue=Actuator#1 Red=ARX MODEL[15 15 2]

(a) Magnitude

Blue=Actuator#1, Red=ARX MODEL[15 15 2]
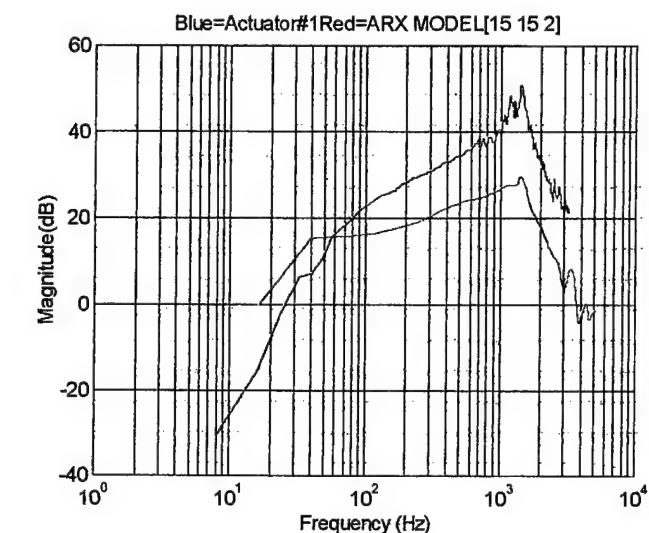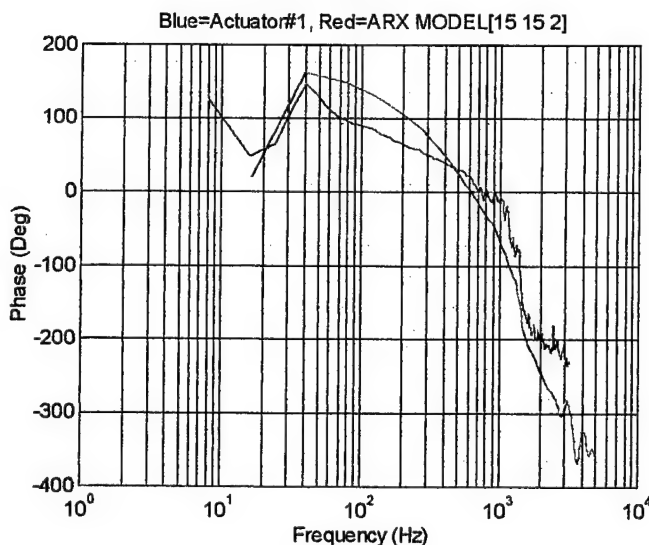
(b) Phase

Figure 3.14
Frequency Response of ARX[15 15 2] Model (Actuator #1)

27

The model's frequency response is similar to that of the actual system (see Figure 3.14). The areas of critical concern are the model behavior at resonance and zero dB crossing for magnitude and -180 degree crossing for phase. The phase is reasonably close however, the magnitude is significantly different. The general shape and resonance peak are in agreement but there is a distinct 10-20dB difference between the actuator and the model.

b)   Output Comparison

In evaluating a model, as stated earlier, it is important to use different input sample data to insure an accurate assessment of the model. In modeling the actuators a 10,000 sample model validation set was held aside for this puppies. Applying the validation input to both the model and the system and comparing the outputs, gives an accurate measure of the model's validity and how close it truly simulates the actual system. Figure 3.15 compares the model output to the actuator output in response to the same input.
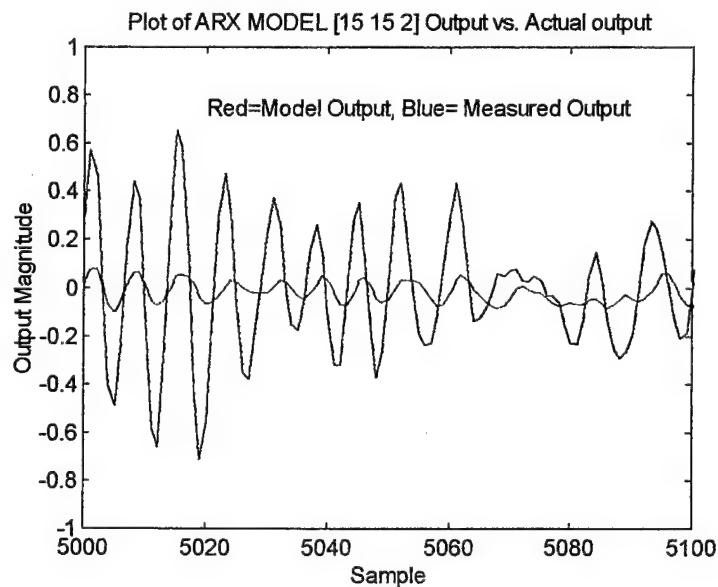
Figure 3.15.
Actual Vs. Model Output For ARX [15 15 2] (Actuator #1)

c) Auto and Cross Correlation Functions

Figure 3.16 provides plots of the auto correlation function of residuals and cross-correlation function between the input and residuals from the output. The difference between the model output and actual output is called the residual. Basically, it is what is left unaccounted for by the model. Recalling equation (3.26):

$$E(t,\rho) = y(t) - \tilde{y}(t,\rho) = \varepsilon(t)$$

where $\varepsilon(t)$ represents the residuals. If $\varepsilon(t)$ is purely "white noise" it is independent of the input. If there is correlation between $\varepsilon(t)$ and $u(t)$, there are elements in the output from the input that are not explained by the model.
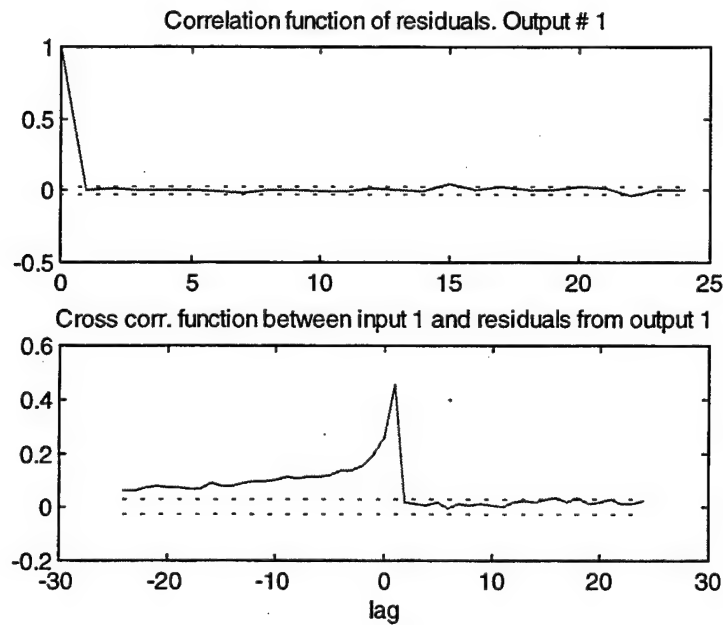
Figure 3.16

Auto and Cross-Correlation Functions for ARX [15 15 2] Model for Actuator #1

The horizontal lines in Figure 3.16 indicate a 99% confidence level. If the function crosses these lines, there is a correlation between $\varepsilon(t)$ and *u(t)* at that point. From Figure 3.16 there appears to be correlation between $\varepsilon(t)$ and *u(t-1)*. This indicates that the input delay might need to be modified to one. The auto-correlation function is acceptable. A plot of residuals versus sample number for 100 samples is given in Figure 3.17.
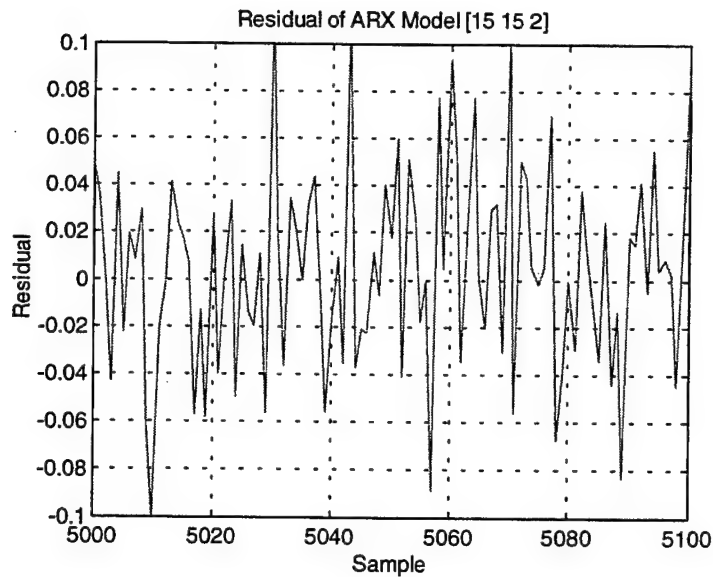
Figure 3.17
Residuals Vs. Sample ARX[15 15 2] For Actuator #1

Over this range of samples the residuals are relatively low. For an average output magnitude of approximately 0.18, the average residual magnitude is on the order of 0.03 or roughly 17% of the output magnitude. Although this percentage is a very rough way of comparison and cannot be considered by itself to determine model validity, it does give a basic idea of how much is left unexplained by the model. A much better method is to use the mean square fit. [Ref.10]

d)   Zero-Pole Plot

The final evaluation tool is the zero-pole plot (see Figure 3.18).
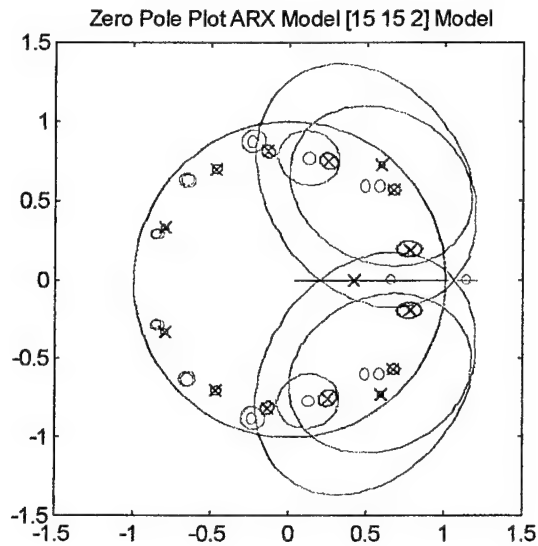
Figure 3.18

Zero-Pole Plot of ARX [15 15 2] For Actuator #1

The ellipses correspond to confidence limits to three standard deviations [Ref.12]. This plot shows that there are numerous possible zero-pole cancellations indicating that a model of lesser degree is desirable.

4.   Model Application and Evaluation (Data Prefiltered)

Based on analysis the ARX [15 15 2] is not a very good model. Following the flow chart the same analysis will be repeated on data pretreated with a 10th order Butterworth filter.

a)   Frequency Response

By prefiltering the data the correlation between the model frequency response and the actual output frequency response is improved. However, there is still an approximate 10 dB difference between the two responses.

31

Blue=Actuator#1, Red=ARX MODEL[15 15 2] *Data Prefiltered*

(a) Magnitude

Blue=Actuator#1, Red=ARX MODEL[15 15 2] *Data Prefiltered*
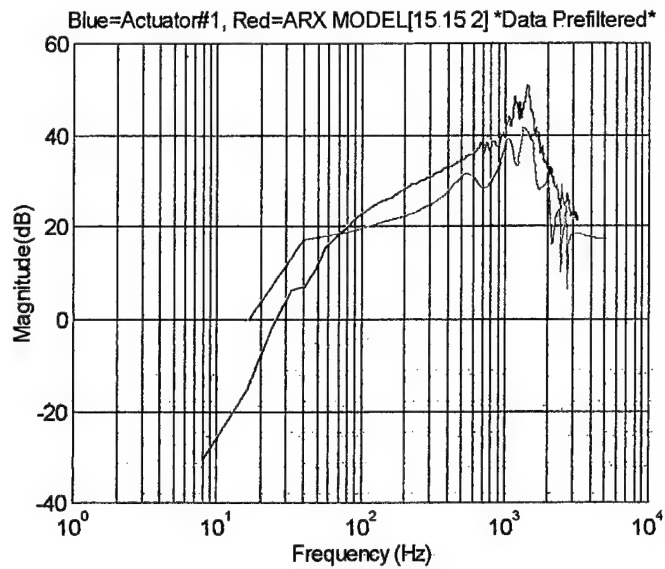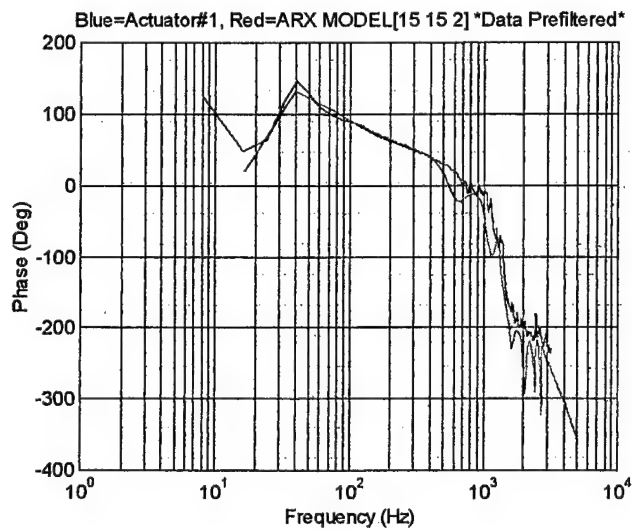
(b) Phase

Figure 3.19

Frequency Response of ARX[15 15 2] Using Prefiltered Data (Actuator#1)

b)   Output Comparison

Figure 3.20 shows an improvement in the correlation between the model and actual output.

Plot of ARX MODEL [15 15 2] Output vs. Actual output *Data Prefiltered*

Red=Model Output, Blue= Measured Output
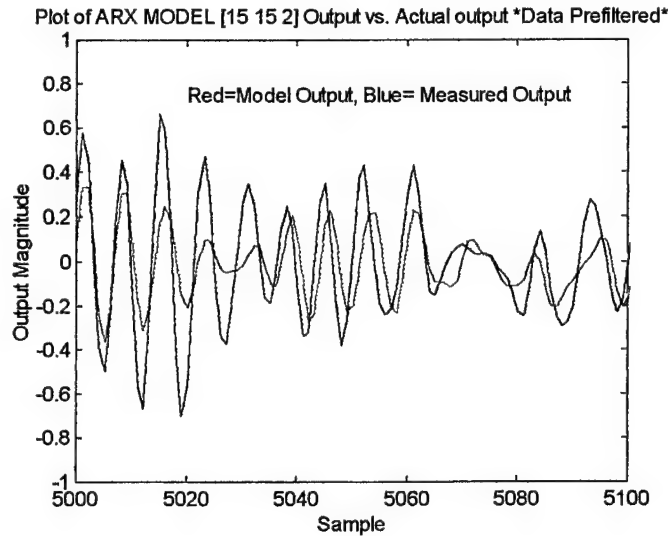
Figure 3.20
Prefiltered ARX[15 15 2] Model Output Vs. Actual Output

c) Auto Correlation and Cross Correlation Functions

As a result of prefiltering there is a degradation of the auto and cross correlation functions (see Figure 3.21). However, the auto-correlation of residuals is relatively small. For cross correlation functions where the crossing occurs in negative lag, this is an indication that the data was possibly collected during feed back vice a problem with the model [Ref. 10:p 284].

Correlation function of residuals. Output # 1

Cross corr. function between input 1 and residuals from output 1
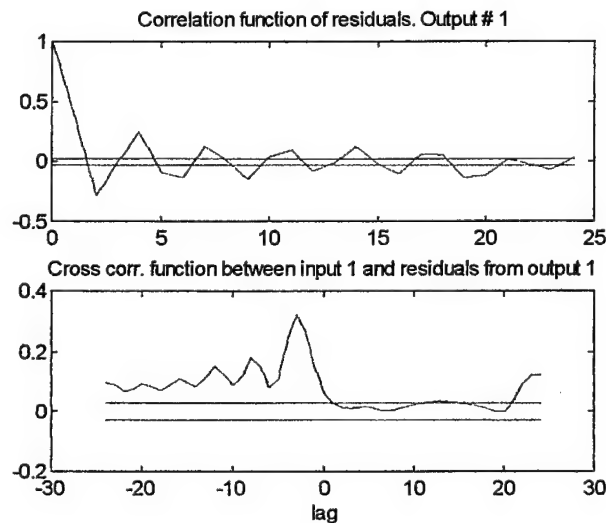
Figure 3.21
Auto and Cross Correlation Functions of Prefiltered ARX[15 15 2] (Actuator #1)

33

d) Residuals

Comparing Figure 3.22 with Figure 3.20, the former residual plot is misleading. This anomaly occurs when large order models (large number of parameters) using prefiltered data are applied to the SITB function. This function uses statistical means to calculate the prediction error and the residuals. A simple plot of the actual output minus the model output is shown in Figure 3.23.
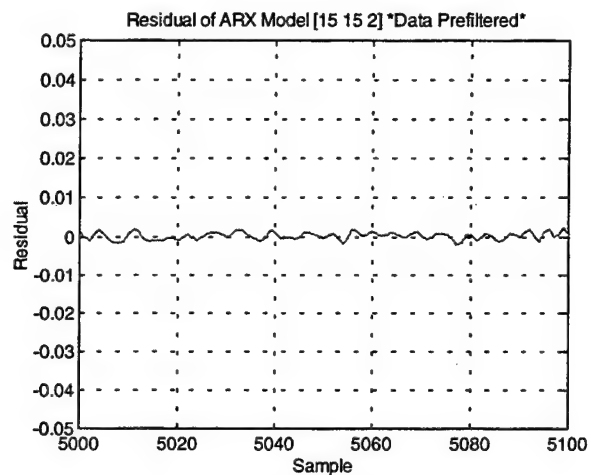
Figure 3.22
Residuals of Prefiltered ARX[15 15 2] (Actuator #1)
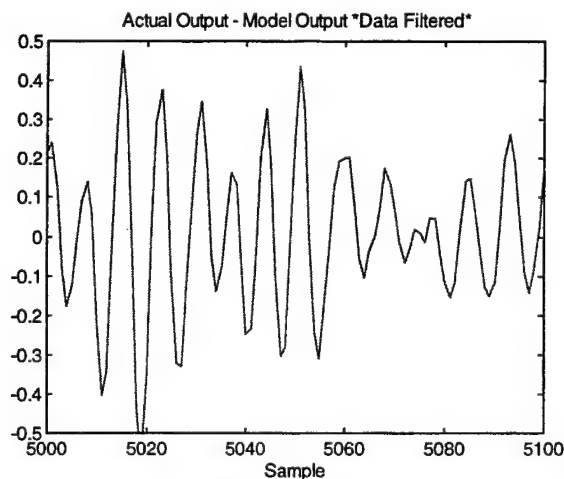
Figure 3.23
Actual Output Minus ARX[15 15 2] Output (Actuator #1)

The average "residual" magnitude for untreated and pretreated data are 0.0041 and 0.0032 respectively, or 2% and 1.7% of the average output magnitude. As previously stated, these are very rough measures of the accuracy but there is a clear improvement in the model by prefiltering the data.

e)   Zero-Pole Plots

The zero-pole plot of the prefiltered model also shows improvement over the unfiltered model (see Figures 3. 18 and 3.24).
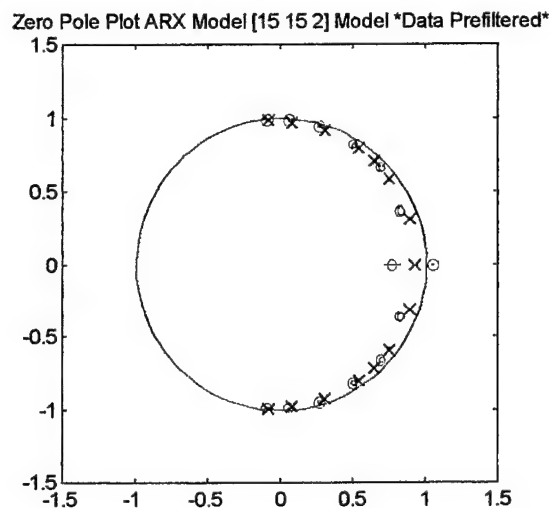
Figure 3.24

Zero-Pole Plot For Prefiltered ARX [15 15 2] (Actuator #1)

However, there are still numerous possible zero-pole cancellations, indicating that use of a lower order model is necessary.

5.   Model Structure Acceptance for Actuator Number One

The goal of the model structure application and evaluation process is to use the ARX based technique to find an acceptable model structure that can be applied to more accurate ARMAX and Box-Jenkins methods. Knowing that prefiltering data provides a better model, the process is repeated. Through the first iteration it was also

determined that a delay change would possibly be beneficial. Returning to the delay selection process, Figure 3.25 plots the loss function for a given number of parameters.

RETURN TO COMMAND SCREEN TO SELECT # OF PARAMETERS TO BE ESTIMATED
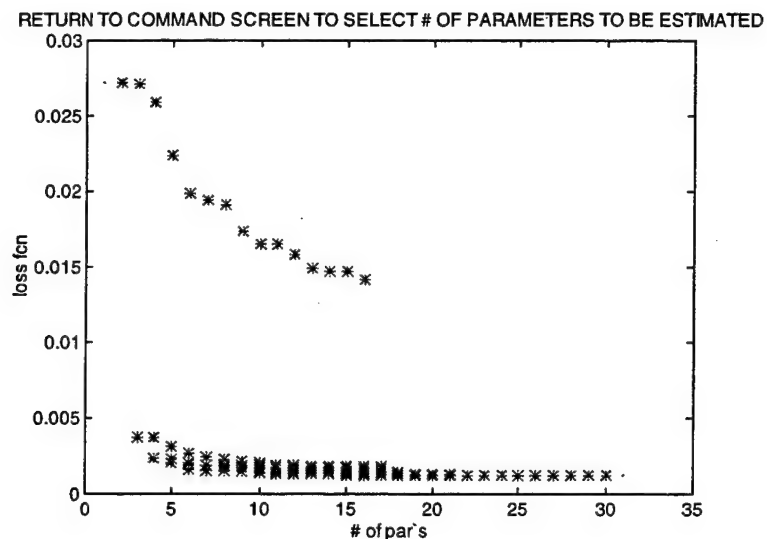
Figure 3.25

Number of Parameters Vs. Loss Function For nk=1 (Actuator #1)

The structures evaluated are contained in table 3.3.

Number of Parameters	Structure [$na\ nb\ nk$]	Notes
30	15 15 1	AIC/MDL Based
24	14 10 1	Automatic
20	7 13 1	Automatic
18	7 11 1	Automatic
15	6 9 1	Automatic
13	6 7 1	Automatic
13	7 6 1	Manual

Table 3.3
Structures For Actuator #1 Input Delay nk=1

After a set of candidate structures was obtained they were used to generate ARX models. The process of model selection and evaluation outlined in Figure 3.11 and described in sections 3 and 4 was applied to each candidate structure based ARX model. The most suitable candidate found was ARX [na=7 nb=6 nk=1] (see Figures 3.26 though 3.32). Table 3.3 lists the [na=7 nb=6 nk=1](or [7 6 1]) structure as a manual selection. In the first iteration the [7 13 1] structure was selected. Upon repeating the selection process for actuator number two, the [7 6 1] structure was generated automatically by the algorithm (see appendix A) based on the choice of 13 parameters. The performance of the resulting model was judged superior and the [7 6 1] structure was applied to actuator number one where it also yielded the best ARX model (see Figure 3.32). However, two design trade-offs were made. First, the auto and cross correlation functions (see Figure 3.28) showed degraded performance, indicating there are still unaccounted input elements in the output. However, it does not affect the frequency response and other criteria used to validate the structure. The second trade-off was the zero-pole plot (see Figure 3.31). The close proximity of two poles and two zeros indicates that a lower order model would be desirable. However, this proved to not be the case. The use of a lower order model showed declining performance over the ARX model using the [7 6 1] structure.

Blue=Actuator#1, Red=ARX MODEL[7 6 1] *Data Prefiltered*

(a) Magnitude

Blue=Actuator#1, Red=ARX MODEL[7 6 1] *Data Prefiltered*
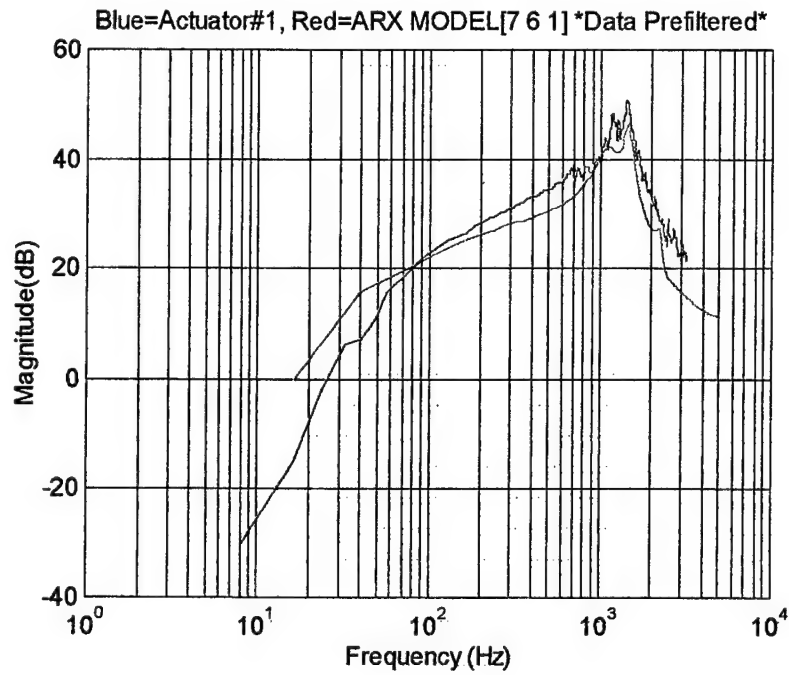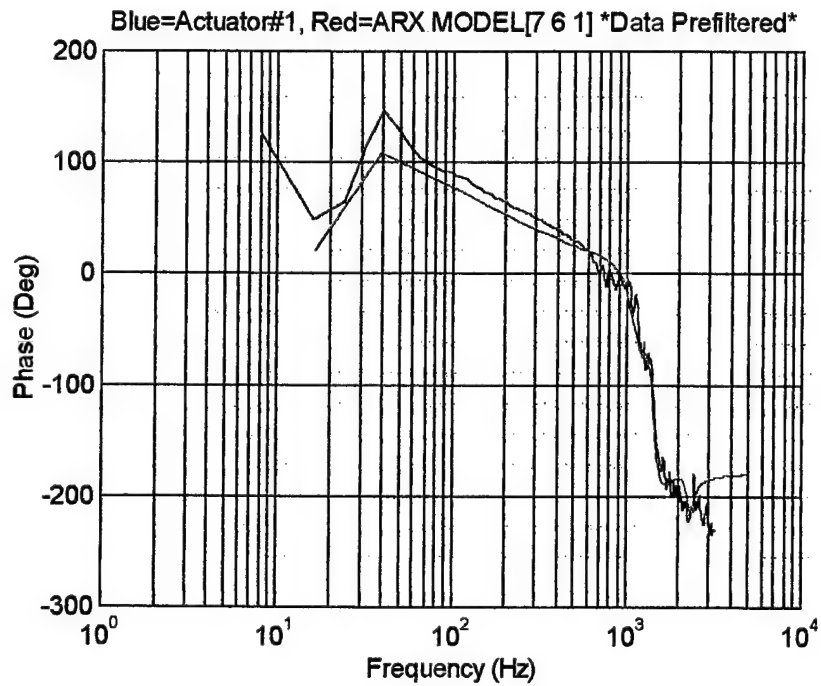
(b) Phase

Figure 3.26
Frequency Response of Prefiltered ARX[7 6 1] (Actuator #1)
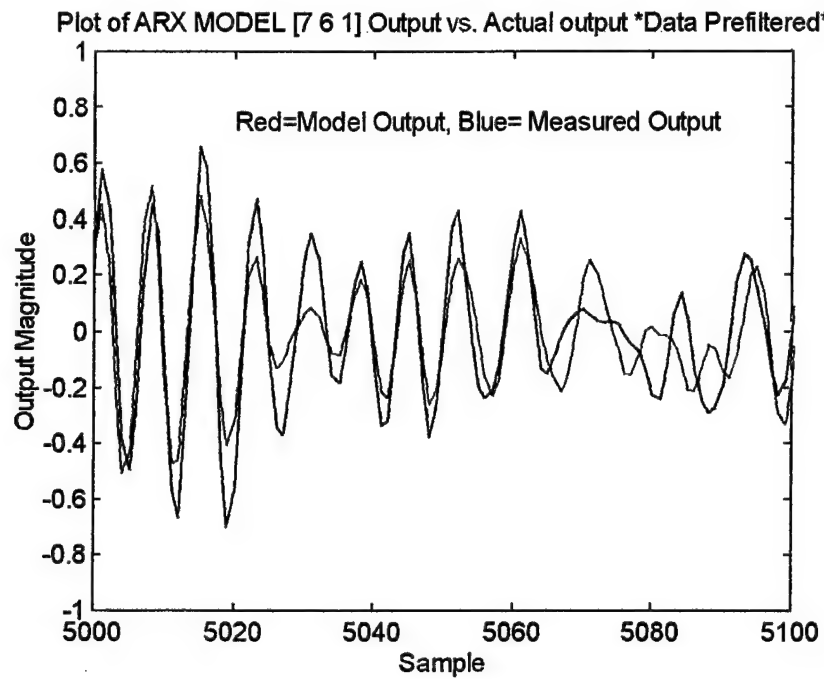
38

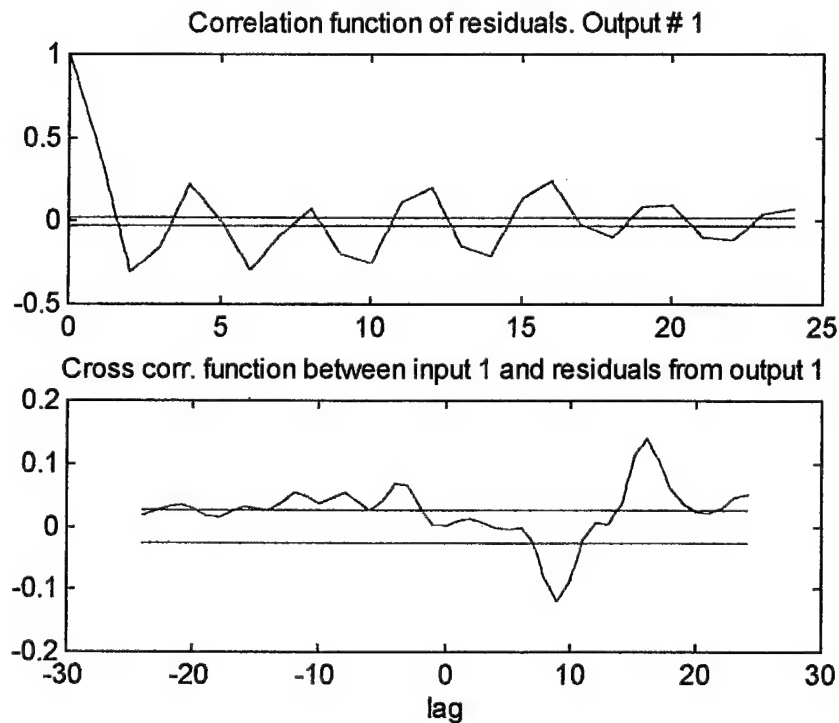Figure 3.27
Actuator #1 Output Vs. ARX[7 6 1] Model

Figure 3.28
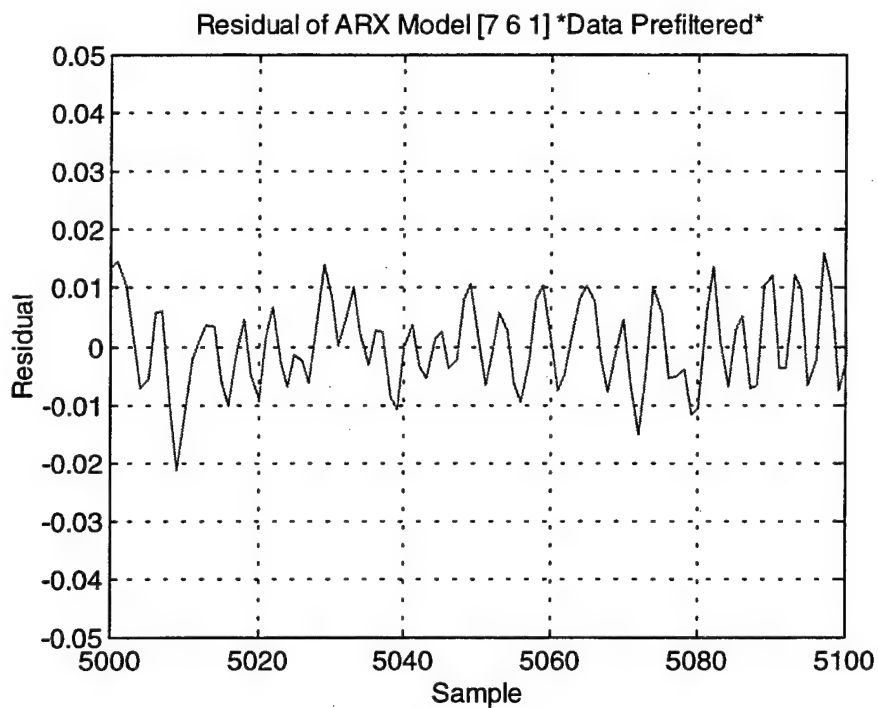Auto and Cross Correlation Functions of ARX[7 6 1] Model (Actuator #1)

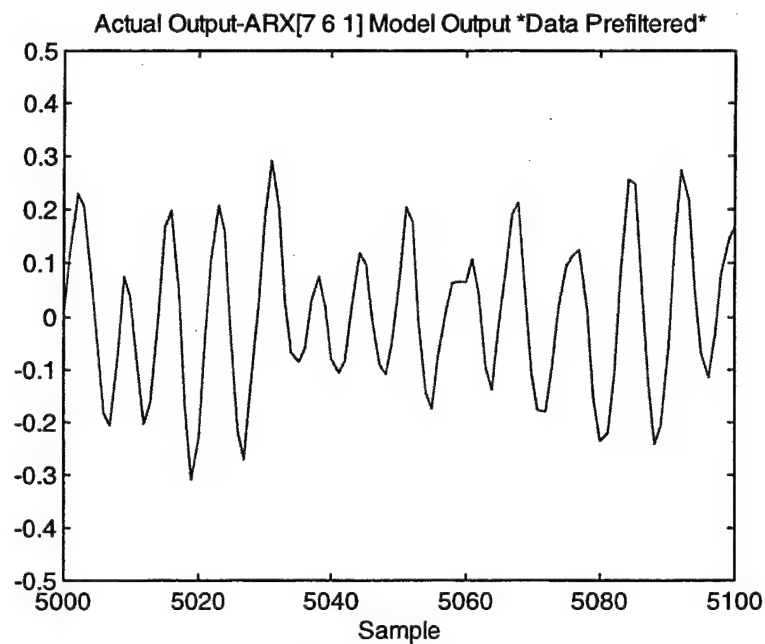Figure 3.29

Residual Vs. Sample for ARX[7 6 1] (Actuator #1)

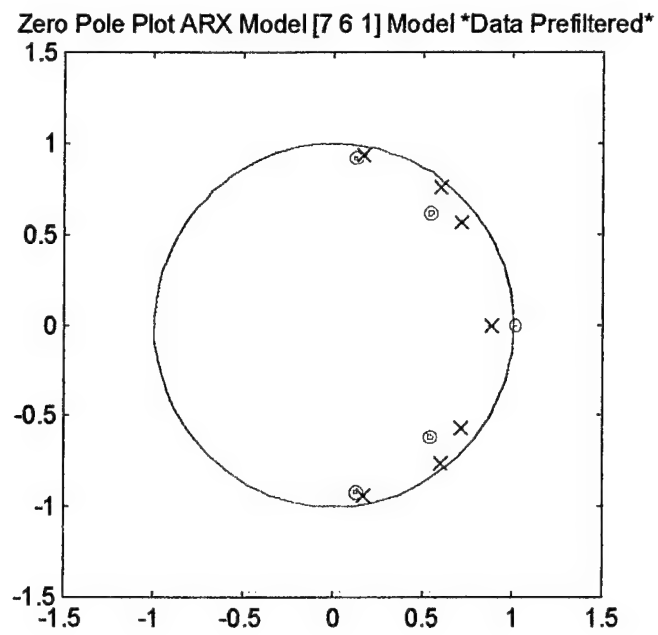Figure 3.30

Actual Output and ARX[7 6 1] Model Output Difference (Actuator #1)

40

Zero Pole Plot ARX Model [7 6 1] Model *Data Prefiltered*

Figure 3.31
Zero-Pole Plot for ARX[7 6 1] Model (Actuator #1)

Strut #1 Magnitude

(a) Magnitude

Strut #1 Phase

Frequency (HZ)
(b) Phase
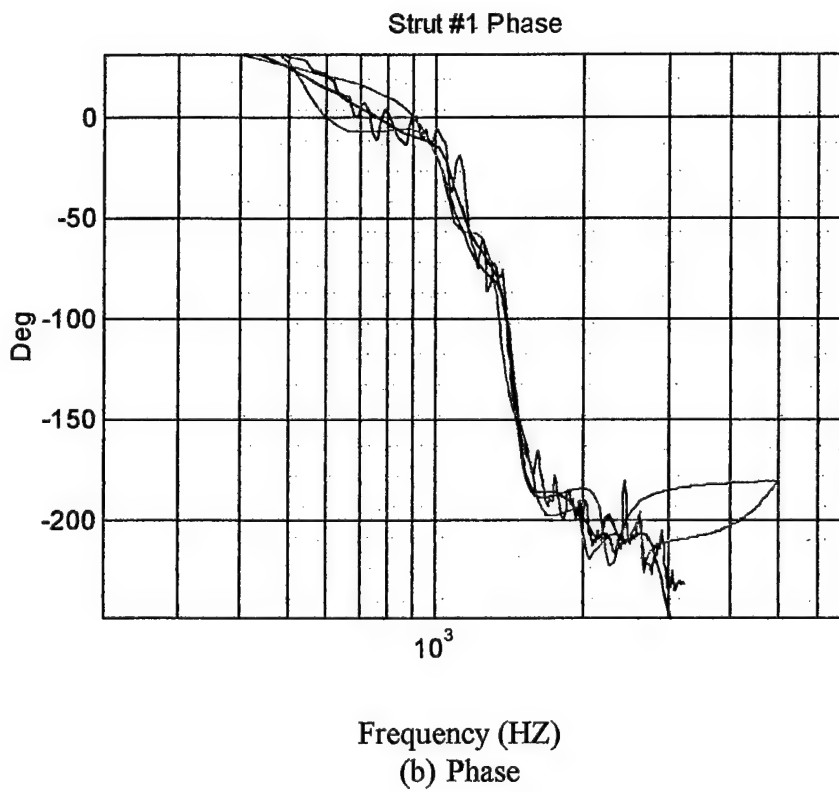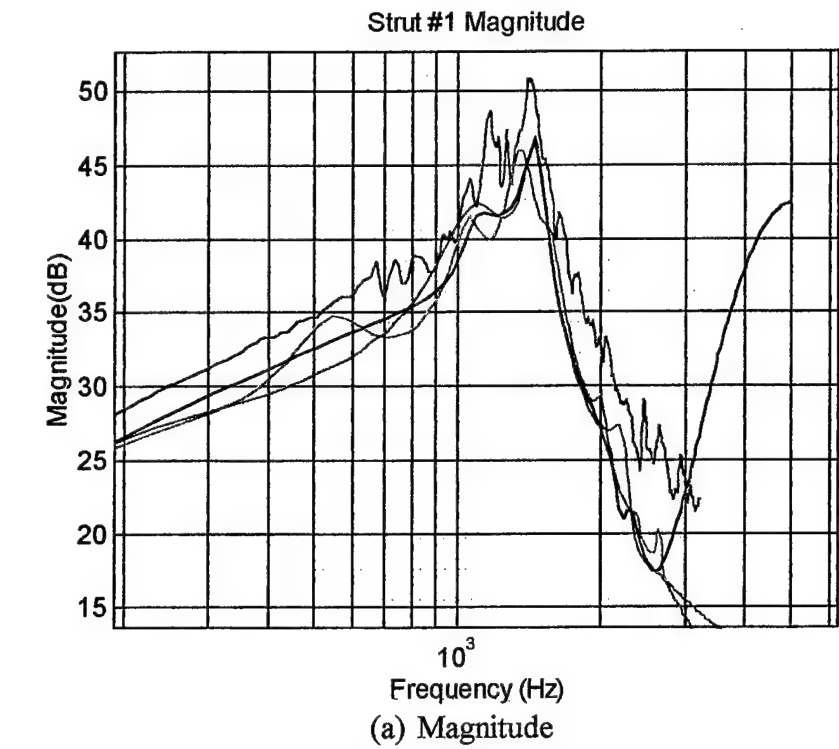
Figure 3.32
ARX Model Frequency Response Comparison
Blue=Actuator#1, Red=[7 6 1], Magenta=[15 15 1], Black=[7 13 1]

42

By increasing the delay the correlation functions improve but performance in all other respects is degraded. The 99% confidence limit may also be too constrictive. Confidence limits of 95% have been used [ref. 10 p.447] to constrain correlation functions. These factors governed the decision to accept the degraded correlation functions as a design trade off. In comparison with models based on various structures (Figure 3.32) this model is acceptable. Table 3.4 summarizes numerical results.

Measure	Result
Average Output Magnitude	0.1870
Average Residual Magnitude	0.0064
Percentage of Average Output	3.4%
Average Output Difference Magnitude	0.0024
Mean Square Fit	0.1562

Table 3.4
Prefiltered ARX[7 6 1] Numerical Results (Actuator #1)

This process was repeated to find the structures for an ARX based model for actuator numbers two through six. This process involved the analysis of hundreds of validation/verification plots and numerical results. Only the validation plots of the accepted structure for each respective actuator were included in this thesis and are shown in appendix B.
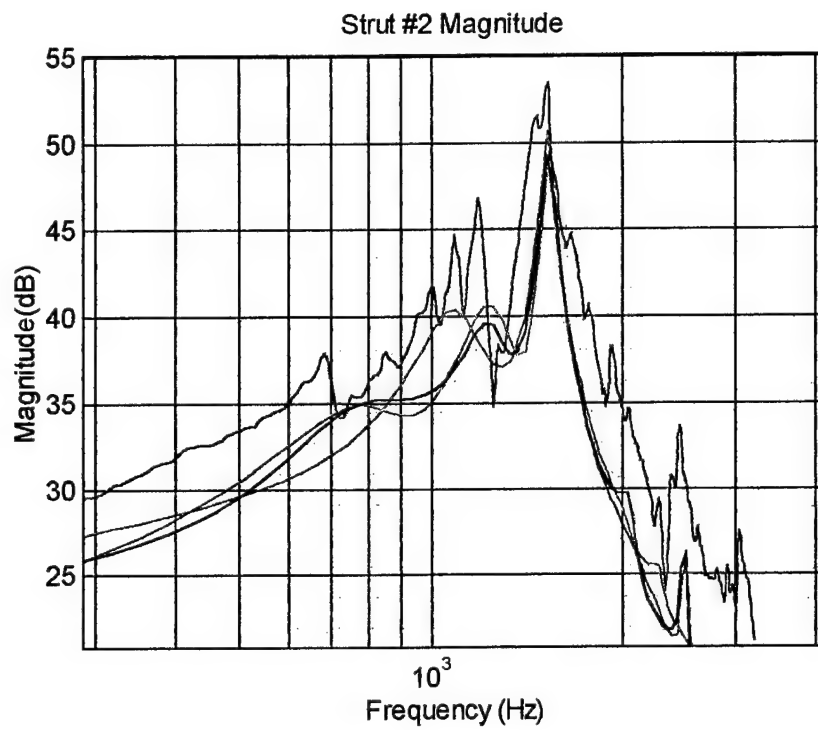
6.   Model Structure Acceptance for Actuator Number Two

The process outlined in section five was repeated for actuator number two. The plots resulting from the acceptance process are listed in appendix B (Figures A.1 through A.7). Based on a delay of nk=1 from table 3.1 and resulting parameter number plot (see appendix B Figure A.1) the structures selected for evaluation are listed in table 3.5.

Number of Parameters	Structure [na nb nk]	Notes
26	12 14 1	AIC Based
25	11 14 1	MDL Based
24	11 13 1	Automatic
22	11 11 1	Automatic
18	9 9 1	Automatic
15	9 6 1	Automatic
13	7 6 1	Automatic
12	6 6 1	Automatic

Table 3.5
Evaluated Model Structures for Actuator #2

After evaluating the graphical and numerical results of the structures listed in table 3.5, the [7 6 1] structure was identified as the best structure. It provides excellent performance for a minimal number of zeros and poles. Figure 3.33 compares the [7 6 1] based model with the next best models.

Strut #2 Magnitude

(a) Magnitude

Strut #2 Phase
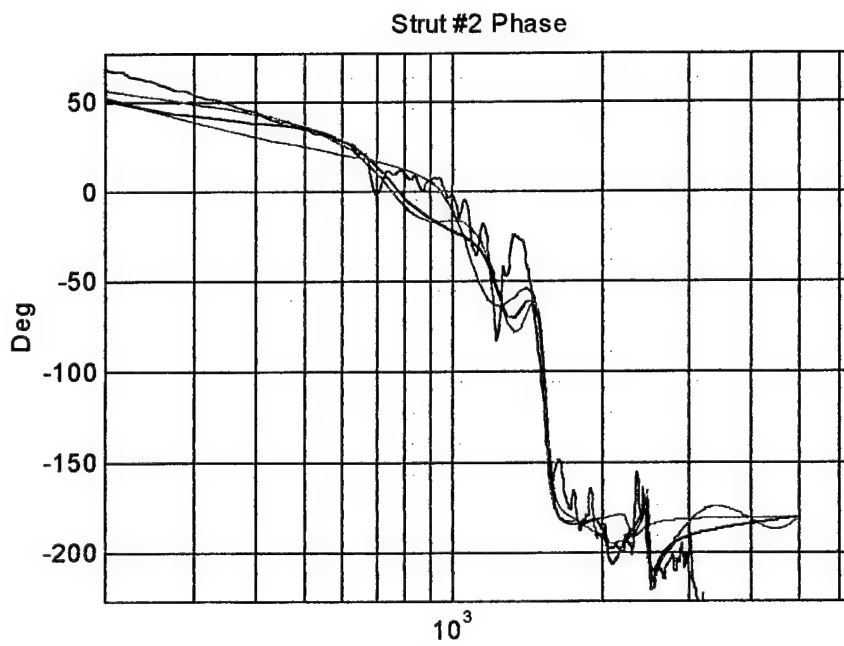
Frequency (Hz)
(b) Phase

Figure 3.33
ARX Model Frequency Response Comparison
Blue=Actuator, Red=[7 6 1], Magenta=[11 14 1], Black=[11 11 1]

Measure	Result
Average Output Magnitude	0.1906
Average Residual Magnitude	0.0073
Percentage of Average Output	3.8%
Average Output Difference Magnitude	0.0025
Mean Square Fit	0.1736

Table 3.6
Numerical Results for Actuator #2

7. Model Structure Acceptance for Actuator Number Three

The plots resulting from the acceptance process are listed in appendix B (Figures B.1 through B.7). Based on a delay of nk=1 from table 3.1 and resulting parameter number plot (see appendix B Figure B.1) the structures selected for evaluation are listed in table 3.7.

Number of Parameters	Structure [na nb nk]	Notes
25	15 10 1	Automatic
24	15 9 1	ADC Based
24	14 10 1	Manual
17	8 9 1	MDL Based
15	8 7 1	Automatic
13	8 5 1	Automatic
13	7 6 1	Manual

Table 3.7
Evaluated Model Structures for Actuator #3

A comparison of the selected structure, [7 6 1], and the next best models is shown in Figure 3.34. Of particular interest, the best structures were those resulting from non-filtered data. A possible explanation is the absence of high frequency disturbances which filtering is designed to remove. Also of note is the fact that during excitation of actuator

46

number three the noise emitted was distinctly different from the other actuators when excited. This could be the result of slight manufacturing differences.
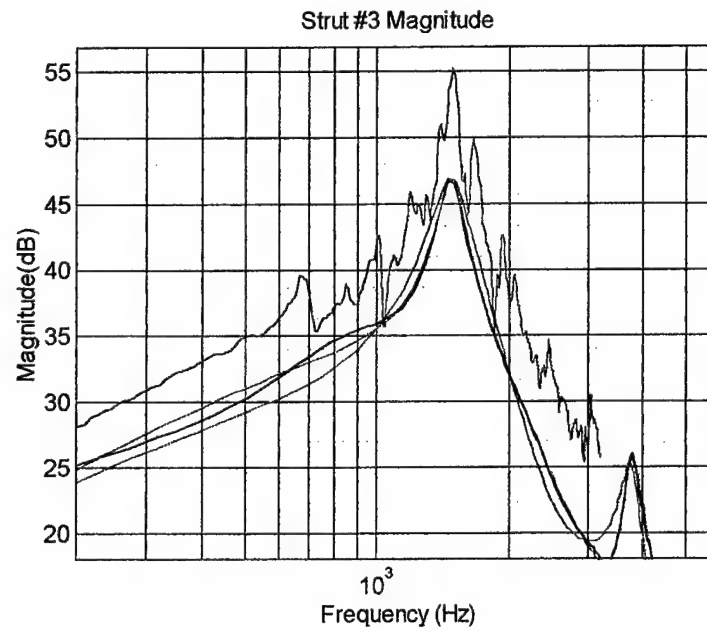
(a) Magnitude
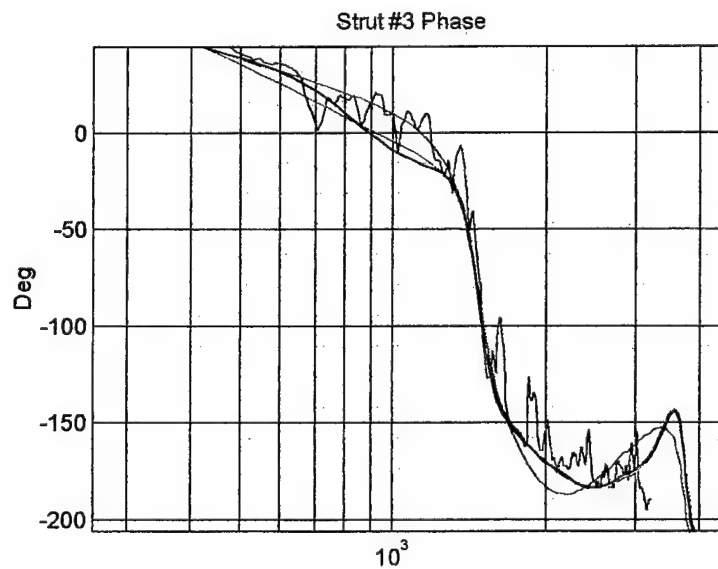
Frequency (Hz)
(b) Phase
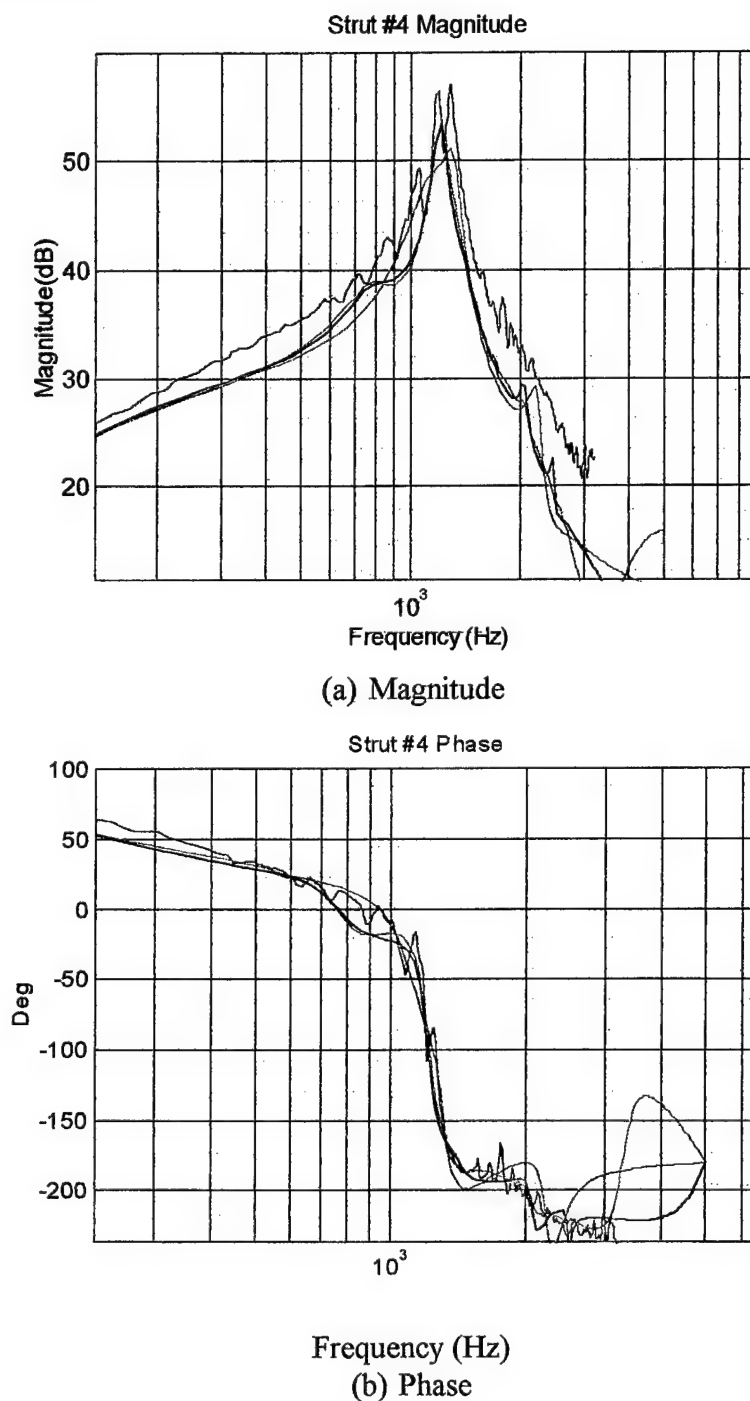
Figure 3.34
ARX Model Frequency Response Comparison
Blue=Actuator#3, Red=[7 6 1], Magenta=[15 15 1], Black=[7 13 1]

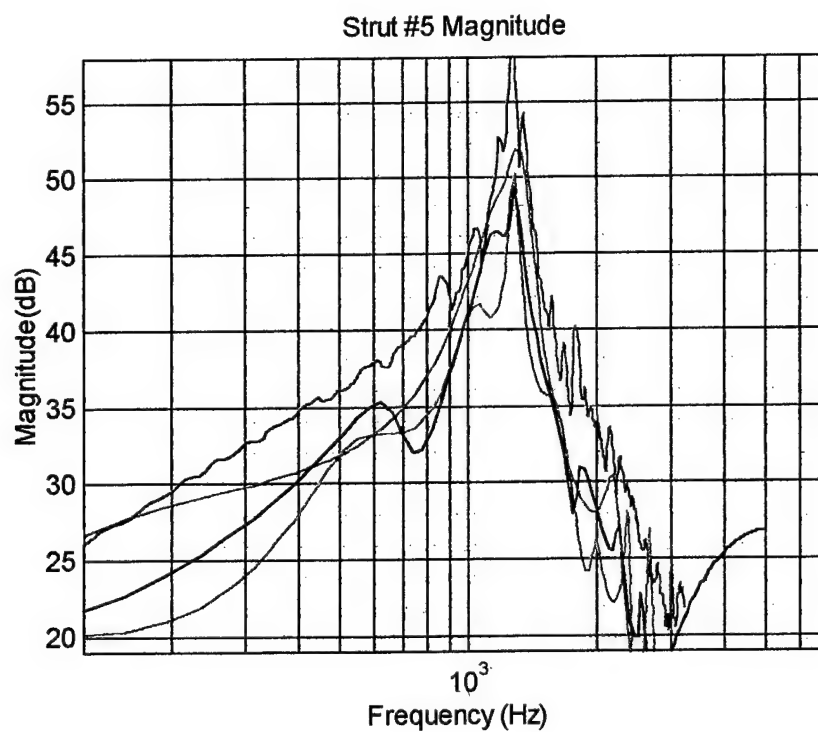| Measure	Result
Average Output Magnitude	0.2298
Average Residual Magnitude	0.0613
Percentage of Average Output	26%
Average Output Difference Magnitude	0.0037
Mean Square Fit	0.2061

Table 3.8
Numerical Results For Actuator #3

8. Model Structure Acceptance for Actuator Number Four

The plots resulting from the acceptance process are listed in appendix B (Figures C.1 through C.7). Based on a delay of nk=1 from table 3.1 and resulting parameter number plot (see appendix B Figure C.1) the structures selected for evaluation are listed in table 3.9.

Number of Parameters	Structure [na nb nk]	Notes
26	11 15 2 .	ADC Based
20	8 12 2	MDL Based
18	10 8 2	Automatic
12	4 8 2	Automatic
26	11 15 1	ADC Based
24	11 13 1	MDL Based
17	8 9 1	Automatic
13	7 6 1	Manual

Table 3.9
Evaluated Model Structures

Similar to the case of actuator number one, the algorithm selected a delay of two. However, the best results were achieved by using a lower delay. The penalty paid was

48

degraded auto and cross correlation functions. This was again taken as a design trade off.
The ARX structure [*na*=7 *nb*=6 *nk*=1] again proved to be the best choice (see Figure
3.35). Numerical results are contained in table 3.10.

Strut #4 Magnitude

(a) Magnitude

Strut #4 Phase

Frequency (Hz)
(b) Phase

Figure 3.35
ARX Model Frequency Response Comparison
Blue=Actuator#4, Red=[7 6 1], Magenta=[11 13 1], Black=[11 11 1]

Measure	Result
Average Output Magnitude	0.3052
Average Residual Magnitude	0.0066
Percentage of Average Output	2.1%
Average Output Difference Magnitude	0.0036
Mean Square Fit	0.2662

Table 3.10
Numerical Results for Actuator #4

9.   Model Structure Acceptance for Actuator Number Five

The plots resulting from the acceptance process are listed in appendix B (Figures D.1 through D.7). Based on a delay of nk=1 from table 3.1 and resulting parameter number plot (see appendix B Figure D.1) the structures selected for evaluation are listed in table 3.12.

Number of Parameters	Structure [na nb nk]	Notes
28	13 15 2	ADC Based
27	12 15 2	MDL Based
22	10 12 2	Automatic
18	12 6 2	Automatic
28	13 15 1	ADC/MDL Based
24	15 9 1	Automatic
15	8 7 1	Automatic
13	7 6 1	Manual

Table 3.11
Evaluated Model Structures

The validation of actuator number five is virtually the same as actuator number four (see appendix B Figures C.2 through C.7, D.2 through D.7 and tables 3.10 and 3.12).

50

Strut #5 Magnitude
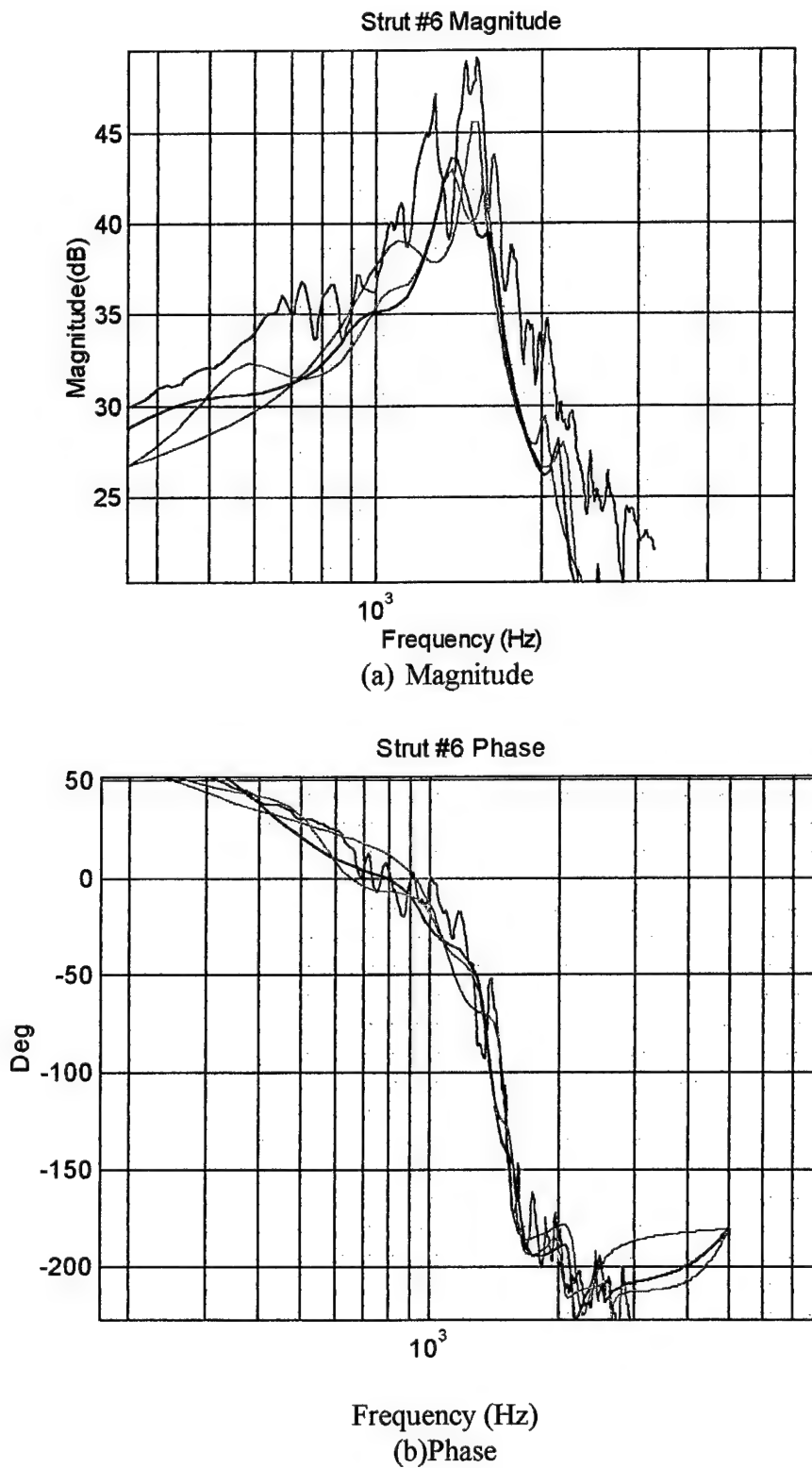

(a) Magnitude

Strut #5 Phase
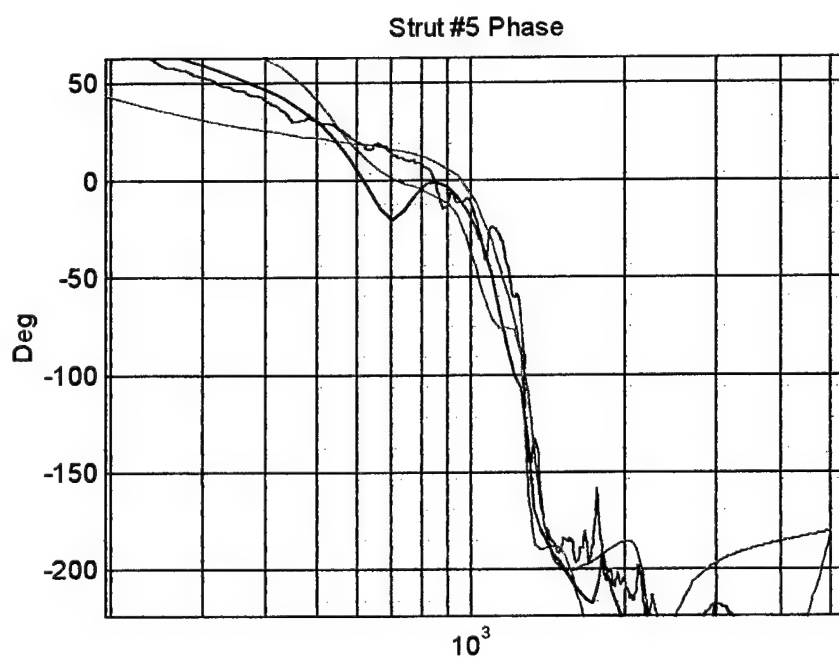
Frequency (Hz)
(b) Phase

Figure 3.36
ARX Model Frequency Response Comparison
Blue=Actuator #5, Red=[7 6 1], Magenta=[15 9 1], Black=[13 15 1]

51

Measure	Result
Average Output Magnitude	0.3070
Average Residual Magnitude	0.0078
Percentage of Average Output	2.5%
Average Output Difference Magnitude	0.0032
Mean Square Fit	0.2830

Table 3.12
Numerical Results for Actuator #5

10.   Model Structure Acceptance for Actuator Number Six

The plots resulting from the acceptance process are listed in appendix B (Figures E.1 through E.7). Based on a delay of $nk=1$ from table 3.1 and resulting parameter number plot (see appendix B Figure E.1) the structures selected for evaluation are listed in table 3.13.

Number of Parameters	Structure [na nb nk]	Notes
30	15 15 1	ADC/MDL Based
24	12 12 1	Automatic
20	11 9 1	Automatic
18	9 9 1	Automatic
13	7 6 1	Manual

Table 3.13
Evaluated Model Structures

The comparison of the best model structures is shown in Figure 3.37 . The [7 6 1] structure selected for the other five actuators is the best choice for actuator number six. Numerical results are listed in table 3.14.

52

Strut #6 Magnitude

(a) Magnitude

Strut #6 Phase

Frequency (Hz)
(b)Phase

Figure 3.37
ARX Model Frequency Response Comparison
Blue=Actuator #6, Red=[7 6 1], Magenta=[15 15 1], Black=[12 12 1]

Measure	Result
Average Output Magnitude	0.1551
Average Residual Magnitude	0.0055
Percentage of Average Output	3.5%
Average Output Difference Magnitude	0.0023
Mean Square Fit	0.1316

Table 3.14
Numerical Results for Actuator #6

D.   APPLICATION OF SELECTED STRUCTURE

The selection of the same basic model structure $na=7$ $nb=6$ $nk=1$ for all six actuators is an indication that the plant dynamics of the actuators can be assumed to be identical. With the exception of actuator number three, all received the best results from prefiltered data. The design trade-offs were the degraded auto and cross correlation functions and the relative proximity of two poles and two zeros. This basic structure was used to develop more accurate ARMAX and Box-Jenkins models. Although the Box-Jenkins is the most accurate parametric estimation method, it was anticipated that the ARMAX would give the best results based on the nature of disturbances and on when they enter into the system (see Figure 3.3).

The application and evaluation process is the same as that used to evaluate selected structures on the ARX model. A second order noise model was used for both the ARMAX and Box-Jenkins models. The standard choices are 2nd and 4th order models [Ref. 11]. Both were applied and the 2nd order yielded a better result. After the application of the ARMAX and Box-Jenkins based models the overall performance of the ARX and ARMAX models was decidedly better. The only exception was on actuator number two. This will be addressed in section two. Based on the results obtained thus far indicating the actuator plants are essentially the same and the excellent performance of the ARX and ARMAX models, only the evaluation plots for the ARMAX model are included and can be found in appendix C. Summary and comparison results are listed for each actuator.

1.   Actuator Number One

A graphical comparison of ARX, ARMAX and Box-Jenkins models is shown in Figure 3.38. Validation plots for the ARMAX [7 6 2 1] model are included as Figures A.1 through A.6 in appendix C. Numerical results are contained in table 3.15.

55

Strut #1 Magnitude

(a) Magnitude

Strut #1 Phase
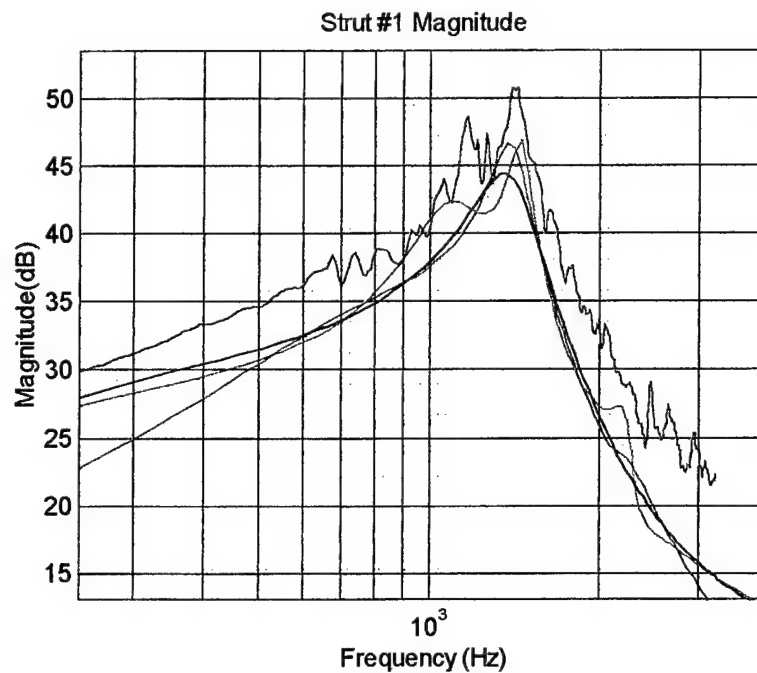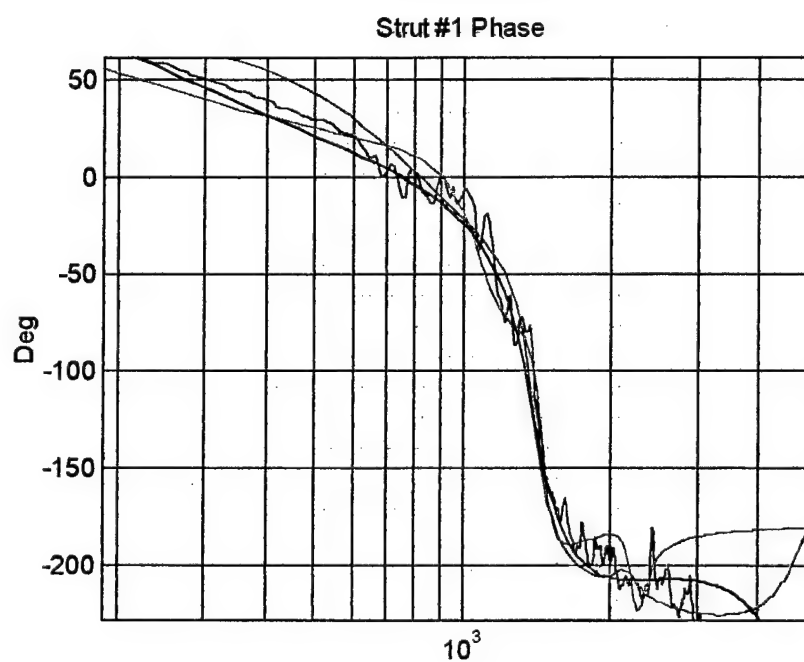
Frequency (Hz)
(b) Phase

Figure 3.38
Model Frequency Response Comparison
Blue=Actuator #1, Red=ARMAX[7 6 2 1], Magenta=ARX[7 6 1], Black=BJ[6 2 2 7 1]

56

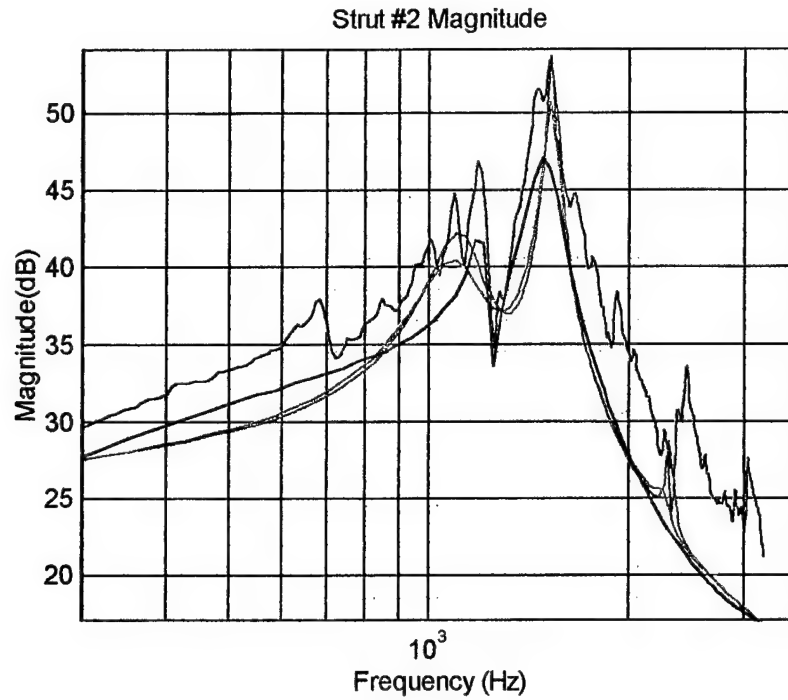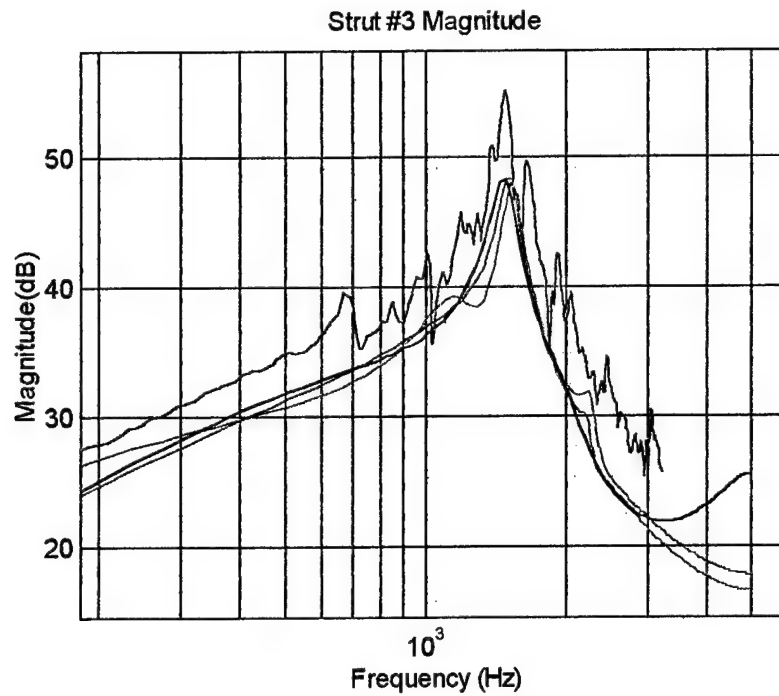| Measure	ARX[7 6 1] (Data Prefiltered)	ARMAX[7 6 2 1] (Data Prefiltered)	BJ[6 2 2 7 1] (Data Prefiltered)
Ave. Output Magnitude	0.1870	0.1870	0.1870
Ave. Residual Magnitude	0.0064	0.0036	0.0094
Percent of Output Mag.	3.4%	2%	5%
Ave. Output Difference	0.0024	0.002	0.0025
Mean Square Fit	0.1562	0.1589	0.1568

Table 3.15
Numerical Results for Actuator #1

Based upon the above results the ARX[7 6 1] model was determined to best fit the performance of actuator number one. The choice between the ARX and ARMAX is a close one. This indicates the assumption that the disturbance or noise entered the system early and is accurately modeled by the dynamics (poles) of the plant. The addition of the $C(q,\theta)$ polynomial is not necessary. The improved performance of the ARX and ARMAX models over the Box-Jenkins further supports the assumption regarding the nature of the disturbance.

2. Actuator Number Two

A graphical comparison of ARX, ARMAX and Box-Jenkins models is shown in Figure 3.39. Validation plots for the ARMAX [7 6 2 1] model are included as Figures B.1 through B.6 in appendix C. Numerical results are contained in table 3.16.

57

(a) Magnitude
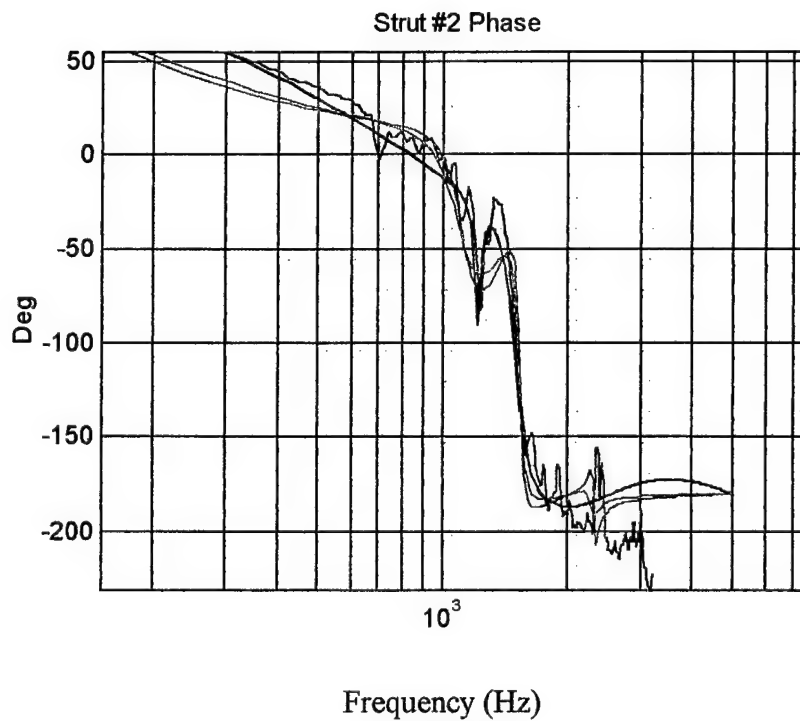
Frequency (Hz)
(b) Phase

Figure 3.39
Model Frequency Response Comparison
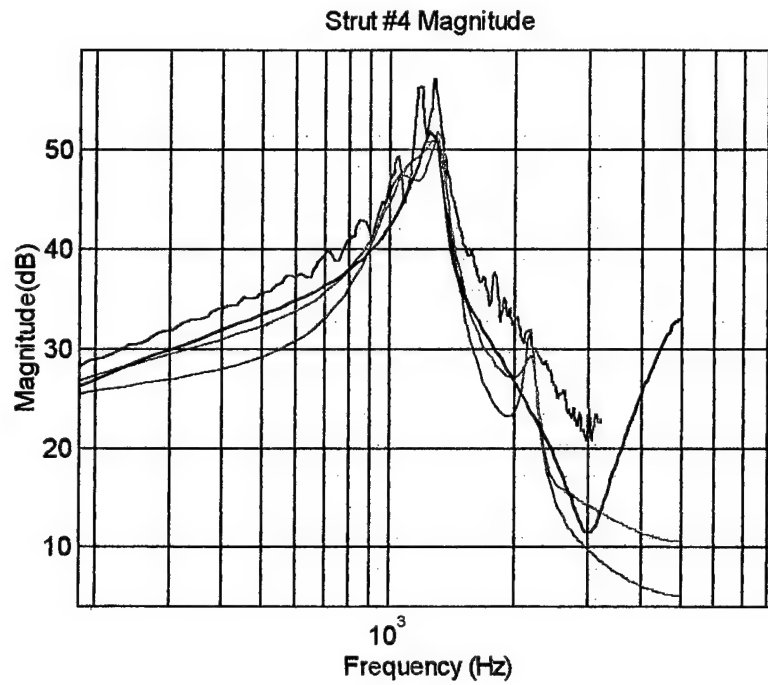Blue=Actuator #2, Red=ARMAX[7 6 2 1], Magenta=ARX[7 6 1], Black=BJ[6 2 2 7 1]

Measure	ARX[7 6 1] (Data Prefiltered)	ARMAX[7 6 2 1] (Data Prefiltered)	BJ[6 2 2 7 1] (Data Prefiltered)
Ave. Output Magnitude	0.1906	0.1906	0.1906
Ave. Residual Magnitude	0.0073	0.003	0.0114
Percent of Output Mag.	3.8%	1.6%	6%
Ave. Output Difference	0.0025	0.0027	0.0023
Mean Square Fit	0.1736	0.1705	0.1616

Table 3.16
Numerical Results for Actuator #2

The Box-Jenkins model showed excellent frequency response correlation, auto and cross correlation functions and some improved numerical results. However, due to the close performance of the ARMAX and Box-Jenkins models, the large uncertainty ellipses in the zero-pole plot (see appendix C) the ARMAX model was selected.

3. Actuator Number Three

A graphical comparison of ARX, ARMAX and Box-Jenkins models is shown in Figure 3.40. Validation plots for the ARMAX [7 6 2 1] model are included as Figures C.1 through C.6 in appendix C. Numerical results are contained in table 3.17.

Strut #3 Magnitude

(a) Magnitude

Strut #3 Phase
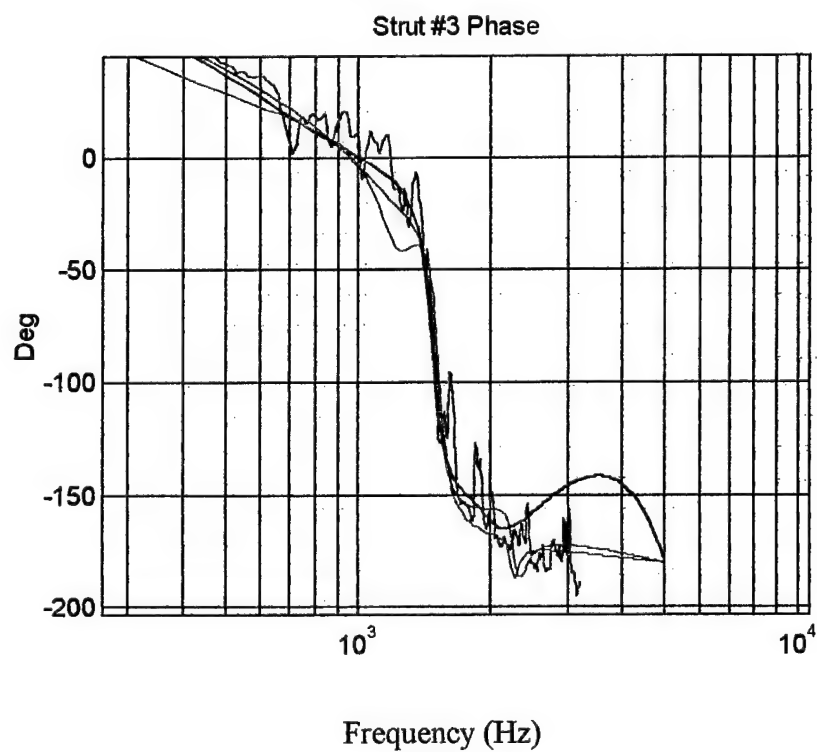
Frequency (Hz)
(b) Phase

Figure 3.40
Model Frequency Response Comparison
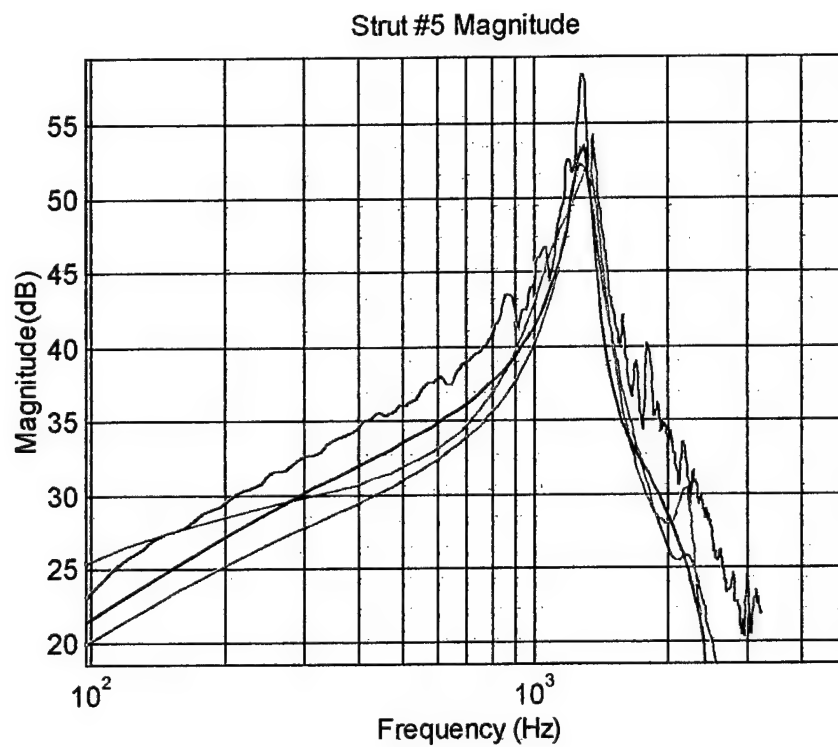Blue=Actuator #3, Red=ARMAX[7 6 2 1], Magenta=ARX[7 6 1], Black=BJ[6 2 2 7 1]

Measure	ARX[7 6 1] (Data not filtered)	ARMAX[7 6 2 1] (Data Prefiltered)	BJ[6 2 2 7 1] (Data Prefiltered)
Ave. Output Magnitude	0.2298	0.2298	0.2298
Ave. Residual Mag.	0.0613	0.0040	0.0215
Percent of Output Mag.	26%	1.7%	9.3%
Ave. Output Difference	0.0037	0.0040	0.0036
Mean Square Fit	0.2061	0.2031	0.2000

Table 3.17
Numerical Results for Actuator #3

Although the non-filtered ARX model was chosen over the prefiltered ARX model, it appears that the performance of the prefiltered ARMAX is much better. This can be explained by possible manufacturing variation in actuator number three which requires the use of the $C(q,\theta)$ polynomial to model the disturbance.

4. Actuator Number Four

A graphical comparison of ARX, ARMAX and Box-Jenkins models is shown in Figure 3.41. Validation plots for the ARMAX [7 6 2 1] model are included as Figures D.1 through D.6 in appendix C. Numerical results are contained in table 3.18.
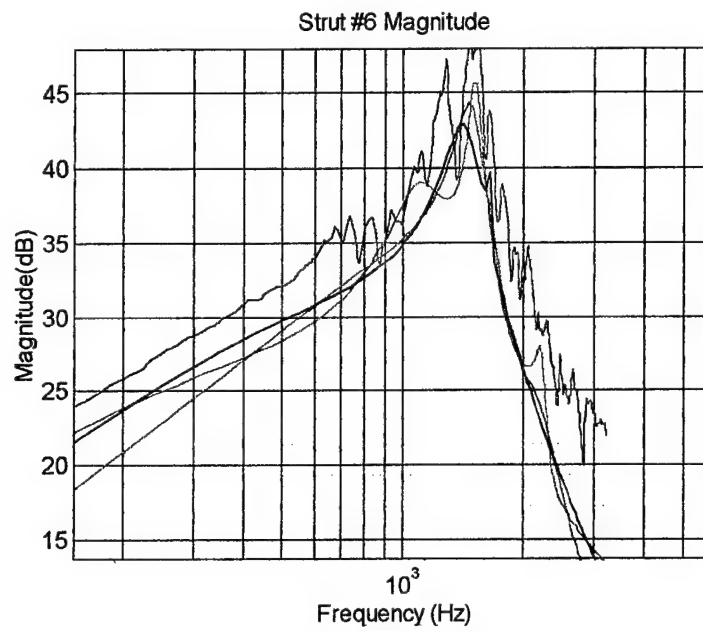
(a) Magnitude
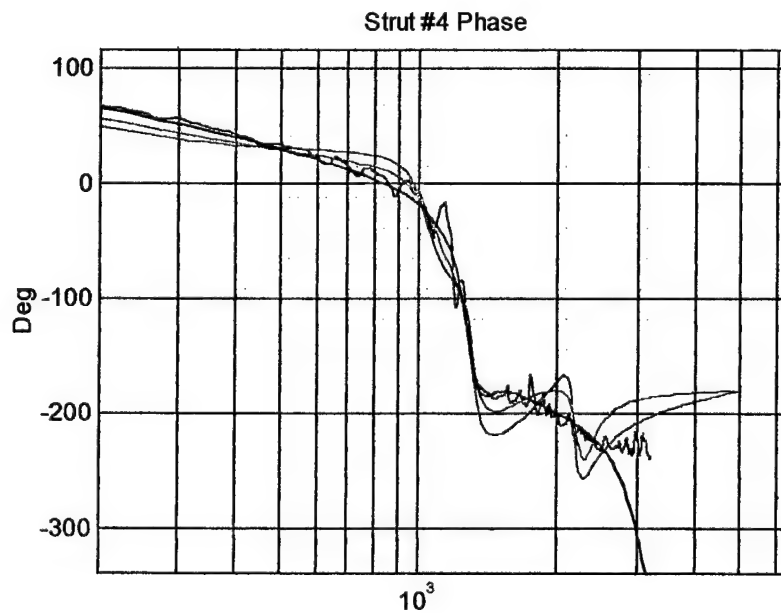
Frequency (Hz)
(b) Phase

Figure 3.41
Model Frequency Response Comparison
Blue=Actuator #4, Red=ARMAX[7 6 2 1], Magenta=ARX[7 6 1], Black=BJ[6 2 2 7 1]

Measure	ARX[7 6 1] (Data Prefiltered)	ARMAX[7 6 2 1] (Data Not Prefiltered)	BJ[6 2 2 7 1] (Data Prefiltered)
Ave. Output Magnitude	0.3052	0.3052	0.3052
Ave. Residual Mag.	0.0066	0.0335	0.0099
Percent of Output Mag.	2.1%	11%	3.2%
Ave. Output Difference	0.0036	0.0034	0.0034
Mean Square Fit	0.2662	0.2661	0.2572

Table 3.18
Numerical Results for Actuator #4

This case appears similar to actuator number one where the disturbance is accurately characterized by the system pole model without the need for the $C(q,\theta)$ polynomial.

5.   Actuator Number Five

A graphical comparison of ARX, ARMAX and Box-Jenkins models is shown in Figure 3.42. Validation plots for the ARMAX [7 6 2 1] model are included as Figures E.1 through E.6 in appendix C. Numerical results are contained in table 3.19.

Strut #5 Magnitude

(a) Magnitude

Strut #5 Phase
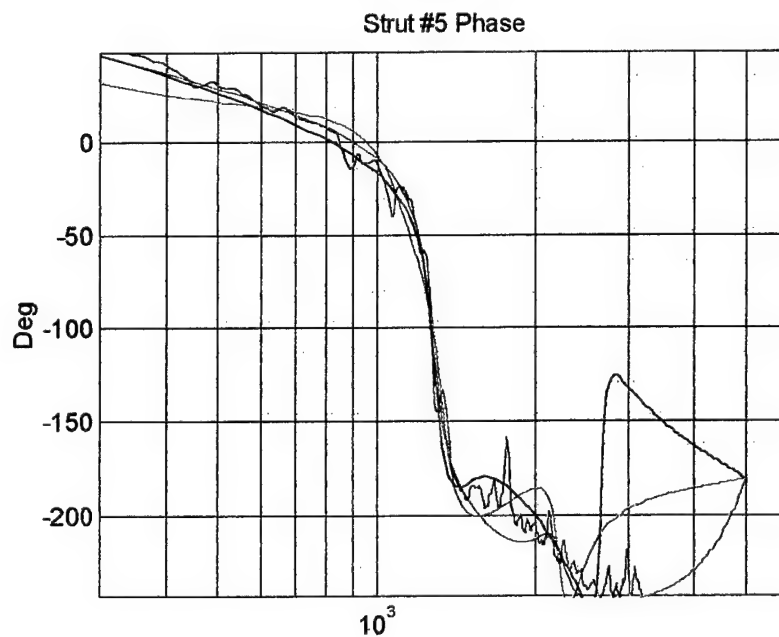
Frequency (Hz)
(b) Phase

Figure 3.42
Model Frequency Response Comparison

64

Measure	ARX[7 6 1] (Data filtered)	ARMAX[7 6 2 1] (Data Prefiltered)	BJ[6 2 2 7 1] (Data Prefiltered)
Ave. Output Magnitude	0.3070	0.3070	0.3070
Ave. Residual Mag.	0.0078	0.0035	0.0151
Percent of Output Mag.	2.5%	1.1%	4.9%
Ave. Output Difference	0.0032	0.0033	0.0034
Mean Square Fit	0.2830	0.2688	0.2698

Table 3.19
Numerical Results for Actuator #5

6.   Actuator Number Six

A graphical comparison of ARX, ARMAX and Box-Jenkins models is shown in Figure 3.43. Validation plots for the ARMAX [7 6 2 1] model are included as Figures F.1 through F.6 in appendix C. Numerical results are contained in table 3.20.

Strut #6 Magnitude

(a) Magnitude

Strut #6 Phase
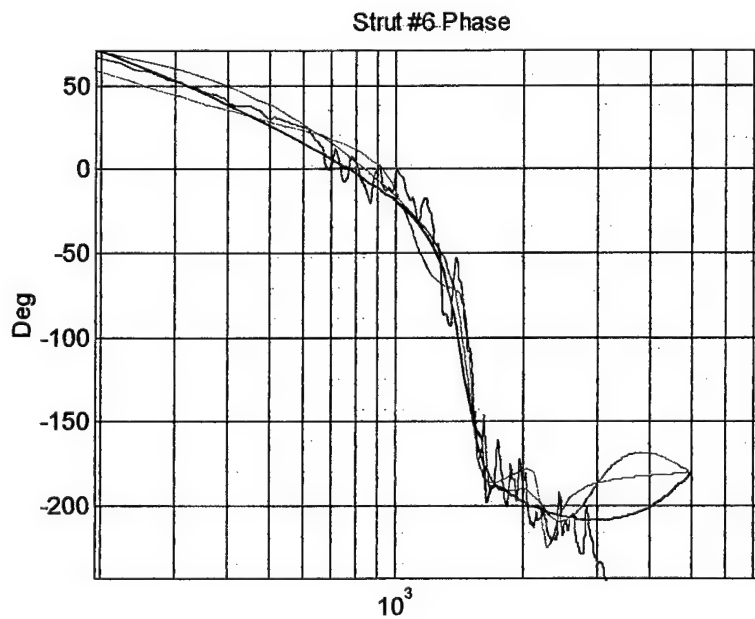
Frequency (Hz)
(b) Phase

Figure 3.43
Model Frequency Response Comparison
Blue=Actuator #6, Red=ARMAX[7 6 2 1], Magenta=ARX[7 6 1], Black=BJ[6 2 2 7 1]

66

Measure	ARX[7 6 1] (Data not filtered)	ARMAX[7 6 2 1] (Data Prefiltered)	BJ[6 2 2 7 1] (Data Prefiltered)
Ave. Output Magnitude	0.1551	0.1551	0.1551
Ave. Residual Mag.	0.0055	0.0035	0.0086
Percent of Output Mag.	3.5%	2.2%	5.5%
Ave. Output Difference	0.0023	0.0020	0.0019
Mean Square Fit	0.1316	0.1312	0.1356

Table 3.20
Numerical Results for Actuator #6

E.   SUMMARY OF RESULTS

Table 3.21 presents a summary of the model selection process.

Actuator	1	2	3	4	5	6
Model [Structure]	ARX [7 6 1]	ARMAX [7 6 2 1]	ARMAX [7 6 2 1]	ARX [7 6 1]	ARMAX [7 6 2 1]	ARMAX [7 6 2 1]
Ave. Out. Mag.	0.1870	0.1906	0.2298	0.3052	0.3070	0.1551
Ave. Res. Mag.	0.0064	0.003	0.0040	0.0066	0.0035	0.0035
% of Out. Mag.	3.4%	1.6%	1.7%	2.1%	1.1%	2.2%
Ave. Out. Dive.	0.0024	0.0027	0.0040	0.0036	0.0033	0.0020
Mean Sq. Fit	0.1562	0.1705	0.2031	0.2662	0.2688	0.1312

Table 3.21
Summary of Numerical Results

F.   POLES AND ZEROS

The ultimate goal in identifying the plant of the platform is to obtain the poles and zeros of the plant transfer function which can be used in design of an active vibration control law for the platform. Tables 3.22 and 3.23 present the poles and zeros extracted from the parameter estimation algorithm listed in appendix A.

1	2	3
0.1252+0.9199i	0.1080+0.9667i	0.1198+0.9204i
0.1252-0.9199i	0.1080-0.9667i	0.1198-0.9204i
1.0137	1.0222	1.0204
0.5371+0.6167i	0.5887+0.6486i	0.4925+0.6206i
0.5371-0.6167i	0.5887-0.6486i	0.4925-0.6206i

(a) Actuators #1 through #3

4	5	6
0.0674 + 0.6235i	0.1971+0.8593i	0.2281+0.7945i
0.0674 + 0.6235i	0.1971-0.8593i	0.2281-0.7945i
-1.2095	1.0098	1.0032
1.0010	-0.5566	-0.1319+0.6080i
-0.5568	0.2913	-0.1319-0.6080i

(b) Actuators #4 through #6

Table 3.22
Actuator Transfer Function Poles

1	2	3
0.1661 + 0.9362i	0.1122 + 0.9803i	0.1410 + 0.9402i
0.1661 - 0.9362i	0.1122 - 0.9803i	0.1410 + 0.9402i
0.8743	0.9035	0.7231
0.5932 + 0.7591i	0.5645 + 0.8101i	0.5584 +0.7771i
0.5932 - 0.7591i	0.5645 - 0.8101i	0.5584 -0.7771i
0.7101 + 0.5677i	0.7220 + 0.6035i	0.5562 + 0.5203i
0.7101 + 0.5677i	0.7220 - 0.6035i	0.5562 + 0.5203i

(a) Actuators #1through #3

4	5	6
0.6905 + 0.6666i	0.1657 + 0.9000i	0.1138 + 0.8029i
0.6905 - 0.6666i	0.1657 - 0.9000i	0.1138 - 0.8029i
0.6386	0.8267	0.6405
-0.3437 + 0.4468i	0.6710 + 0.6870i	0.5522 + 0.7348i
-0.3437 - 0.4468i	0.6710 - 0.6870i	0.5522 -0.7348i
0.2640 + 0.4531i	0.4532 + 0.4747i	0.3908 + 0.4466i
0.2640 - 0.4531i	0.4532 - 0.4747i	0.3908 -0.4466i

(b) Actuators #4 through #6

Table 3.23
Actuator Transfer Function Zeros

A review of the poles and zeros shows that zeros are very similar, especially among actuators one, two, three and six. The magnitude of the real parts of zeros for actuators four and five appear to vary more than the others. This is also true for the poles. This was unexpected and no explanation is offered. Any expected difference would have been attributed to actuator number three based on previous results and analysis. However, actuator number three is in relative concurrence with the other actuators.

G.   TRANSFER FUNCTIONS

The actuator transfer functions are as follows;

ACTUATOR Number One

$$\frac{13.5362S^6 - 31.6493S^5 + 42.5317S^4 - 39.4886S^3 + 22.8012S^2 - 7.9085S}{S^7 - 3.8132S^6 + 7.7793S^5 - 10.3532S^4 + 9.7102S^3 - 6.3907S^2 + 2.7336S - 0.6064}$$

ACTUATOR Number Two

$$\frac{15.1709S^6 - 36.6464S^5 + 51.4596S^4 - 49.9296S^3 + 30.8599S^2 - 11.2584S}{S^7 - 3.7010S^6 + 7.5692S^5 - 10.2511S^4 + 9.9482S^3 - 6.8762S^2 + 3.1332S - 0.7594}$$

ACTUATOR Number Three

$$\frac{21.6875S^6 - 48.6904S^5 + 64.5198S^4 - 59.8485S^3 + 33.8370S^2 - 11.9673S}{S^7 - 3.2342S^6 + 6.0679S^5 - 7.5022S^4 + 6.6380S^3 - 4.1175S^2 + 1.6454S - 0.3361}$$

ACTUATOR Number Four

$$\frac{13.4875S^6 - 30.7993S^5 + 40.4032S^4 - 36.9017S^3 + 21.2236S^2 - 7.5489S}{S^7 - 3.9270S^6 + 8.0953S^5 - 10.8076S^4 + 10.1338S^3 - 6.6348S^2 + 2.8015S - 0.6022}$$

ACTUATOR Number Five

$$\frac{8.5131S^6 + 3.9823S^5 - 9.4237S^4 - 4.2242S^3 + 0.93002S^2 - 0.1950S}{S^7 - 2.0359S^6 + 1.743S^5 - 0.4824S^4 + 0.0175S^3 - 0.2773S^2 + 0.2577S - 0.1089}$$

ACTUATOR Number Six

$$\frac{9.6768S^6 - 11.5692S^5 + 11.0591S^4 - 9.1858S^3 + 2.5227S^2 - 2.5671S}{S^7 - 2.7542S^6 + 4.5011S^5 - 4.7744S^4 + 3.6582S^3 - 1.9692S^2 + 0.6811S - 0.1253}$$

There is greater concurrence among actuators one, two, three and six. However, overall comparison of zeros, poles and transfer functions indicates that all six plants are very similar.

IV.   ACTUATOR COUPLING AND VIBRATION CONTROL APPLICATION

A.   ACTUATOR COUPLING

With the dynamic models constructed in Chapter Three it is now possible to model and investigate the interaction between actuators to see if indeed they can be controlled independently. The basic ARX method has been proved to be quite accurate in modeling the plant transfer function of each actuator. To determine the presence of actuator coupling each actuator was excited with 50mV pink noise and the output response of all six actuators measured. The input-output data gathered was introduced to the ARX[7 6 1] model and the resulting model frequency response was plotted. Figures 4.1 through 4.5 show the results from the excitation of actuator number one.
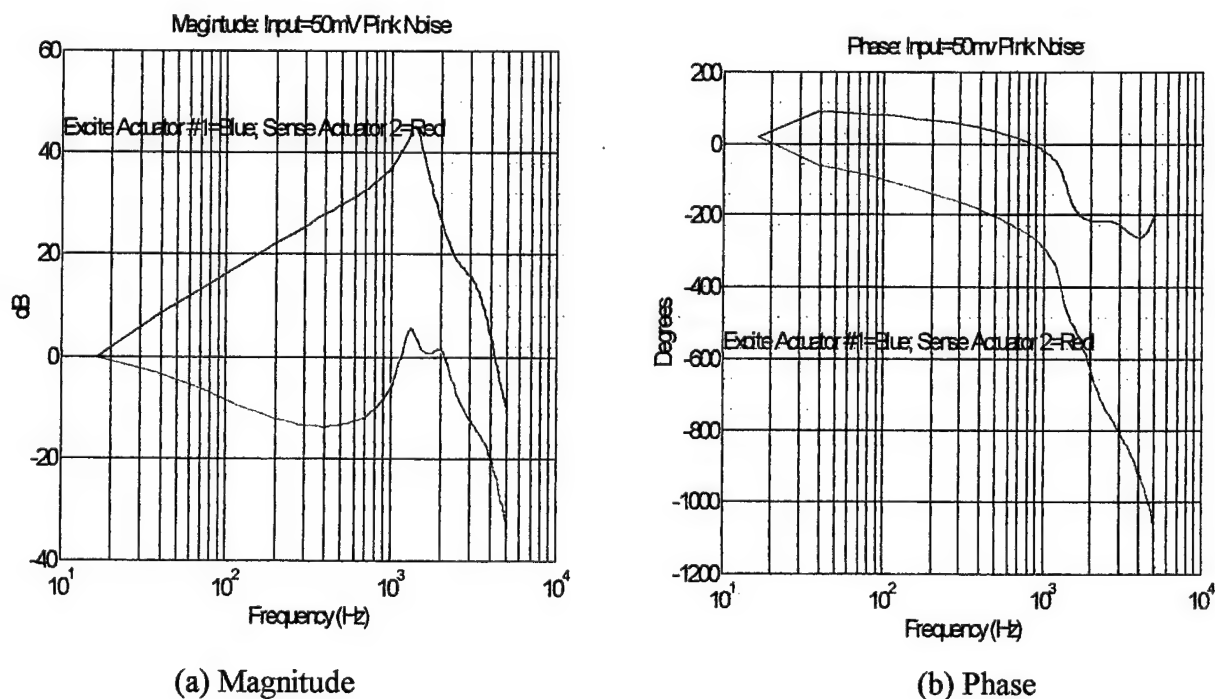
(a) Magnitude   (b) Phase

Figure 4.1
Frequency Response Actuator #1 Vs. Actuator #2
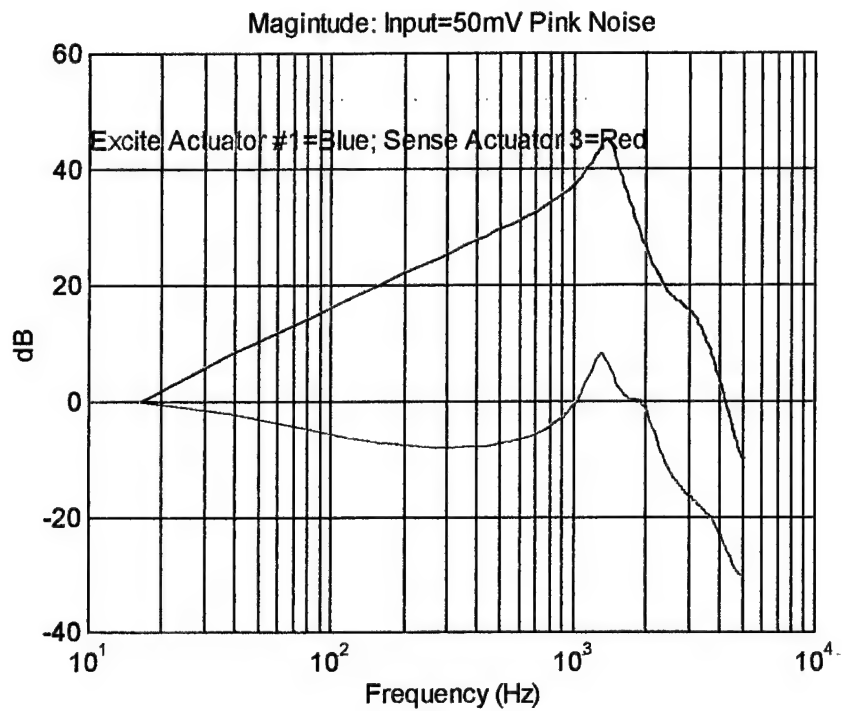
(a) Magnitude
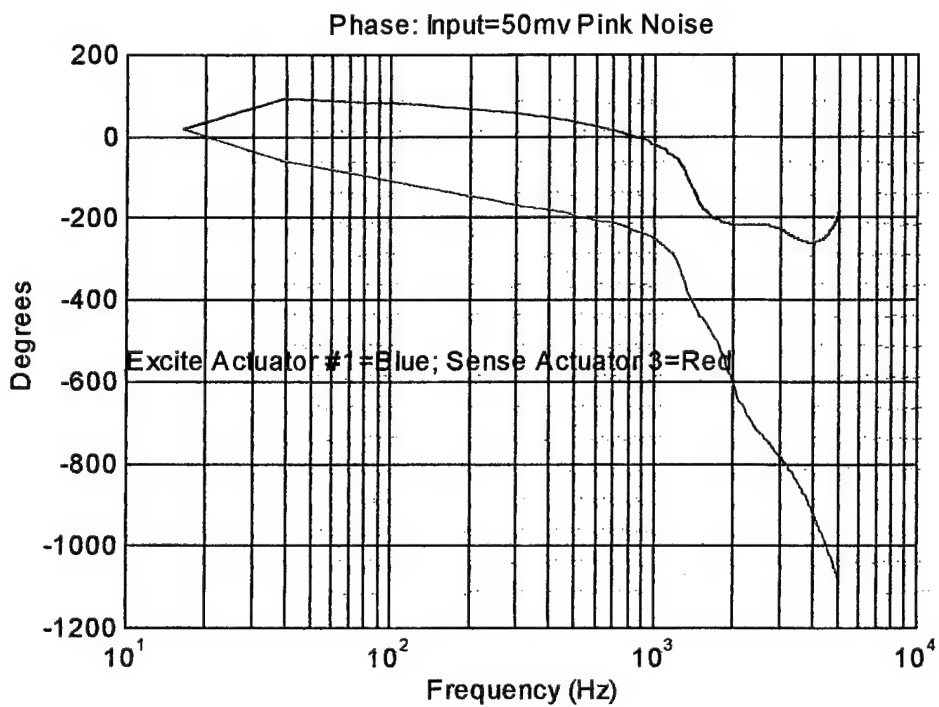
(b) Phase

Figure 4.2
Frequency Response Actuator #1 Vs. Actuator #3

72
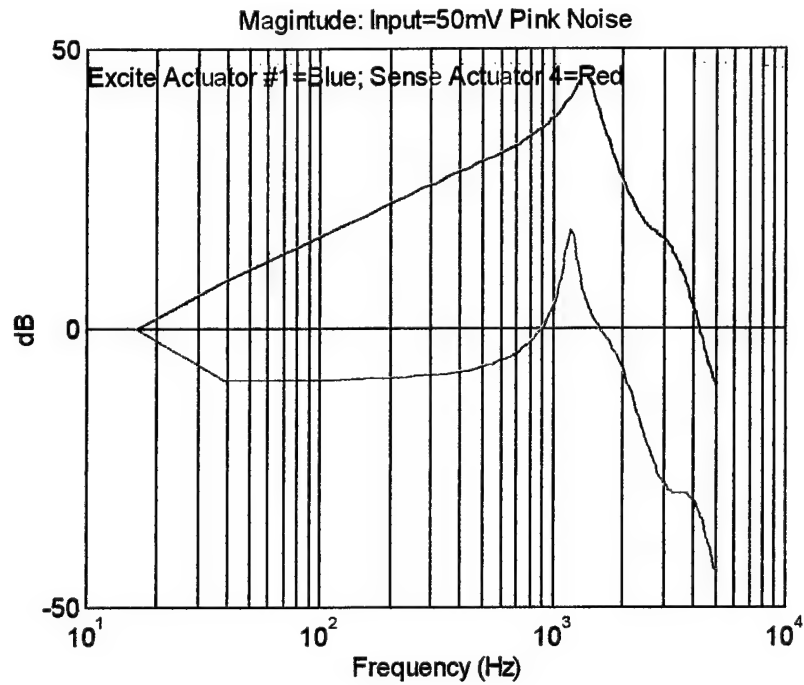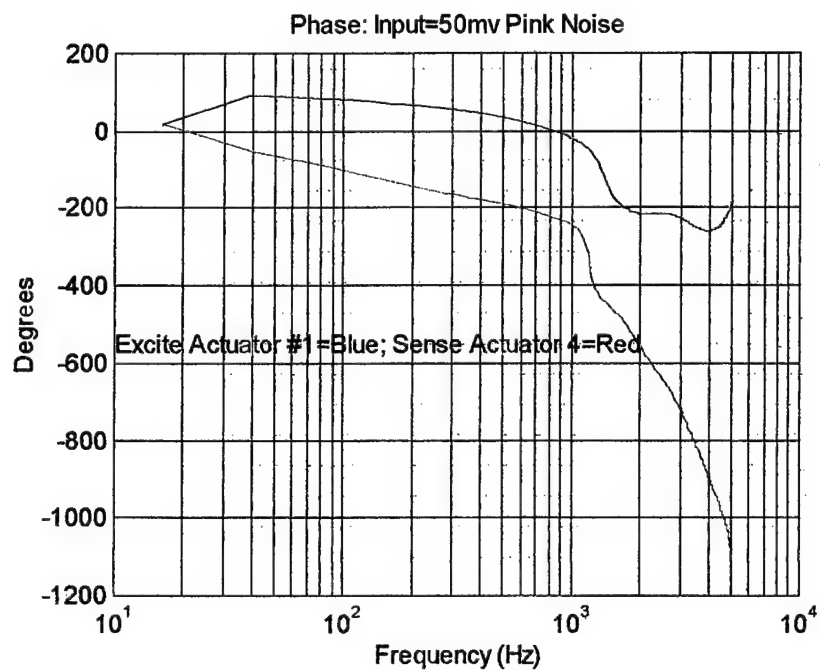
(a)Magnitude

(b) Phase

Figure 4.3
Frequency Response Actuator #1 Vs. Actuator #4

73
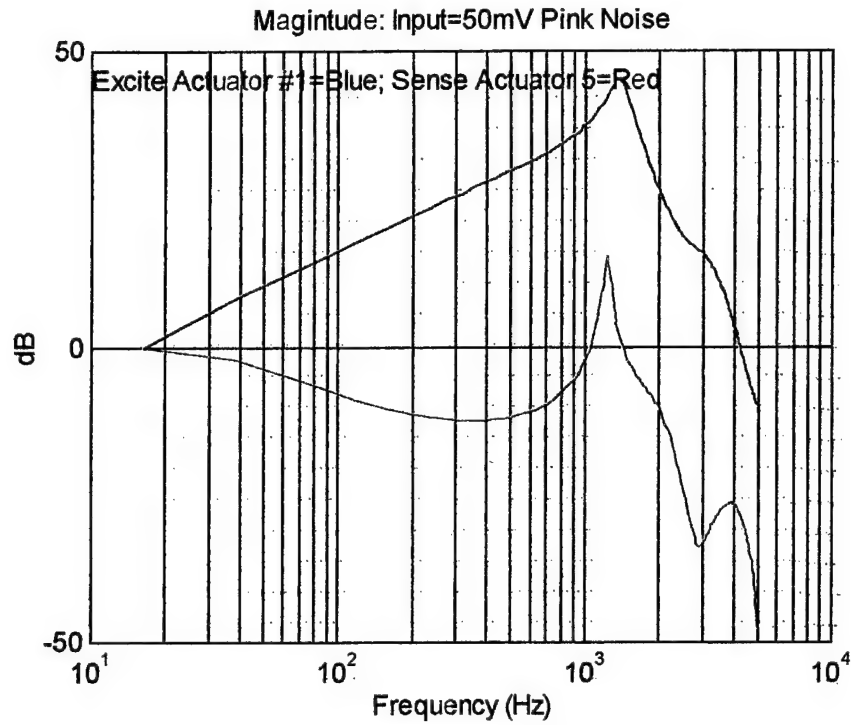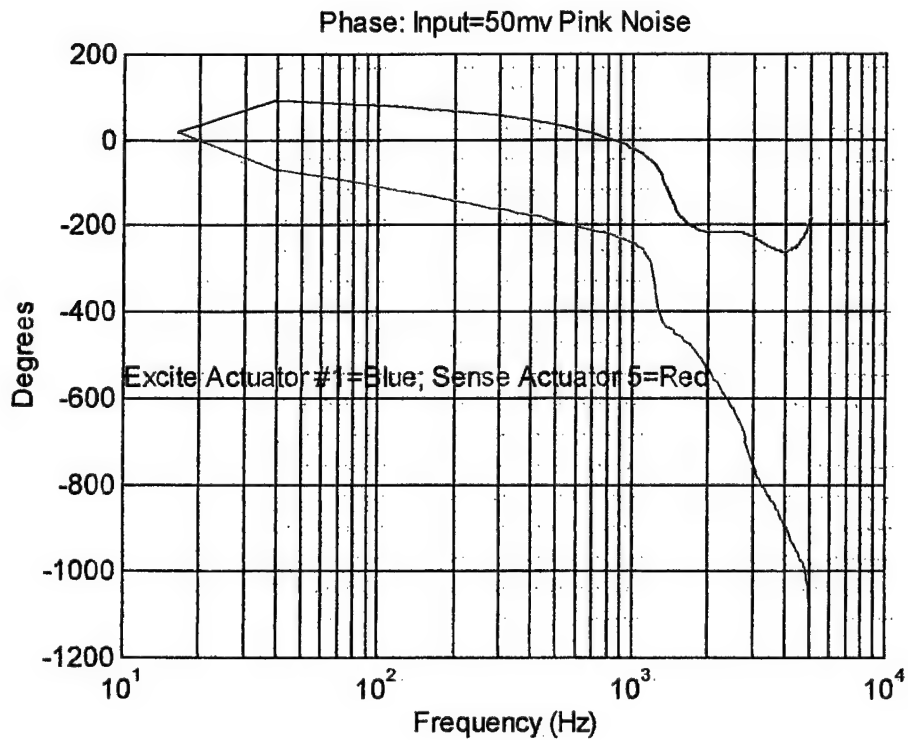
(a) Magnitude

(b) Phase

Figure 4.4
Frequency Response Actuator #1 Vs. Actuator #5

74
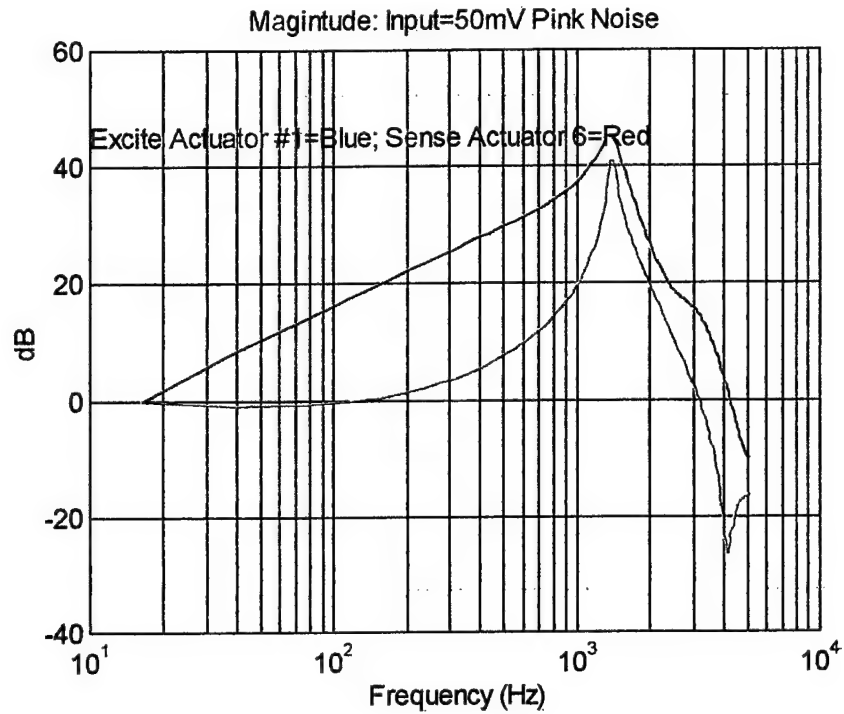
(a) Magnitude
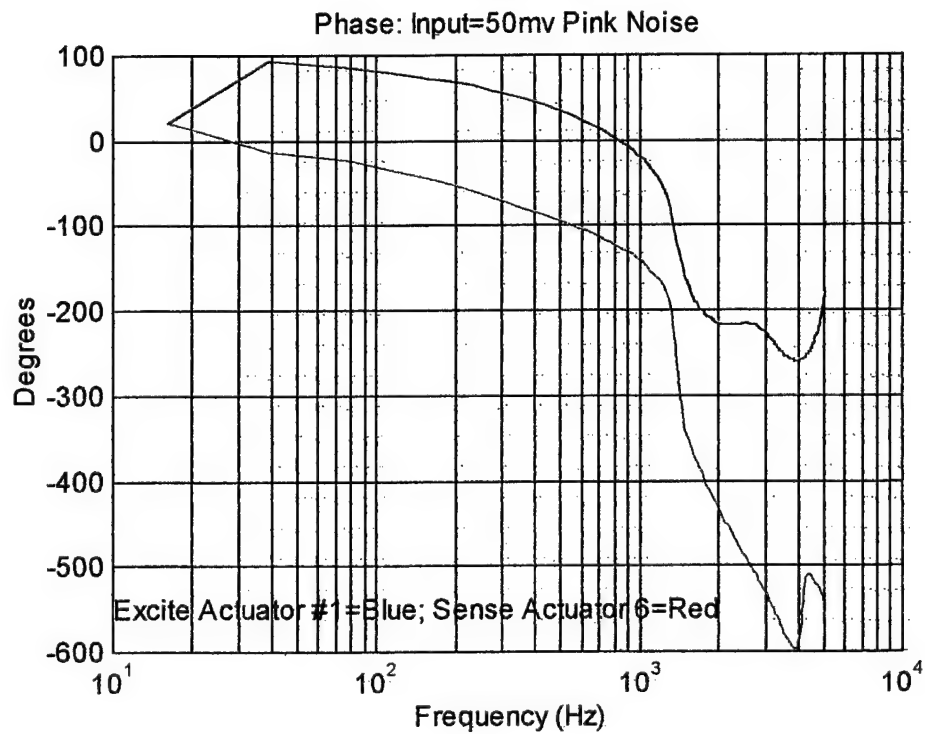
(b) Phase

Figure 4.5
Frequency Response Actuator #1 Vs. Actuator #6

75

In Figures 4.1 through 4.4 there is discernible correlation between the frequency response of actuator number one and the frequency response of actuators two through five to the excitation of actuator number one. Of particular interest is the response at the resonance frequency of 1.4 kHz. On average there is approximately a 10 dB difference at 1.4 kHz for these actuators. In the frequencies below 1kHz the response is in the negative dB range. This would indicate that the passive stage is performing well in eliminating the low frequency disturbances. Although coupling is present, it is relatively low in comparison to the response of actuator one. However this is not the case with actuator number six. As in actuators two through five the response below 1 k is small. Above 1kHz, particularly at 1.4 kHz the response is close to a mirror image of the response of actuator number one. This suggests that there is significant high frequency coupling

B.   CONTROL APPLICATION AND COUPLING VERIFICATION

Given the results of the previous section it is necessary to verify on the UQP. This was accomplished by applying a control law to the platform and checking for any evidence of coupling. The first evaluation conducted consisted of controlling an individual actuator and the second applied control to all six actuators simultaneously. There are numerous control candidates for use in AVC. For random broad band noise/vibrations, feedback control is preferable. Feed forward controllers are good candidates when a specific frequency of the disturbance is known. Local (decoupled) force feedback [Ref. 5], adaptive vibration control using two least mean square filters [Ref. 4], and absolute velocity feedback [Ref. 6] are examples that have been used in AVC. The latter of the three also used a geophone for sensing. The control law currently programmed for the system is a lead-lag compensator. This type of compensator is a variant of derivative and integral control. Lead compensation has the effect of lowering rise time and decreasing overshoot while lag compensation is used mainly to gain steady state accuracy of the system[Ref. 7]. A lead-lag controller was provided by CSA Engineering and was used to ensure the operation of each individual strut. This control

law was modified to apply the same lead-lag compensator to all six actuators simultaneously based on the initial assumption of independently controllable actuators. The results previously obtained indicate that this cannot be done.

1.   Compensator Transfer Function

A Bode Plot of the magnitude and phase of the compensator (See Figure 4.6) shows an infinite gain margin and a phase margin of approximately 60 degrees.
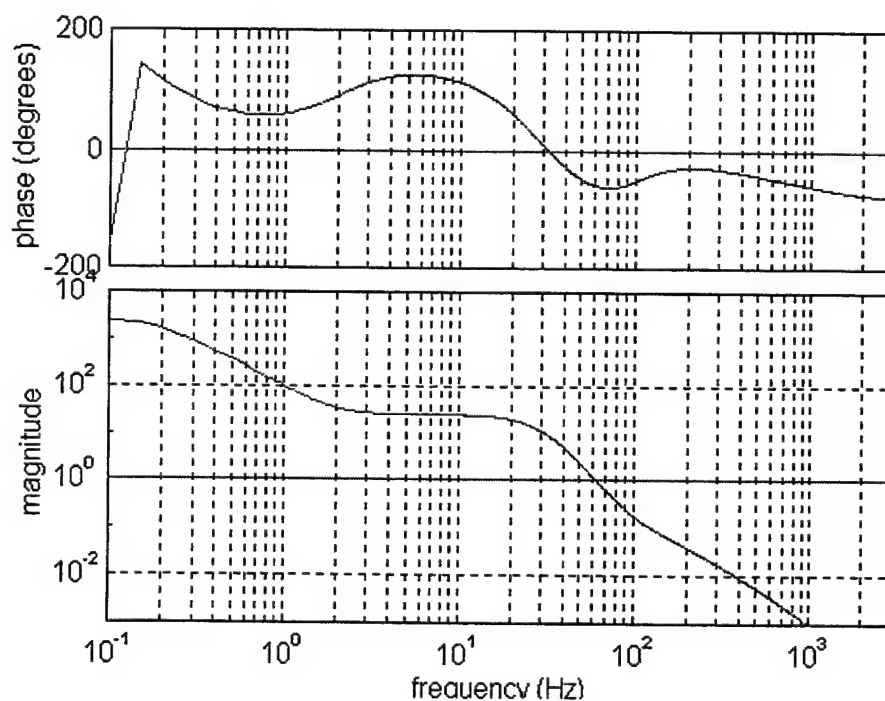

Figure 4.6
Compensator Bode Plot

77

A bode plot of the open loop tranfer function is provided in Figure 4.7.
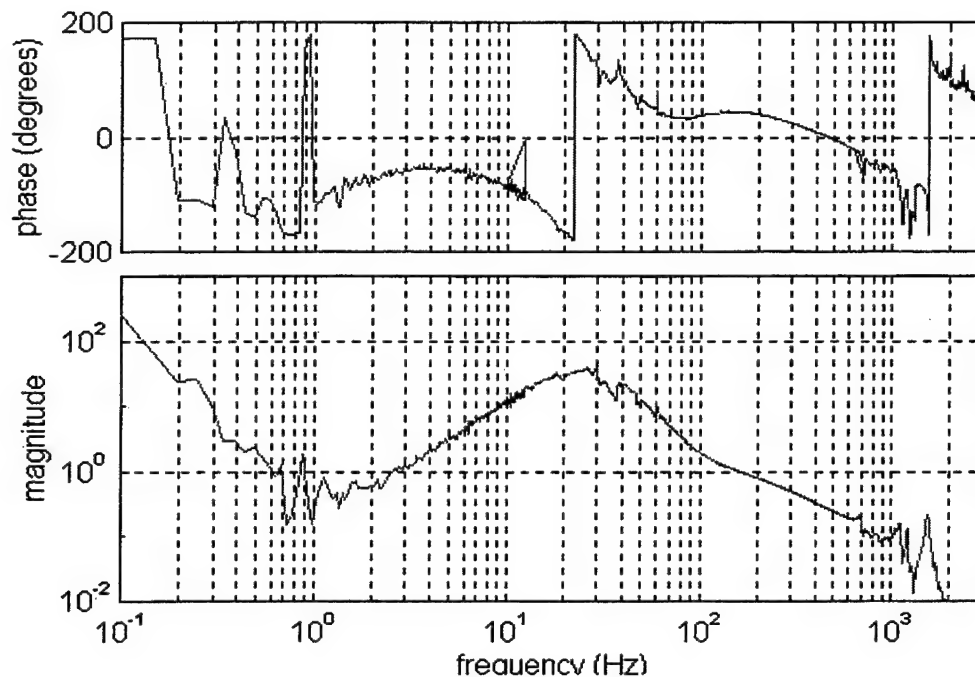
Figure 4.7
Open Loop Transfer Function (Compensator*Actuator)

Finally, a magnitude plot in terms of dB of closed to open loop is shown in Figure 4.8. From this plot it is observed that the best performance for this compensator will be between 12 Hz to 48 Hz with maximum reduction of 32dB at 25 Hz. A reduction of approximately 25 dB can be seen at 42 Hz. This controller was designed with an approximate bandwidth of 100 Hz. The spike at approximately 10 Hz is a faulty value resulting from system noise or an error in data collection.
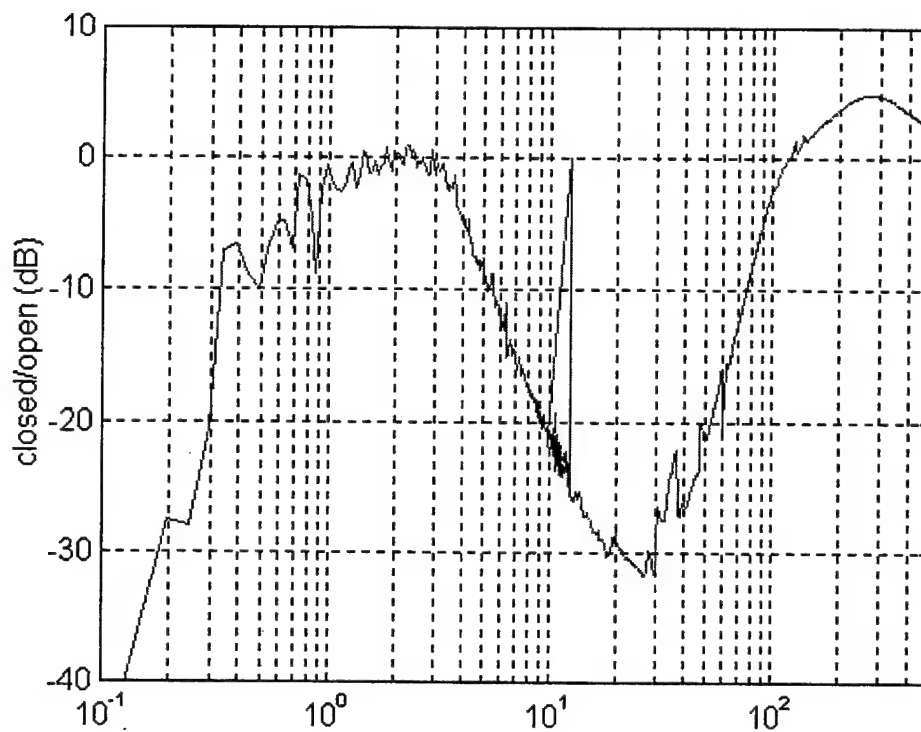
Figure 4.8

Closed Loop/Open Loop

2. Control Application

The controller described in section one was first applied to actuator number two and then the modified controller was applied to all six actuators simultaneously. Table 4.1 details the equipment preparation and settings.

Equipment	Setting	
HP 33120A Function Generator	Waveform	Sinusoid
	Frequency	42 Hz
	Amplitude	500mv peak-to-peak
KEPCO Bipolar Operational Power Supply/Amplifier	Current Control Mode	+/- 1 Amp

Table 4.1
Equipment Settings

3.   Experiment

The first task is to look at the platform in open loop mode. From this the local environment can be assessed. The plots in Figures 4.9 and 4.10 show what is sensed by the geophone on actuator two with the 42 Hz disturbance and no control (open loop).
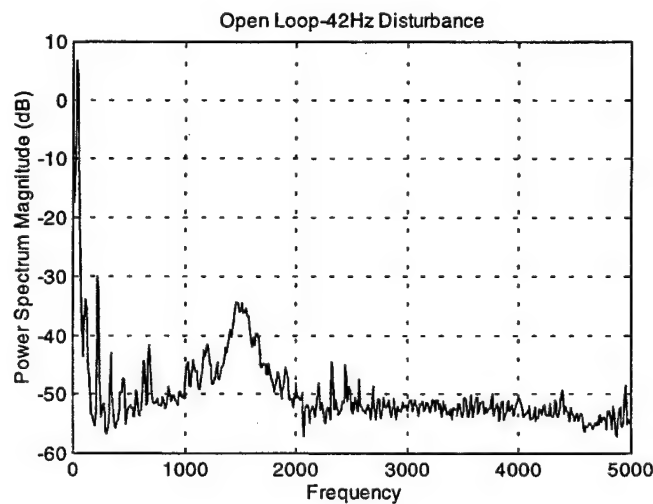
Figure 4.9
Ambient PSD (0-5kHz)
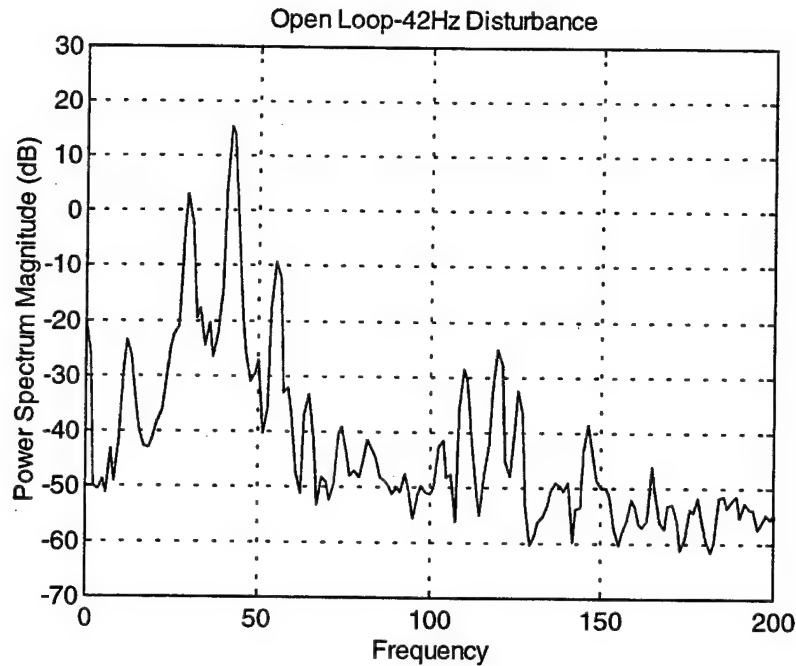
Figure 4.10
Ambient PSD (0-200Hz)

Of note in Figure 4.9 is the 1.4 kHz resonance frequency. This is the result of power being applied to the actuator from the HVPS. At approximately 30 Hz there is an environmental disturbance of unknown origin. In the open loop mode the 42Hz disturbance is clearly visible (see Figure 4.10). Figure 4.11 shows the power spectral density (PSD) of the sensor output for actuator number two for open and closed loop operations (both single and all six actuators). With only power applied to the piezoceramic actuator (no control), excitation of the resonance frequency is visible as the blue trace in Figure 4.11(a). Closing the control loop for single and multi-actuator control increases the excitation. Figure 4.12 shows the sensor output for actuators two, three, and six with control applied to actuator number two. Actuator number three shares the same base node with actuator number two. The coupling between actuators two and three can be seen in Figure 4.12(a). The application of control excites the resonance of all three actuators, but the interaction between actuators two and three is the most pronounced.

Blue-Open Loop; Magenta-Strut #2 Closed Loop; Red-All 6 Struts Closed Loop
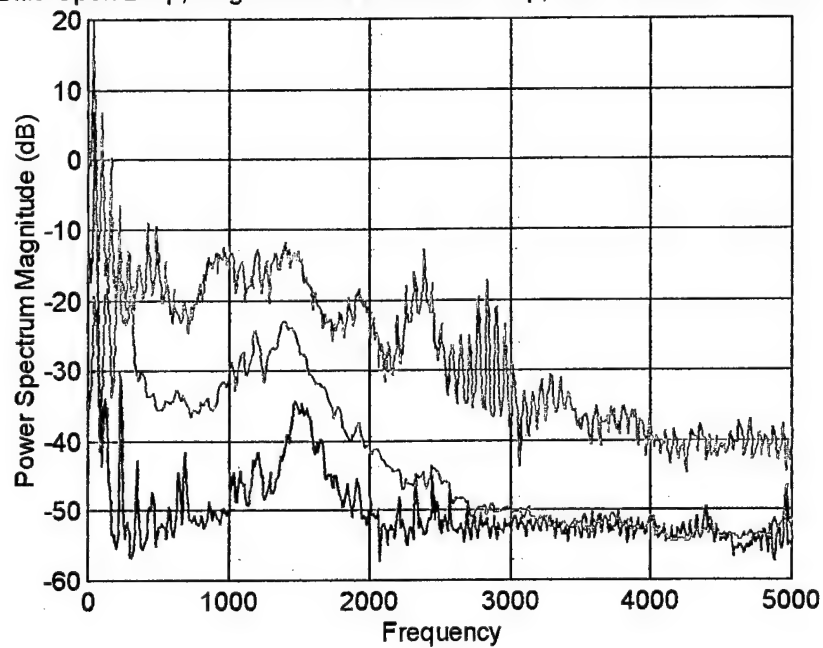
(a) PSD (0-5kHz) Sensed By Geophone on Actuator #2

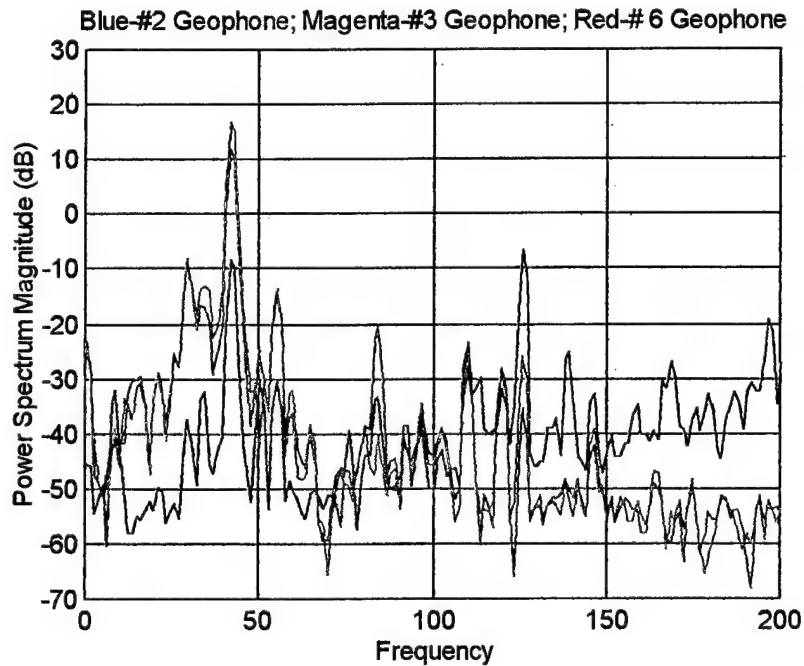Blue-Open Loop; Magenta-Strut #2 Closed Loop; Red-All 6 Struts Closed Loop
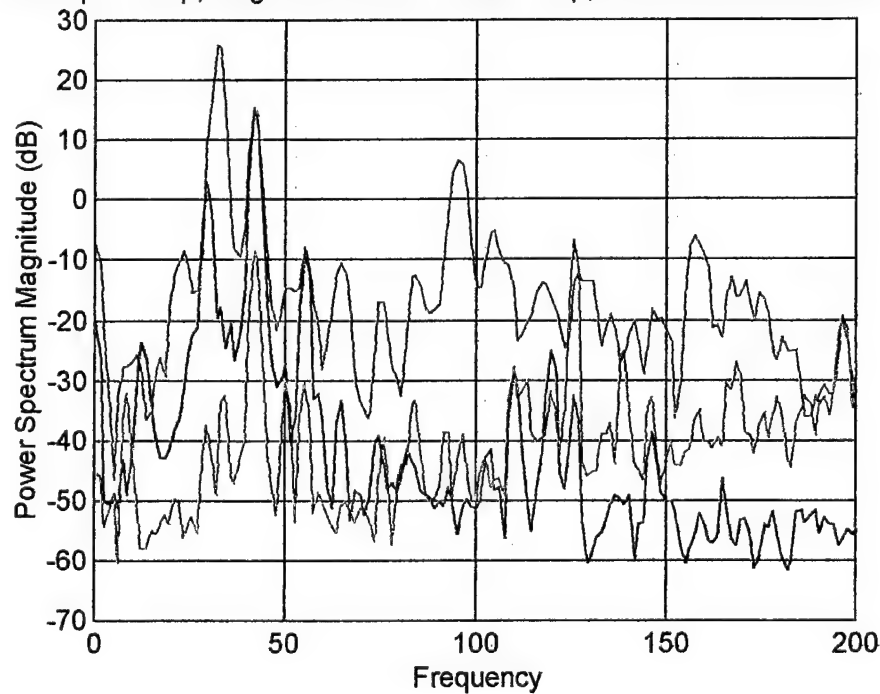
(b) PSD (0-200Hz) Sensed By Geophone on Actuator #2

Figure 4.11
Open Vs. Closed Loop Performance PSD

Blue-#2 Geophone; Magenta-#3 Geophone; Red-# 6 Geophone
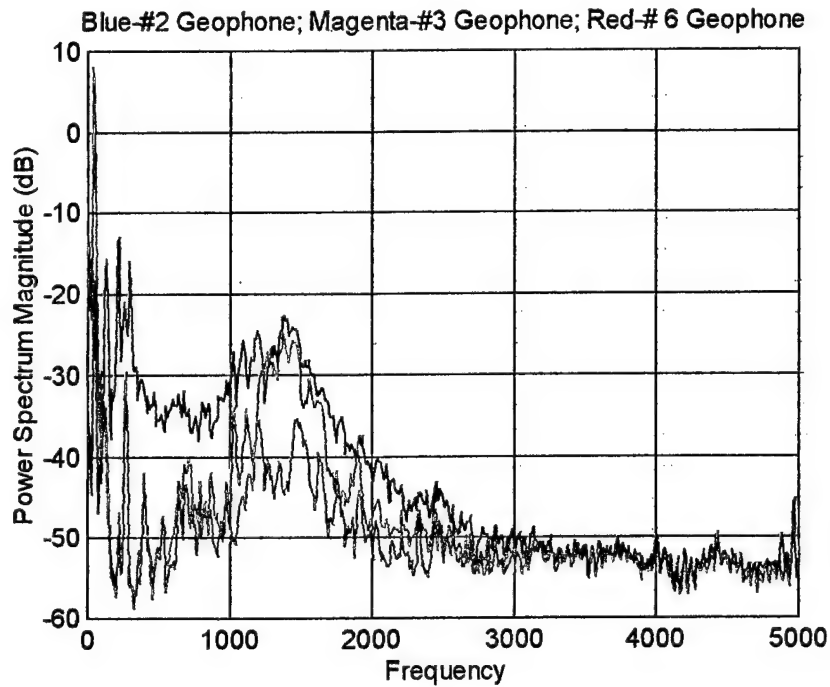
(a) PSD (0-5kHz) Sensor Outputs

Blue-#2 Geophone; Magenta-#3 Geophone; Red-# 6 Geophone

(b) PSD (0-200Hz) Sensor Outputs

Figure 4.12
Actuator #2 Closed Loop Performance PSD

V.   SUMMARY

A.   CONCLUSIONS

The process of system identification provided valuable insight into the UQP. By treating the UQP as a "Black Box" and using ready-made models the complex system dynamics were overcome and very accurate models of the system were developed. Some possible reasons for differences between the models and the actual system can be explained by non-removal of faulty values. Due to the number of samples used to build and validate the models, hand smoothing of the data was not practical. Based on the average residuals for each actuator being less than 4% of the average model output, outliers did not pose a significant problem. In comparing the validation data (numerical and graphical), actual frequency responses, and zeros, poles and transfer functions there are distinct similarities. The fact that all six are described by seven poles and six zeros was anticipated. However, some variation among actuators was expected. There is strong correlation of actuators one, two, three and six are. Although the numerical values for the zeros, poles and transfer function of actuators four and five did not correlate with the other actuators as strongly, they still retained the same pole-zero structure. Based on this it can be stated that for the purposes of characterizing the system and control design, all six actuators are identical.

The sensitivity of the geophones resulting in the introduction of external disturbances could be a source of inaccuracy, however, they are considered small in comparison to the disturbances generated by the other actuators. The emergence of ARX and ARMAX models as the most accurate models validates the assumption that these disturbances to the system entered the process early on. The disturbance created by the excitation of an actuator in turn causes excitation of other actuators, especially for actuators that share the same aluminum base in the region above 200 Hz. Since the disturbance is caused by another actuator, the choice of modeling the noise with the system dynamics (poles) was an accurate one. The interaction or coupling among

actuators, particularly between base adjoining actuators is distinct. Although the passive damping mechanism works well in eliminating low frequency interaction, high frequency disturbances are readily transmitted between actuators. For actuators not sharing a common base node this interaction is minimal and could possibly be ignored. However, for base node sharing elements this problem is significant.

The lead-lag compensator worked well for the single actuator in the 1Hz to 100Hz range, providing over 20dB damping of the 42Hz disturbance. However, above 200 Hz the controller exacerbates the disturbances. This problem is amplified in the case where all six actuators are controlled simultaneously. The interaction between actuators compounds the high frequency degraded performance of the controller. This causes it to go unstable. The high frequency interaction between base sharing nodes must be addressed before attempting to control all six actuators simultaneously.

B.   RECOMMENDATIONS FOR FUTURE WORK

With accurate plant models of the actuators the next logical step is control law design. With knowledge of the system it is possible to design controllers using either classical or modern techniques. The main concern in the design is the high frequency interaction in the range of 1kHz to 1.5 kHz. The revelation of actuator interaction does not necessarily mean that it is impossible to control each actuator independently. The dynamic compensator applied to an individual actuator worked well below 100Hz but did not roll off sufficiently. This resulted in high frequency instability in control of all six actuators. With knowledge of the plant transfer function it is possible to design a dynamic compensator capable of controlling each actuator independently. However, the design must be such that it does not excite the 1.4 kHz resonance. On the other hand, it may be necessary to treat the UQP as a multiple input/multiple output (MIMO) system and a modern control design is therefore required. Another possible remedy to the interaction between base node sharing elements is to change the material of the attachment node. The use of aluminum acts as an excellent conductor of vibration from one actuator to another. By using vibration absorbing material such as high stiffness rubber it may be possible to reduce the interaction sufficiently such that each actuator

could be controlled independently using single input/single output (SISO) classical design techniques. Replacing the upper node material could also reduce the overall transmission of unwanted vibration, not only from interaction but external sources as well.

APPENDIX A. COMPUTER PROGRAMS

All computer codes included in this thesis were written by Naval Postgraduate School Space Research and Design Center unless otherwise noted. The code included in this appendix is organized along lines of the thesis.

A. SYSTEM IDENTIFICATION AND MODEL CONSTRUCTION
```
% sysident.m : MAIN PROGRAM
% Written by:  George D. Beavers          June 1997
% This MATLAB ".m" file reads in the user requested actuator input output data
% from the "4h*.mat" files. "*" represents the actuator that is being excited by the
% 50mV "pink noise". It calls the user written functions
% "arxmod.m", "armaxmod.m" and "bjmod.m" to calculate models based on the
% ARX, ARMAX and Box-Jenkins parameter estimation methods respectively
% The zeros, poles and transfer functions are then extracted from the models
% returned by the user written functions.
% Each "4h*.mat" file has 7 rows of data
%        rows 1-6 = geophone output from the respective actuator (row1=actuator #1)
%        row 7 is the 50mv "pink noise" input
% Information on the MATLAB SITB functions can be found in reference[12]


clear
dum='y';
while (dum=='y'),
j=input('Enter strut number >> ');
disp(['load 4h' int2str(j)])
eval(['load ' '4h' int2str(j) ])            %Load input output data %
z2=[trace_y(j,1:10000)' trace_y(7,1:10000)'];    %Pull out requested channel %
z2=dtrend(z2);                              %Remove trends & adjust levels%
z3=[trace_y(j,10001:20000)' trace_y(7,10001:20000)'];
z3=dtrend(z3);

disp(['Choose Structure Selection Method'])
disp(['1==Automatic'])                      % Use algorithm to determine %
disp(['2==Manual'])                         %[na, nb, nk] or input them    %
temp=input('>>> ');                         % manually                     %

disp(['Choose a Parametric Estimation Model'])
disp(['arx   =1';   'armax =2';   'bj    =3'])
chc=input('>>> ')

% The following subroutine is used to determine input delay and number of parameters%
% and structure na,nb based on that delay for an ARX based model%
if temp==1
        V=arxstruct(z2,z3,struc(2,2,1:5));
```

89

```
[nn,Vm]=selstruc(V,'AIC')
inp=input('enter delay')
V=arxstruct(z2,z3,struc(1:15,1:15,inp));
nnA=selstruct(V,'AIC')
nnM=selstruct(V,'MDL')
Figure(1)
nns=selstruct(V)                              % Generate parameter Vs. Loss fcn%
                                              % plot                            %
% Determine which model to construct then call the function%
% Using the automatically generated ARX based Structure   %
if chc==1
        arxmod(j,nns,z2,z3);
elseif chc==2
        nc=input('Enter Order of Noise model nc >>');
        itr=input('Enter Maximum Number of Iterations >>');
        narm=[nns(1,1) nns(1,2) nc nns(1,3)];
        armaxmod(j,narm,itr,z2,z3)
else
        on=input('Enter Order of Noise model [nc nd] >>')
        itr=input('Enter Maximum Number of Iterations >>')
        nbj=[nns(1,2) on nns(1,1) nns(1,3)]
        bjmod(j,nbj,itr,z2,z3)
end


% Generate models based on manually entered structure %
else

    if chc==1
            nns=input('Enter Structure [na nb nk] >>');
            [arxm,arxmft]=arxmod1(j,nns,z2,z3);
            [zepo1,k1]=th2zp(arxm)            % Extracts zeros-poles
            [num1,den1]=th2tf(arxm)           % Extracts transfer function
            [zepo1f,k1f]=th2zp(arxmft)  % Extracts zeros-poles (filtered data)
            [num1f,den1f]=th2tf(arxmft)  % Extracts tranfer function(filtered data)
            present(arxm)                     % Extracts parameters
            present(arxmft)                   % Extracts parameters(filtered data)
    elseif chc==2
            narm=input('Enter Structure [na nb nc nk] >>');
            itr=input('Enter Maximum Number of Iterations >>')
            [armxm,armxmft]=armaxmdf(j,narm,itr,z2,z3);
            [zepo2,k2]=th2zp(armxm)     % Extracts zeros-poles
            [num2,den2]=th2tf(armxm)    % Extracts tranfer function
            [zepo2f,k2f]=th2zp(armxmft) % Extracts zeros-poles (filtered data)
            [num2f,den2f]=th2tf(armxmft) % Extracts tranfer function(filtered data)
            present(armxm)                    % Extracts parameters
```

90

```
                present(armxmft)              % Extracts parameters(filtered data)
        else
                nbj=input('Enter Structure [nb nc nd nf nk] >>')
                itr=input('Enter Maximum Number of Iterations >>')
                [bjm,bjmft]=bjmdf(j,nbj,itr,z2,z3);
        end
end

dum=input('Continue ?>> ','s');


end


%%%%%%%%%%%%%%%%%%%%%%%%%%%%%%%%%%%%%%%%%%%%%%%%%%
% arxmod.m                                                              %
%                    ARX Model Construction and Analysis                %
%                          George D. Beavers                            %
%                             June 1997                                 %
%%%%%%%%%%%%%%%%%%%%%%%%%%%%%%%%%%%%%%%%%%%%%%%%%%
% This program generates a model based on the input-output data of a system using   %
% the ARX parameter estimation method.  It also generated a series of graphical and %
% numerical results in order to evaluate the suitability of the model               %
%%%%%%%%%%%%%%%%%%%%%%%%%%%%%%%%%%%%%%%%%%%%%%%%%%

function [arxm,arxmft]=arxmod(j,nns,z2,z3)
%%%%%%%%%%%%%%%%%%%%%%%%%%%%%%
% arxm=ARX based model                          %
% arxmft=ARX based model (filtered data)        %
% j=actuator                                    %
% nns=structure([na nb nc])                     %
% z2=input-output data for model construction   %
% Z3=input-ouput data for model evaluation      %
%%%%%%%%%%%%%%%%%%%%%%%%%%%%%%

na=nns(1,1);
NA=int2str(na);
nb=nns(1,2);
NB=int2str(nb);
nk=nns(1,3);
NK=int2str(nk);


%****************ARX MODEL ************************
arxm=arx(z2,nns);
arxm=sett(arxm,0.1e-3);              % Set sample interval %
garxm=th2ff(arxm);                   % Convert to frequency function%
```

91

% This section loads separate data to compute the actual actuator frequency response%
% and then plot it against the model's frequency response   %
Figure(2)

eval(['load s',int2str(j),'m'])   %
X1=o2i1x;
Y1=20.*log10(abs(o2i1));

semilogx(X1,Y1,'b'),
hold on
semilogx(garxm(:,1)/(2*pi),20*log10(garxm(:,2)),'r');
title(['Blue=Actuator#',num2str(j),'Red=ARX MODEL[',NA,' ',NB,' ',NK,']'])
xlabel('Frequency (Hz)')
ylabel('Magnitude(dB)')
grid
hold off

Figure(3)

eval(['load s',int2str(j),'p'])
X2=o2i1x;
Y2=180*unwrap(angle(o2i1))/pi;

semilogx(X2,Y2,'b')
hold on
semilogx(garxm(:,1)/(2*pi),(garxm(:,4)),'r');
title(['Blue=Actuator#',num2str(j),', Red=ARX MODEL[',NA,' ',NB,' ',NK,']'])
xlabel('Frequency (Hz)')
ylabel('Phase (Deg)')
grid
hold off

%*****************ARX MODEL (DATA PREFILTERED)*****************%
% The above process is repeated using prefiltered data. A 10th order Butterworth filter %
% is used. The passband is given in terms of fractions of the Nyquist frequency (0.52)%
% This is a low pass filter with an upper bound of approximately 1.5kHz
%
zf=idfilt(z2,10,.52);   %Prefilter model construction data%

arxmft=arx(zf,nns);
arxmft=sett(arxmft,0.1e-3);
garxmft=th2ff(arxmft);

eval(['load s',int2str(j),'m'])
X1=o2i1x;

92

```
Y1=20.*log10(abs(o2i1));

Figure(4)

semilogx(X1,Y1,'b')
hold on
semilogx(garxmft(:,1)/(2*pi),20*log10(garxmft(:,2)),'r');
title(['Blue=Actuator#',num2str(j),', Red=ARX MODEL[',NA,' ',NB,' ',NK,'] *Data
Prefiltered*'])
xlabel('Frequency (Hz)')
ylabel('Magnitude(dB)')
grid
hold off

Figure(5)

eval(['load s',int2str(j),'p'])
X2=o2i1x;
Y2=180*unwrap(angle(o2i1))/pi;
semilogx(X2,Y2,'b')

hold on
semilogx(garxmft(:,1)/(2*pi),(garxmft(:,4)),'r');
title(['Blue=Actuator#',num2str(j),', Red=ARX MODEL[',NA,' ',NB,' ',NK,'] *Data
Prefiltered*'])
xlabel('Frequency (Hz)')
ylabel('Phase (Deg)')
grid
hold off
%*****************GRAPHICAL AND NUMERICAL ANALYSIS***********%
%  This section generates plots and numerical results used in evaluating the model %
Figure(6)
%  Apply the input row of the validation data to the model and then compare with      %
%  the actual output of the system corresponding to the validation data and plot results%
[yh,fit]=compare(z3,arxm);
axis([5000,5100,-1.0,1.0])
title(['Plot of ARX MODEL [',NA,' ',NB,' ',NK,'] Output vs. Actual output'])
text(5020,0.75,'Red=Model Output, Blue= Measured Output')
xlabel('Sample')
ylabel('Output Magnitude')
Figure(7)

[yhf,fitf]=compare(zfv,arxmft);                 %Prefiltered data%
title(['Plot of ARX MODEL [',NA,' ',NB,' ',NK,'] Output vs. Actual output *Data
Prefiltered*'])
```

```
axis([5000,5100,-1.0,1.0])
text(5020,0.75,'Red=Model Output, Blue= Measured Output')
xlabel('Sample')
ylabel('Output Magnitude')


%  Calculate the residuals and plot the auto and cross correlation functions %
Figure(8)
e1=resid(z3,arxm);              %  Non-filtered data
Figure(9)
e2=resid(zfv,arxmft);           %  Prefiltered data


%  Plot the residuals  %
Figure(10)
plot(e1,'m'),grid
title(['Residual of ARX Model [',NA,' ',NB,' ',NK,']'])
ylabel('Residual')
xlabel('Sample')
axis([5000,5100,-0.1,0.1])
Figure(11)
plot(e2,'m'),grid
title(['Residual of ARX Model [',NA,' ',NB,' ',NK,'] *Data Prefiltered*'])
axis([5000,5100,-0.05,0.05])
xlabel('Sample')
ylabel('Residual')


%  Calculate Numerical Results%
e1pos=abs(e1);
e2pos=abs(e2);
ypos=abs(z3(:,1));
ave=mean(e1pos)              %  Average residual
aveft=mean(e2pos)            %  Average residual
outave=mean(ypos)           %  Average actual output
fit                         %Mean Square Fit calculated above
fitf                        %Mean Square Fit calculated above
% Calculate and plot the actual output-model output
z3out=z3(:,1);
for i=5000:5100;
  difft(i)=z3out(i)-yhf(i);
end
z3out=z3(:,1);
for j=5000:5100;
  diff(j)=z3out(j)-yh(j);
end
Figure(14)
plot(diff,'r')
```

```
axis([5000,5100,-0.5,0.5])
title(['Actual Output - ARX Model [',NA,' ',NB,' ',NK,'] Model'])
xlabel('Sample')
Figure(15)
plot(difft,'r')
axis([5000,5100,-0.5,0.5])
title(['Actual Output - ARX Model [',NA,' ',NB,' ',NK,'] Model *Data Prefiltered*'])
xlabel('Sample')
avediff=mean(abs(diff))        %Ave. difference between actual and model outputs
avedft=mean(abs(difft))        % Ave. difference between actual and model outputs (filter)


%  Generate Zero-Pole plots
Figure(12)
zpplot1(th2zp(arxm),3,[],1.2)
title(['Zero Pole Plot ARX Model [',NA,' ',NB,' ',NK,'] Model'])
Figure(13)
zpplot1(th2zp(arxmft),3,[],1.2)
title(['Zero Pole Plot ARX Model [',NA,' ',NB,' ',NK,'] Model *Data Prefiltered*'])



%%%%%%%%%%%%%%%%%%%%%%%%%%%%%%%%%%%%%%%%%%%
% armaxmod.m                                               %
%            ARMAX Model Construction and Analysis         %
%                   George D. Beavers                      %
%                      June 1997                           %
%%%%%%%%%%%%%%%%%%%%%%%%%%%%%%%%%%%%%%%%%%%
% This program generates a model based on the input-output data of a system using   %
% the ARMAX parameter estimation method.  It also generated a series of graphical   %
% and numerical results in order to evaluate the suitability of the model           %
%%%%%%%%%%%%%%%%%%%%%%%%%%%%%%%%%%%%%%%%%%%


function [arxm,arxmft]=armaxmod(j,nns,itr,z2,z3)
%%%%%%%%%%%%%%%%%%%%%%%%%%%%%%%
%  arxm=ARMAX based model                    %
%  arxmft=ARMAX based model (filtered data)  %
%  j=actuator                                %
%  nns=structure([na nb nc])                 %
%  z2=input-output data for model construction %
%  Z3=input-ouput data for model evaluation  %
%%%%%%%%%%%%%%%%%%%%%%%%%%%%%%%


na=nns(1,1);
NA=int2str(na);
nb=nns(1,2);
NB=int2str(nb);
```

```
nc=nns(1,3);
NC=int2str(nc);
nk=nns(1,4);
NK=int2str(nk);
```

```
%****************ARMAX MODEL *********************************%
% This section loads separate data to compute the actual actuator frequency response%
% and then plot it against the model's frequency response                           %
```

```
arxm=armax(z2,nns,itr);
arxm=sett(arxm,0.1e-3);              % Set sampling interval        %
garxm=th2ff(arxm);                   % Convert to frequency function%
```

```
eval(['load s',int2str(j),'m'])      % Load actual actuator data (magnitude)%
X1=o2i1x;
Y1=20.*log10(abs(o2i1));
Figure(2)
semilogx(X1,Y1,'b'),
hold on
semilogx(garxm(:,1)/(2*pi),20*log10(garxm(:,2)),'r');
title(['Blue=Actuator#',num2str(j),'Red=ARMAX MODEL[',NA,' ',NB,' ',NC,' ',NK,']'])
xlabel('Frequency (Hz)')
ylabel('Magnitude(dB)')
grid
hold off
```

```
eval(['load s',int2str(j),'p'])      % Load actual actuator data (phase)%
X2=o2i1x;
Y2=180*unwrap(angle(o2i1))/pi;
Figure(3)
semilogx(X2,Y2,'b')
hold on
semilogx(garxm(:,1)/(2*pi),(garxm(:,4)),'r');
title(['Blue=Actuator#',num2str(j),'Red=ARMAX MODEL[',NA,' ',NB,' ',NC,' ',NK,']'])
xlabel('Frequency (Hz)')
ylabel('Phase (Deg)')
grid
hold off
```

```
%*************ARMAX MODEL (DATA PREFILTERED********************%
% The above process is repeated using prefiltered data.  A 10th order Butterworth filter %
% is used.  The passband is given in terms of fractions of the Nyquist frequency  (0.52)%
```

```
%  This is a low pass filter with an upper bound of approximately 1.5kHz
%
zf=idfilt(z2,10,.52);                % Prefilter model construction data %
arxmft=armax(zf,nns,itr);
arxmft=sett(arxmft,0.1e-3);
garxmft=th2ff(arxmft);

eval(['load s',int2str(j),'m'])
X1=o2i1x;
Y1=20.*log10(abs(o2i1));

Figure(4)
semilogx(X1,Y1,'m')
hold on
semilogx(garxmft(:,1)/(2*pi),20*log10(garxmft(:,2)),'g');
title(['Blue=Actuator#',num2str(j),'Red=ARMAX MODEL[',NA,' ',NB,' ',NC,' ',NK,']
*Data Prefiltered*'])
xlabel('Frequency (Hz)')
ylabel('Magnitude(dB)')
grid
hold off

eval(['load s',int2str(j),'p'])
X2=o2i1x;
Y2=180*unwrap(angle(o2i1))/pi;

Figure(5)
semilogx(X2,Y2,'b')
hold on
semilogx(garxmft(:,1)/(2*pi),(garxmft(:,4)),'r');
title(['Blue=Actuator#',num2str(j),'Red=ARMAX MODEL[',NA,' ',NB,' ',NC,' ',NK,']
*Data Prefiltered*'])
xlabel('Frequency (Hz)')
ylabel('Phase (Deg)')
grid
hold off

%*****************GRAPHICAL AND NUMERICAL ANALYSIS***********%
%  This section generates plots and numerical results used in evaluating the model     %
%  Apply the input row of the validation data to the model and then compare with       %
%  the actual output of the system corresponding to the validation data and plot results
%
Figure(6)
[yh,fit]=compare1(z3,arxm);
axis([5000,5100,-1.0,1.0])
```

```
title(['Plot of ARMAX MODEL[',NA,' ',NB,' ',NC,' ',NK,'] Output vs. Actual output'])
text(5020,0.75,'Red:Model Output, Green: Measured Output')
grid
Figure(7)
[yhf,fitf]=compare1(zfv,arxmft);
title(['Plot of ARMAX MODEL[',NA,' ',NB,' ',NC,' ',NK,'] Output vs. Actual output
*Data Prefiltered*'])
axis([5000,5100,-1.0,1.0])
xlabel('Sample')
grid


%  Calculate residuals and generate and plot auto & cross correlation functions %
Figure(8)
e1=resid1(z3,arxm);
Figure(9)
e2=resid1(zfv,arxmft);


%  Plot Residuals   %
Figure(10)
plot(e1,'m'),grid
title(['Residual of ARMAX MODEL[',NA,' ',NB,' ',NC,' ',NK,']'])
ylabel('Residual')
axis([5000,5100,-0.1,0.1])
Figure(11)
plot(e2,'m'),grid
title(['Residual of ARMAX MODEL[',NA,' ',NB,' ',NC,' ',NK,'] *Data Prefiltered*'])
axis([5000,5100,-0.05,0.05])
xlabel('Sample')
ylabel('Residual')


%  Calculate Numerical Results%
e1pos=abs(e1);
e2pos=abs(e2);
ypos=abs(z3(:,1));
ave=mean(e1pos)          % Average residual
aveft=mean(e2pos)        % Average residual (Prefiltered)
outave=mean(ypos)        % Average actual output

fit                      % Mean Square Fit calculated above
fitf                     % Mean Square Fit (Prefiltered)


%  Calculate actual output minus model output an plot results %

z3out=z3(:,1);
for i=5000:5100;
```

98

```
    difft(i)=z3out(i)-yhf(i);
end
z3out=z3(:,1);
for j=5000:5100;
   diff(j)=z3out(j)-yh(j);
end
Figure(14)
 plot(diff,'r')
axis([5000,5100,-0.5,0.5])
title(['Actual Output - ARMAX[',NA,' ',NB,' ',NC,' ',NK,'] Model Output'])
grid
Figure(15)
plot(difft,'r')
axis([5000,5100,-0.5,0.5])
title(['Actual Output - ARMAX[',NA,' ',NB,' ',NC,' ',NK,']Model Output *Data
Filtered*'])
grid
avediff=mean(abs(diff))                    % Ave. output difference
avedft=mean(abs(difft))                    % Ave. output difference (Prefiltered)


%  Generate Zero-Pole Plots
Figure(12)
zpplot(th2zp(arxm),3,[],1.2)
title(['Zero Pole Plot ARMAX MODEL[',NA,' ',NB,' ',NC,' ',NK,']'])
Figure(13)
zpplot(th2zp(arxmft),3,[],1.2)
title(['Zero Pole Plot ARMAX [',NA,' ',NB,' ',NC,' ',NK,'] Model *Data Prefiltered*'])


%%%%%%%%%%%%%%%%%%%%%%%%%%%%%%%%%%%%%%%%%%%%%
% bjmod.m                                                                                      %
%                 Box-Jenkins Model Construction and Analysis                %
%                            George D. Beavers                                           %
%                               June 1997                                                 %
%%%%%%%%%%%%%%%%%%%%%%%%%%%%%%%%%%%%%%%%%%%%%
% This program generates a model based on the input-output data of a system using    %
% the Box-Jenkins parameter estimation method.  It also generated a series of graphical%
% and numerical results in order to evaluate the suitability of the model                  %
%%%%%%%%%%%%%%%%%%%%%%%%%%%%%%%%%%%%%%%%%%%%%
function [bjm,bjmft]=bjmod(j,nns,itr,z2,z3)
%%%%%%%%%%%%%%%%%%%%%%%%%%%%%
%  bjm=Box-Jenkins based model                        %
%  bjmft=Box-Jenkins based model (filtered data)   %
%  j=actuator                                         %
%  nns=structure([na nb nc])                          %
%  itr=number of iterations                           %
```

```
%  z2=input-output data for model construction        %
%  Z3=input-ouput data for model evaluation           %
%%%%%%%%%%%%%%%%%%%%%%%%%%%%%%%%
nb=nns(1,1);
NB=int2str(nb);
nc=nns(1,2);
NC=int2str(nc);
nd=nns(1,3);
ND=int2str(nd);
nf=nns(1,4);
NF=int2str(nf);
nk=nns(1,5);
NK=int2str(nk);


%****************BOX-JENKINS MODEL*****************************%
%  This section loads separate data to compute the actual actuator frequency response  %
%  and then plot it against the model's frequency response                             %


arxm=bj(z2,nns,itr);              %Build the model              %
arxm=sett(arxm,0.1e-3);           % Set the sampling interval   %
garxm=th2ff(arxm);                % Convert to frequency function  %

eval(['load s',int2str(j),'m'])           %Load data for actuator frequency function%
X1=o2i1x;
Y1=20.*log10(abs(o2i1));
Figure(2)
semilogx(X1,Y1,'b'),
hold on
semilogx(garxm(:,1)/(2*pi),20*log10(garxm(:,2)),'r');
title(['Blue=Actuator#',num2str(j),'Red=Box-Jenkins MODEL[',NB,' ',NC,' ',ND,' ',NF,'
',NK,']'])
xlabel('Frequency (Hz)')
ylabel('Magnitude(dB)')
grid
hold off

eval(['load s',int2str(j),'p'])
X2=o2i1x;
Y2=180*unwrap(angle(o2i1))/pi;
Figure(3)
semilogx(X2,Y2,'b')
hold on
semilogx(garxm(:,1)/(2*pi),(garxm(:,4)),'r');
title(['Blue=Actuator#',num2str(j),'Red=Box-Jenkins MODEL[',NB,' ',NC,' ',ND,' ',NF,'
',NK,']'])
```

```
xlabel('Frequency (Hz)')
ylabel('Phase (Deg)')
grid
hold off


%*************BOX-JENKINS MODEL (DATA PREFILTERED*************%
% The above process is repeated using prefiltered data.  A 10th order Butterworth filter %
%  is used.  The passband is given in terms of fractions of the Nyquist frequency  (0.52)%
%  This is a low pass filter with an upper bound of approximately 1.5kHz                 %
zf=idfilt(z2,10,.52);                    % Prefilter model construction data  %
arxmft=bj(zf,nns,itr);                   % Construct model                    %
arxmft=sett(arxmft,0.1e-3);              % Set sampling interval              %
garxmft=th2ff(arxmft);                   % Convert to frequency function      %

eval(['load s',int2str(j),'m'])          % Load data for actuator frequency response
X1=o2i1x;
Y1=20.*log10(abs(o2i1));

Figure(4)
semilogx(X1,Y1,'b')
hold on
semilogx(garxmft(:,1)/(2*pi),20*log10(garxmft(:,2)),'r');
title(['Blue=Actuator#',num2str(j),'Red=Box-Jenkins MODEL[',NB,' ',NC,' ',ND,' ',NF,'
',NK,']*Data Prefiltered*'])
xlabel('Frequency (Hz)')
ylabel('Magnitude(dB)')
grid
hold off

eval(['load s',int2str(j),'p'])
X2=o2i1x;
Y2=180*unwrap(angle(o2i1))/pi;

Figure(5)
semilogx(X2,Y2,'m')
hold on
semilogx(garxmft(:,1)/(2*pi),(garxmft(:,4)),'g');
title(['Blue=Actuator#',num2str(j),'Red=Box-Jenkins MODEL[',NB,' ',NC,' ',ND,' ',NF,'
',NK,']*Data Prefiltered*'])
xlabel('Frequency (Hz)')
ylabel('Phase (Deg)')
grid
hold off
```

101

```
%******************GRAPHICAL AND NUMERICAL ANALYSIS***********%
% This section generates plots and numerical results used in evaluating the model   %
% Comparison of model output to actual output                                        %
% Apply the input row of the validation data to the model and then compare with     %
% the actual output of the system corresponding to the validation data and plot results
%


Figure(6)
[yh,fit]=compare(z3,arxm);
axis([5000,5100,-1.0,1.0])
title(['Plot of Box-Jenkins [',NB,' ',NC,' ',ND,' ',NF,' ',NK,'] Output vs. Actual output'])
text(5020,0.75,'Red:Model Output, Blue: Measured Output')
xlabel('Sample')


Figure(7)
[yhf,fitf]=compare(z3,arxmft);
title(['Plot of Box-Jenkins MODEL [',NB,' ',NC,' ',ND,' ',NF,' ',NK,'] Output vs. Actual
output *Data Prefiltered*'])
text(5020,0.75,'Red:Model Output, Blue: Measured Output')
axis([5000,5100,-1.0,1.0])
xlabel('Sample')


% Calculate residuals and auto and cross correlation functions and plot results

Figure(8)
e1=resid1(zfv,arxm);
Figure(9)
e2=resid1(zfv,arxmft);
Figure(10)
plot(e1,'m'),grid
title(['Residual of Box-Jenkins Model [',NB,' ',NC,' ',ND,' ',NF,' ',NK,']'])
ylabel('Residual')
xlabel('Sample')
axis([5000,5100,-0.1,0.1])
Figure(11)
plot(e2,'m'),grid
title(['Residual of Box-Jenkins Model [',NB,' ',NC,' ',ND,' ',NF,' ',NK,'] *Data
Prefiltered*'])
axis([5000,5100,-0.05,0.05])
xlabel('Sample')
ylabel('Residual')
```

```
% Numerical results
e1pos=abs(e1);
e2pos=abs(e2);
ypos=abs(z3(:,1));
ave=mean(e1pos)                    % Average residual
aveft=mean(e2pos)                  % Average residual (Prefiltered Data)
outave=mean(ypos)                  % Average actuator output
fit                                % Mean Square Fit calculated above
fitf                               % Mean Square Fit (Prefiltered)


% Calculate and plot actual output minus model output
z3out=z3(:,1);
for i=5000:5100;
  difft(i)=z3out(i)-yhf(i);
end
z3out=z3(:,1);
for j=5000:5100;
  diff(j)=z3out(j)-yh(j);
end
Figure(12)
plot(diff,'r')
axis([5000,5100,-0.5,0.5])
title('Actual Output - Model Output')
Figure(13)
plot(difft,'r')
axis([5000,5100,-0.5,0.5])
title('Actual Output - Model Output *Data Filtered*')
avediff=mean(abs(diff))                  % Average output difference
avedft=mean(abs(difft))                  % Average output difference(Prefiltered)


% Generate Zero-Pole Plot
Figure(14)
zpplot1(th2zp(arxm),3,[],1.2)
title(['Zero Pole Plot Box-Jenkins Model [',NB,' ',NC,' ',ND,' ',NF,' ',NK,'] '])
Figure(15)
zpplot1(th2zp(arxmft),3,[],1.2)
title(['Zero Pole Plot Box-Jenkins Model [',NB,' ',NC,' ',ND,' ',NF,' ',NK,'] *Data
Prefiltered*'])


%%%%%%%%%%%%%%%%%%%%%%%%%%%%%%%%%%%%%%%%%%%%
% plotarx.m                                                              %
%                    Compare Three ARX Model Structures                  %
%                            George D. Beavers                           %
%                               June 1997                                %
%%%%%%%%%%%%%%%%%%%%%%%%%%%%%%%%%%%%%%%%%%%%
```

```
% This program generates the frequency response plots of the three best ARX model   %
% structures for evaluation and structure selection                                  %
%%%%%%%%%%%%%%%%%%%%%%%%%%%%%%%%%%%%%%%%%%%%%%%%%%%


j=input('enter strut>>');

eval(['load 4h',int2str(j)])
eval(['load s',int2str(j),'m'])


z2=[trace_y(j,1:10000)' trace_y(7,1:10000)'];
z2=dtrend(z2);
z3=[trace_y(j,10001:20000)' trace_y(7,10001:20000)'];
z3=dtrend(z3);


nn1=[7 6 1]                          % Top three structures
nn2=[15 15 1]
nn3=[12 12 1]

X1=o2i1x;
Y1=20.*log10(abs(o2i1));


zf=idfilt(z2,10,.52);
%  Construct the models  %
fm1=arx(zf,nn1);
fm1=sett(fm1,0.1e-3);
gfm1=th2ff(fm1);


fm2=arx(zf,nn2);
fm2=sett(fm2,0.1e-3);
gfm2=th2ff(fm2);



fm3=arx(zf,nn3);
fm3=sett(fm3,0.1e-3);
gfm3=th2ff(fm3);


%  Generate comparison plots
Figure(1)
semilogx(X1,Y1,'b'),
title(['Strut #',int2str(j),' Magnitude'])
xlabel('Frequency (Hz)')
ylabel('Magnitude(dB)')
hold on
```

104

```
semilogx(gfm1(:,1)/(2*pi),20*log10(gfm1(:,2)),'r');
semilogx(gfm2(:,1)/(2*pi),20*log10(gfm2(:,2)),'m');
semilogx(gfm3(:,1)/(2*pi),20*log10(gfm3(:,2)),'w');,grid;
hold off


Figure(2);
eval(['load s',int2str(j),'p'])
X2=o2i1x;
Y2=180*unwrap(angle(o2i1))/pi;
semilogx(X2,Y2,'b'),
title(['Strut #',int2str(j),' Phase'])
xlabel('Frequency (Hz)');
ylabel('Deg');
hold on
semilogx(gfm1(:,1)/(2*pi),(gfm1(:,4)),'r');
semilogx(gfm2(:,1)/(2*pi),(gfm2(:,4)),'m');
semilogx(gfm3(:,1)/(2*pi),(gfm3(:,4)),'w');,grid;


hold off
%%%%%%%%%%%%%%%%%%%%%%%%%%%%%%%%%%%%%%%%%%%%
% plotamb.m                                                                %
%                           Model Comparison                              %
%                           George D. Beavers                             %
%                                June 1997                                %
%%%%%%%%%%%%%%%%%%%%%%%%%%%%%%%%%%%%%%%%%%%%
% This program generates the frequency response plots of the three best models based  %
% on the ARX structure[7 6 1].   ARX, ARMAX and BOX-JENKINS models are      %
% compared to select the best model                                       %
%%%%%%%%%%%%%%%%%%%%%%%%%%%%%%%%%%%%%%%%%%%%
j=input('enter strut>>');

eval(['load 4h',int2str(j)])
eval(['load s',int2str(j),'m'])


z2=[trace_y(j,1:10000)' trace_y(7,1:10000)'];
z2=dtrend(z2);
z3=[trace_y(j,10001:20000)' trace_y(7,10001:20000)'];
z3=dtrend(z3);

%  Define model structure  %
nn1=[7 6 2 1]
nn2=[7 6 1]
nn3=[6 2 2 7 1]


X1=o2i1x;
```

```
Y1=20.*log10(abs(o2i1));
%  Generate models (non-filtered)  %
%m1=armax(z2,nn1,60);
%m1=sett(m1,0.1e-3);
%gm1=th2ff(m1);
%m2=arx(z2,nn2);
%m2=sett(m2,0.1e-3);
%gm2=th2ff(m2);
%m3=bj(z2,nn3,60);
%m3=sett(m3,0.1e-3);
%gm3=th2ff(m3);


zf=idfilt(z2,10,.52);

%  Generate Models (Prefiltered)
fm1=armax(zf,nn1,60);
fm1=sett(fm1,0.1e-3);
gfm1=th2ff(fm1);

fm2=arx(zf,nn2);
fm2=sett(fm2,0.1e-3);
gfm2=th2ff(fm2);


fm3=bj(zf,nn3,60);
fm3=sett(fm3,0.1e-3);
gfm3=th2ff(fm3);

%  Generate plots
Figure(1)
semilogx(X1,Y1,'b')
title(['Strut #',int2str(j),' Magnitude'])
xlabel('Frequency (Hz)')
ylabel('Magnitude(dB)')
hold on
semilogx(gfm1(:,1)/(2*pi),20*log10(gfm1(:,2)),'r');
semilogx(gfm2(:,1)/(2*pi),20*log10(gfm2(:,2)),'m');
semilogx(gfm3(:,1)/(2*pi),20*log10(gfm3(:,2)),'w');,grid;
hold off

Figure(2);
eval(['load s',int2str(j),'p'])
X2=o2i1x;
Y2=180*unwrap(angle(o2i1))/pi;
```

```
semilogx(X2,Y2,'b')
title(['Strut #',int2str(j),' Phase'])
xlabel('Frequency (Hz)');
ylabel('Deg');
hold on
semilogx(gfm1(:,1)/(2*pi),(gfm1(:,4)),'r');
semilogx(gfm2(:,1)/(2*pi),(gfm2(:,4)),'m');
semilogx(gfm3(:,1)/(2*pi),(gfm3(:,4)),'w');,grid;

hold off
%%%%%%%%%%%%%%%%%%%%%%%%%%%%%%%%%%%%%%%%%%%%%%%%%%%%%%%%%
% compid.m                                                                          %
%                          Interaction Comparison                                   %
%                                June 1997                                          %
%%%%%%%%%%%%%%%%%%%%%%%%%%%%%%%%%%%%%%%%%%%%%%%%%%%%%%%%%
% This program generates the  frequency response plots of the actuators when actuator %
% number one is excited with 50mV "pink noise".  These plots use the ARX[7 6 1]      %
% model frequency repines of the respective actuator.  This is compared with the     %
% modeled response of actuator number one  These plots are used to check for         %
% interaction between actuators                                                      %
%%%%%%%%%%%%%%%%%%%%%%%%%%%%%%%%%%%%%%%%%%%%%%%%%%%%%%%%%


function []=compid(j)
% j= actuator number%
int2str(j)

disp(['load 4h' int2str(j)])
eval(['load ' '4h' int2str(j) '.mat'])


        z1=[trace_y(1,1:10000)' trace_y(7,1:10000)'];
        z1=dtrend(z1);
        z1a=[trace_y(1,10001:20000)' trace_y(7,10001:20000)'];
        z1a=dtrend(z1a);

        th1=arx(z1,[7 6 1]);
        th1=sett(th1,0.1e-3);
        gth1=th2ff(th1);



for i=2:6

        z2=[trace_y(i,1:10000)' trace_y(7,1:10000)'];
        z2=dtrend(z2);
        z7=[trace_y(i,10001:20000)' trace_y(7,10001:20000)'];
```

```
        z7=dtrend(z7);

        th=arx(z2,[7 6 1]);
        th=sett(th,0.1e-3);
        gth=th2ff(th);


        Figure(i-1);

        semilogx(gth1(:,1)/(2*pi),20*log10(gth1(:,2)),'b');
        hold on
        semilogx(gth(:,1)/(2*pi),20*log10(gth(:,2)),'r');
        title('Magnitude: Input=50mV Pink Noise')
        xlabel('Frequency (Hz)')
        ylabel('dB')
        text(10,45,['Excite Actuator #' num2str(j) 'Blue; Sense Actuator ',
num2str(i),'=Red'])
        grid
        hold off

end

for i=2:6
        z2=[trace_y(i,1:10000)' trace_y(7,1:10000)'];
        z2=dtrend(z2);
        z7=[trace_y(i,10001:20000)' trace_y(7,10001:20000)'];
        z7=dtrend(z7);

        th=arx(z2,[7 6 1]);
        th=sett(th,0.1e-3);
        gth=th2ff(th);

        Figure(i+4)
        semilogx(gth1(:,1)/(2*pi),(gth1(:,4)),'b');
        hold on
        semilogx(gth(:,1)/(2*pi),(gth(:,4)),'r');
        title('Phase: Input=50mv Pink Noise')
        text(10,-550,['Excite Actuator #' num2str(j) '=Blue; Sense Actuator ',num2str(i),
'=Red'])
        xlabel('Frequency (Hz)')
        ylabel('Degrees')
        grid
      hold off
```

end

```
%%%%%%%%%%%%%%%%%%%%%%%%%%%%%%%%%%%%%%%%%%%
% fig1.m, fig2.m, fig3.m, fig4.m                                              %
%                          PSD of Applied Controllers                         %
%                                  June 1997                                  %
%%%%%%%%%%%%%%%%%%%%%%%%%%%%%%%%%%%%%%%%%%%
% This program generates the power spectral density plots resulting from applying      %
% a lead-lag compensator to an individual actuator and the all six actuators to evaluate %
% the effects of actuator interaction                                          %
%%%%%%%%%%%%%%%%%%%%%%%%%%%%%%%%%%%%%%%%%%%
%fig1.m%
% Plots over range of 0-5kHz%
clear
load s1                      %Open loop data with 42 Hz disturbance on%
Figure(1)
clg
psd(trace_y(2,1:20000),1024*1,10000,[]);
%[popen,fopen]=psd(trace_y(2,1:20000),1024*12,10000,[]);
hold on
load s2                      %Compensator applied to actuator #2 (
psd(trace_y(2,1:20000),1024*1,10000,kaiser(512,5),256);
%[ps2,fs2]=psd(trace_y(2,1:20000),1024*12,10000,[]);
load s3                      %Compensator applied to all six actuators
psd(trace_y(2,1:20000),1024*1,10000,[]);
%[ps3,fs3]=psd(trace_y(2,1:20000),1024*12,10000,[]);
hold off
%semilogx((fopenk),20*log10(popenk),'r',(fs2k),20*log10(fs2k),'y',(fs3k),20*log10(fs3k)
,'b')
Title('Blue-Open Loop; Magenta-Strut #2 Closed Loop; Red-All 6 Struts Closed Loop' )


%%%%%%%%%%%%%%%%%%%%%%%%%%%%%%%%%%%%%%%%%%%
%fig2.m%
% Plots same Figure as fig1.m over range of 0-200 Hz%

clear
load s1                      %Open loop-42 Hz Disturbance on%
Figure(2)
clg
psdb(trace_y(2,1:20000),1024*8,10000,[]);
%[popen,fopen]=psd(trace_y(2,1:20000),1024*12,10000,[]);
hold on
```

```
load s2                           %Compensator applied to actuator #2%
psd(trace_y(2,1:20000),1024*8,10000,[]);
%[ps2,fs2]=psd(trace_y(2,1:20000),1024*12,10000,[]);
load s3                           % Compensator applied to actuator #2%
psd(trace_y(2,1:20000),1024*8,10000,[]);
%[ps3,fs3]=psd(trace_y(2,1:20000),1024*12,10000,[]);
hold off
%semilogx((fopenk),20*log10(popenk),'r',(fs2k),20*log10(fs2k),'y',(fs3k),20*log10(fs3k)
,'b')
Title('Blue-Open Loop; Magenta-Strut #2 Closed Loop; Red-All 6 Struts Closed Loop' )
%Title('Open Loop-42Hz Disturbance' )
axis([0 200 -70 30])


%%%%%%%%%%%%%%%%%%%%%%%%%%%%%%%%%%%%%%%%%%%%%%
%fig3.m%
%plots PSD sensed by 3 geophones; actuator #2, #3 and #6 over range of 0-200Hz%


clear
load s2                           % Compensator applied to actuator #2 %
Figure(3)
clg
psd(trace_y(2,1:20000),1024*1,10000,[]);
%[popen,fopen]=psd(trace_y(2,1:20000),1024*12,10000,[]);
hold on
psd(trace_y(3,1:20000),1024*1,10000,[]);
%[ps2,fs2]=psd(trace_y(3,1:20000),1024*12,10000,[]);
psd(trace_y(6,1:20000),1024*1,10000,[]);
%[ps3,fs3]=psd(trace_y(6,1:20000),1024*12,10000,[]);
hold off
%semilogx((fopenk),20*log10(popenk),'r',(fs2k),20*log10(fs2k),'y',(fs3k),20*log10(fs3k)
,'b')
Title('Blue-#2 Geophone; Magenta-#3 Geophone; Red-# 6 Geophone' )
%axis([0 200 -70 30])


%%%%%%%%%%%%%%%%%%%%%%%%%%%%%%%%%%%%%%%%%%%%%%
%fig3.m%
%plots PSD sensed by 3 geophones; actuator #2, #3 and #6 over range of 0-5kHz%


clear
load s2                           %Compensator applied to actuator #2 %
Figure(4)
clg
psd(trace_y(2,1:20000),1024*8,10000,[]);
%[popen,fopen]=psd(trace_y(2,1:20000),1024*12,10000,[]);
hold on
```

```
psd(trace_y(3,1:20000),1024*8,10000,[]);
%[ps2,fs2]=psd(trace_y(3,1:20000),1024*12,10000,[]);
psd(trace_y(6,1:20000),1024*8,10000,[]);
%[ps3,fs3]=psd(trace_y(6,1:20000),1024*12,10000,[]);
hold off
%semilogx((fopenk),20*log10(popenk),'r',(fs2k),20*log10(fs2k),'y',(fs3k),20*log10(fs3k)
,'b')
Title('Blue-#2 Geophone; Magenta-#3 Geophone; Red-# 6 Geophone' )
axis([0 200 -70 30])
```

APPENDIX B. MODEL STRUCUTURE SELECTION PLOTS

A. Structure Acceptance Plots for Actuator Two

The following plots were utilized in selecting the ARX structure [na=7 nb=6 nk=1] for actuator number two.

RETURN TO COMMAND SCREEN TO SELECT # OF PARAMETERS TO BE ESTIMATED
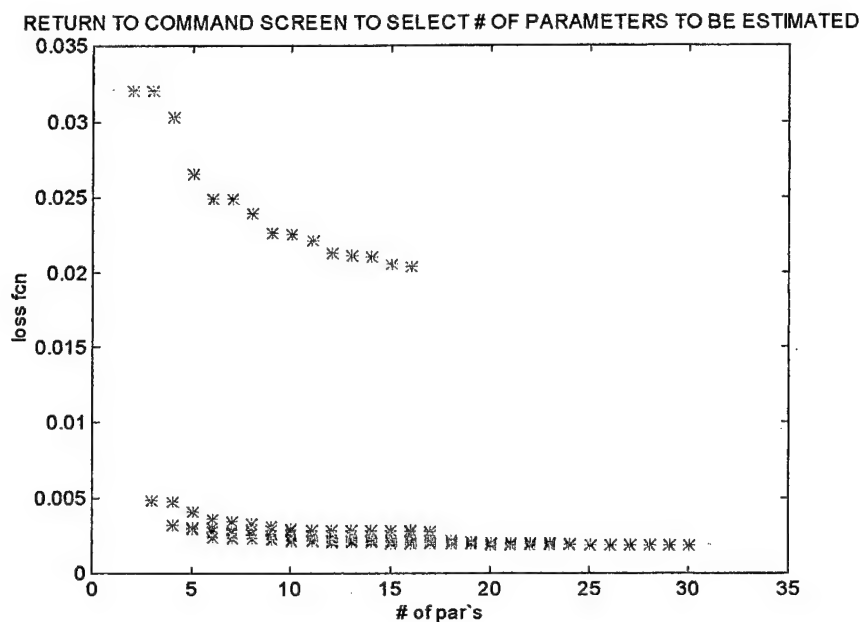
Figure A.1
Parameter Number Vs. Loss Function For *nk*=1

Zero Pole Plot ARX Model [7 6 1] Model *Data Prefiltered*

Figure A.2
Zero-Pole Plot

113

Blue=Actuator#2, Red=ARX MODEL[7 6 1] *Data Prefiltered*

(a) Magnitude

Blue=Actuator#2, Red=ARX MODEL[7 6 1] *Data Prefiltered*
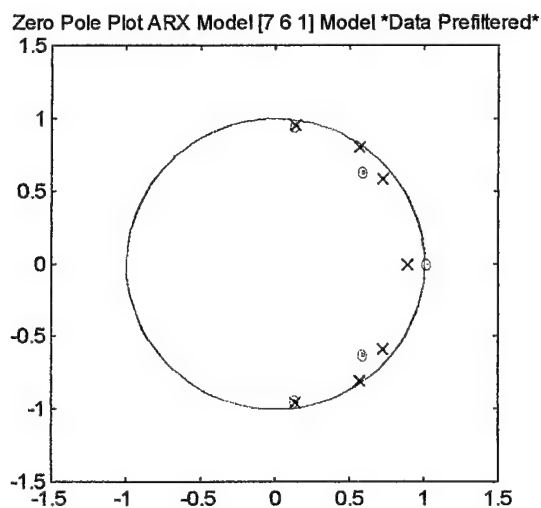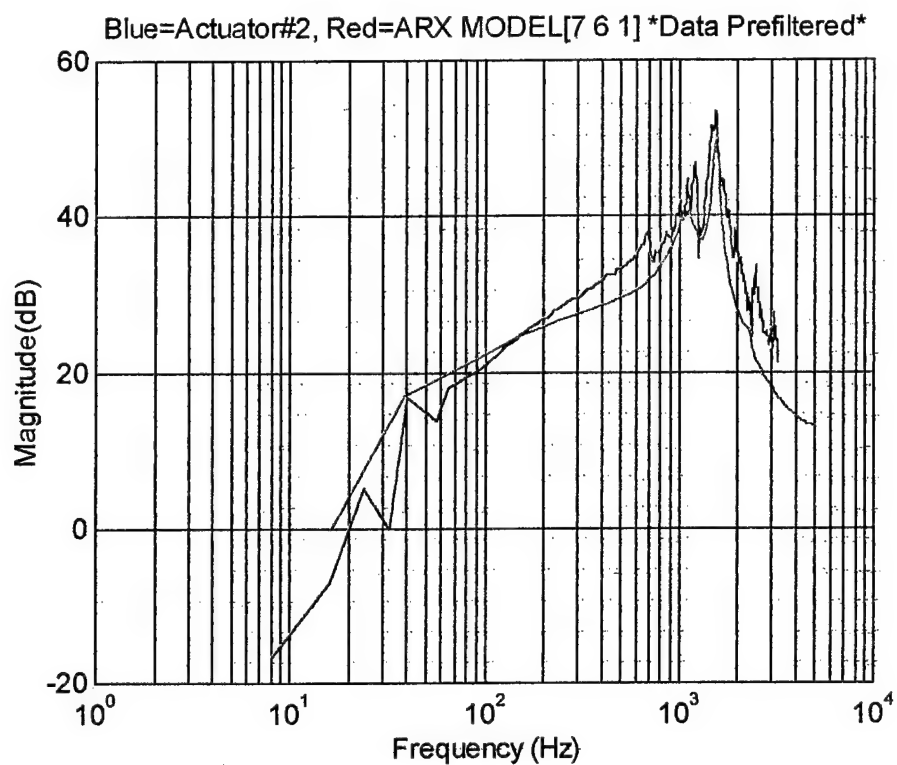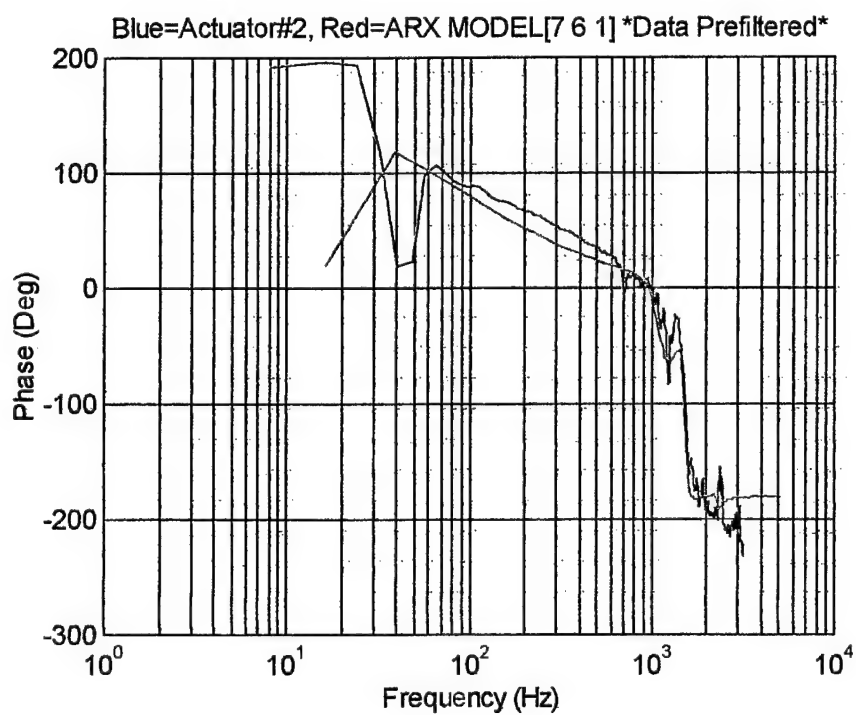
(b) Phase

Figure A.3
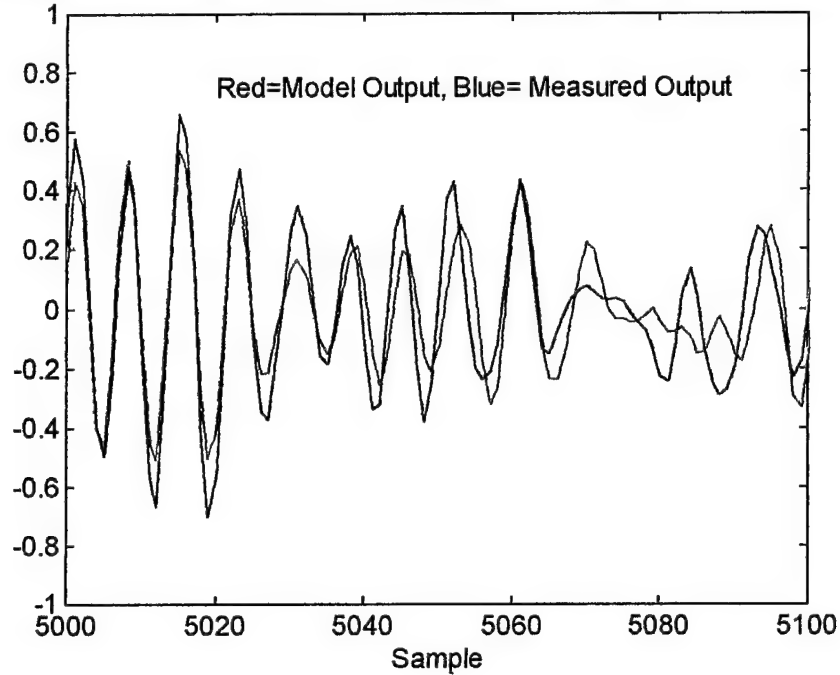Frequency Response Comparison
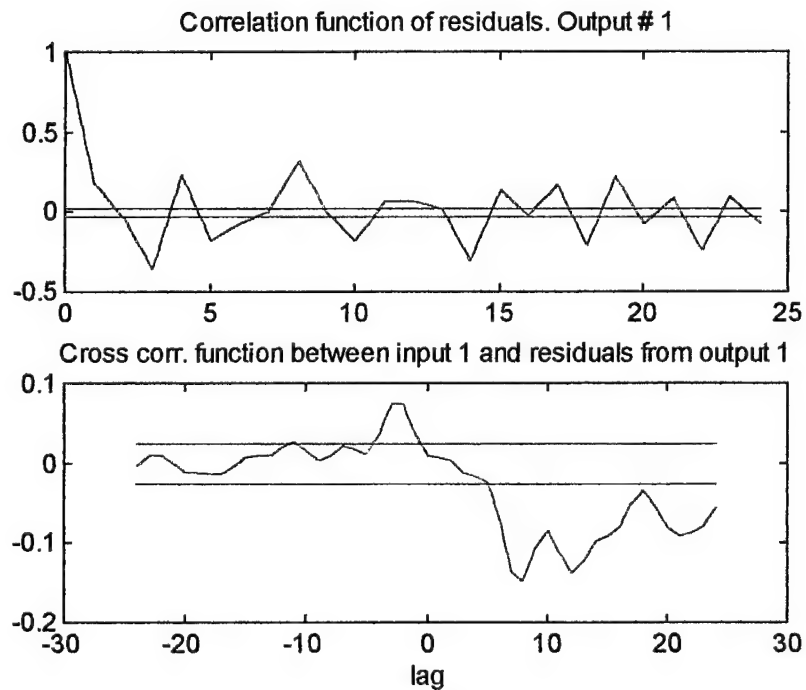
114
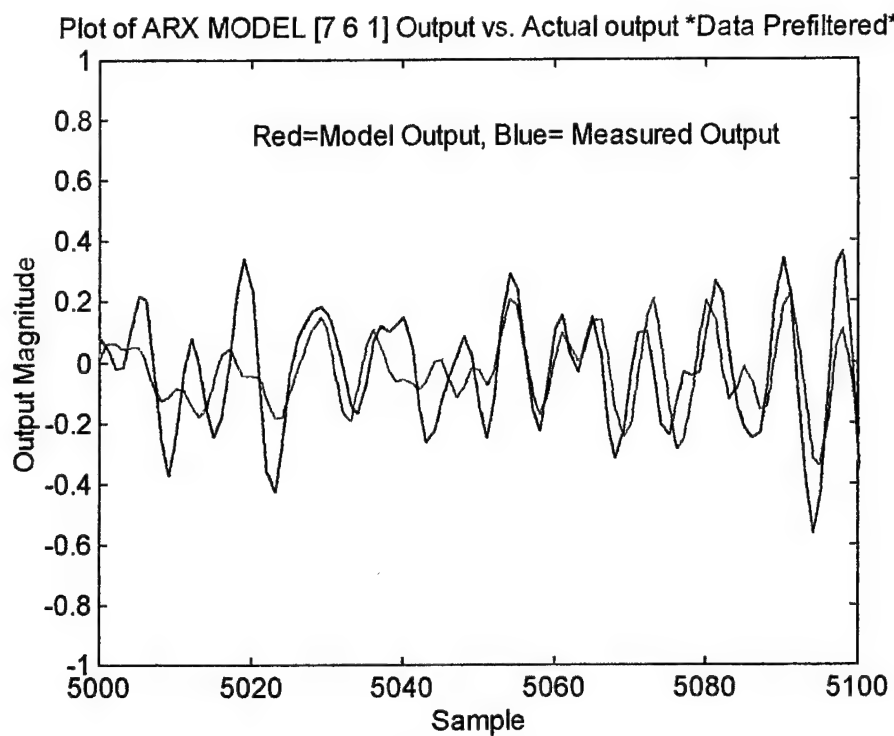
Figure A.4
Model Output Vs. Actual Output
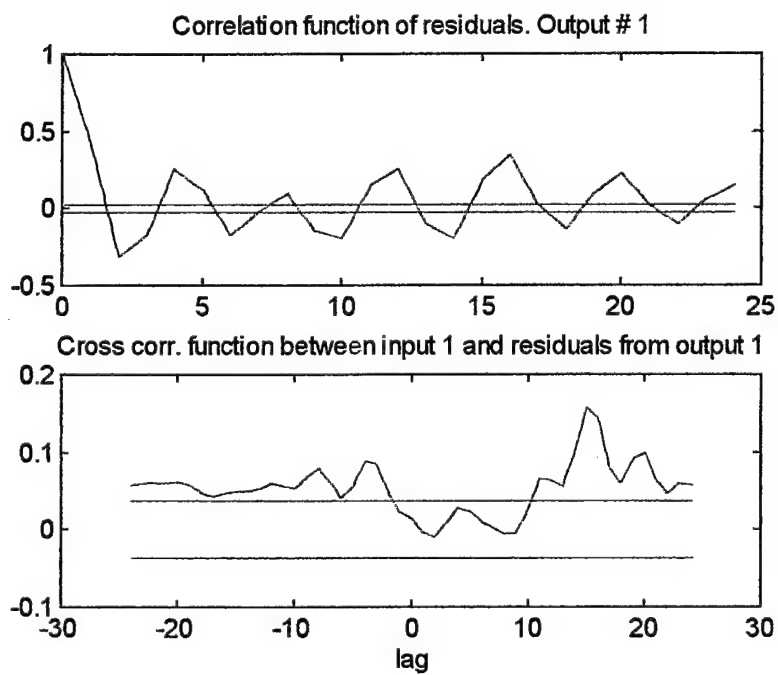
Figure A.5
Auto and Cross Correlation Functions

115
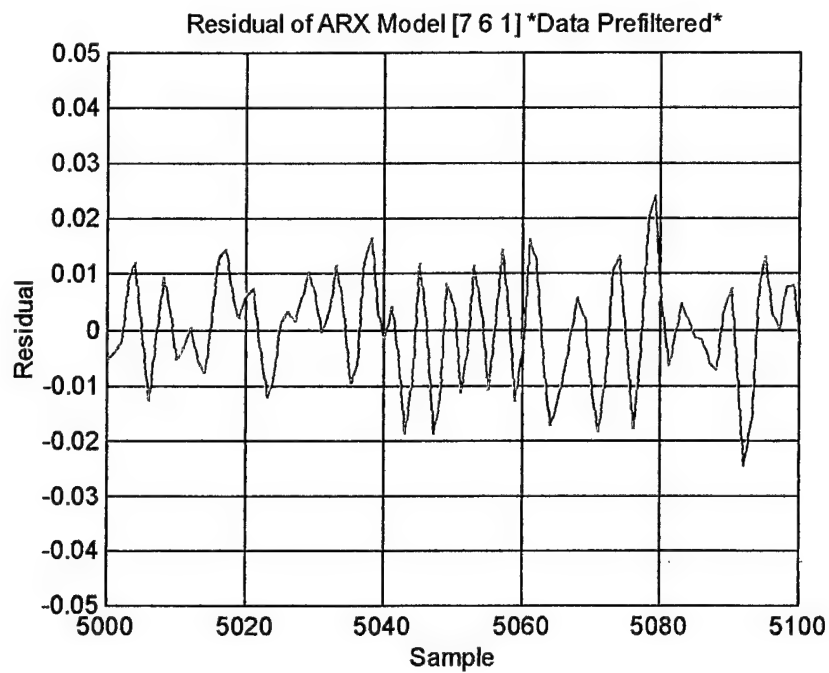
Figure A.6
Residual Vs. Sample
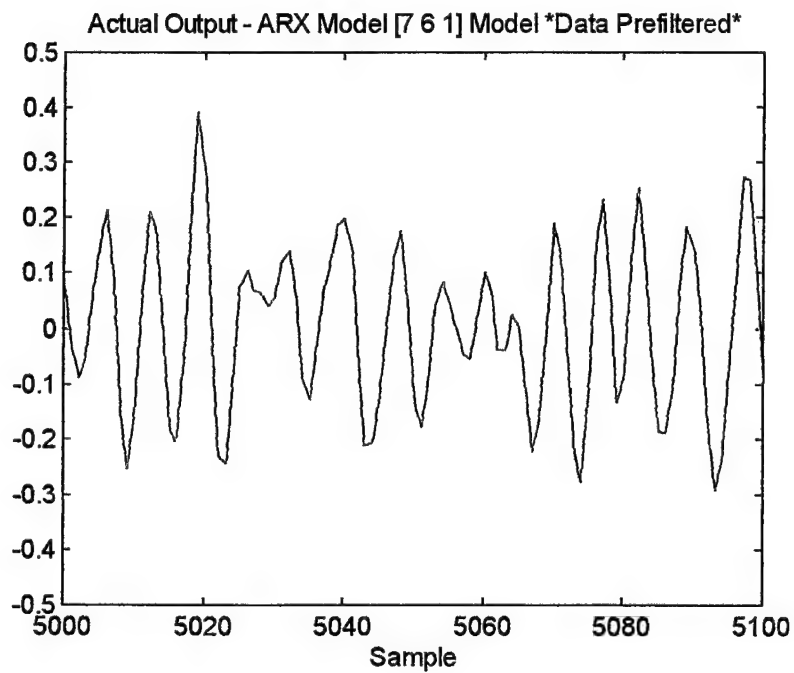
Figure A.7
Actual Output and Model Output Difference

116

B. Model Structure Acceptance for Actuator Three

The following plots were utilized in selecting the ARX structure [na=7 nb=7 nk=1] for actuator number three.
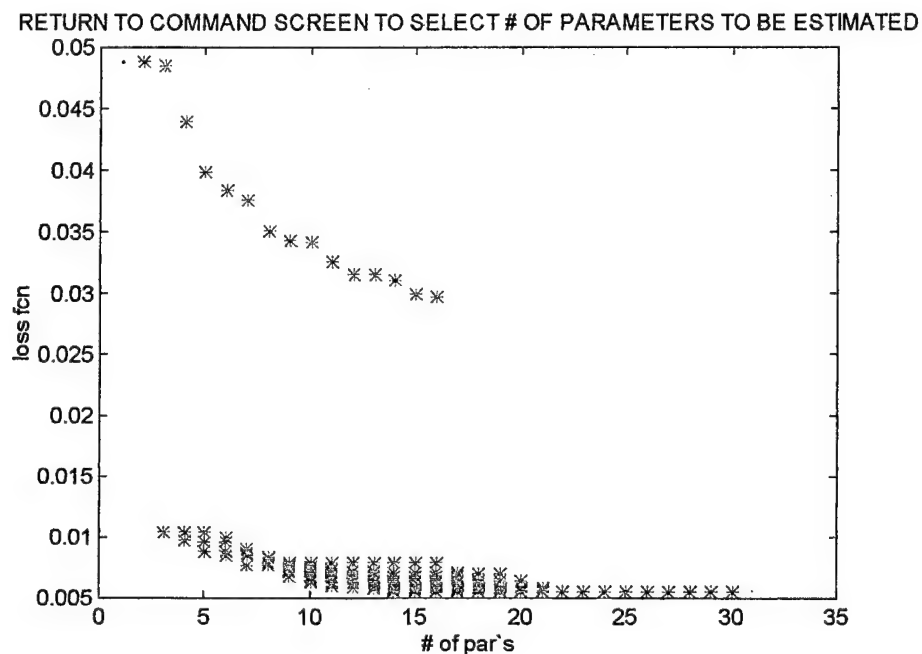
Figure B.1
Parameter Number Vs. Loss Function For *nk*=1

Figure B.2
Zero-Pole Plot

Blue=Actuator#3Red=ARX MODEL[7 6 1]

(a) Magnitude

Blue=Actuator#3, Red=ARX MODEL[7 6 1]
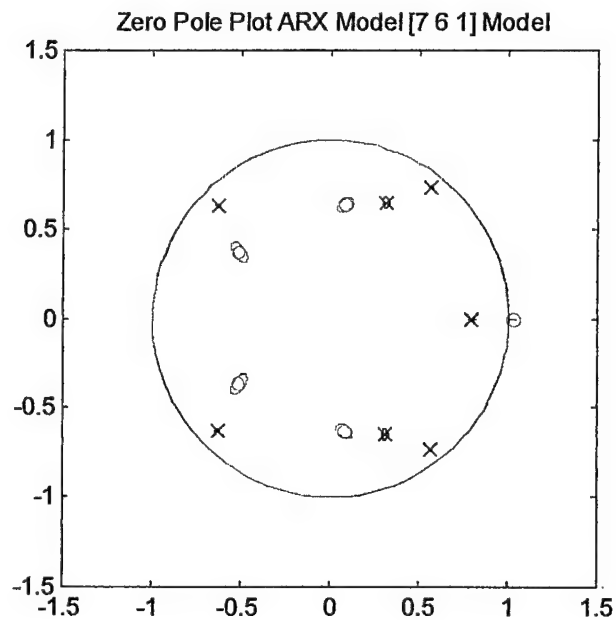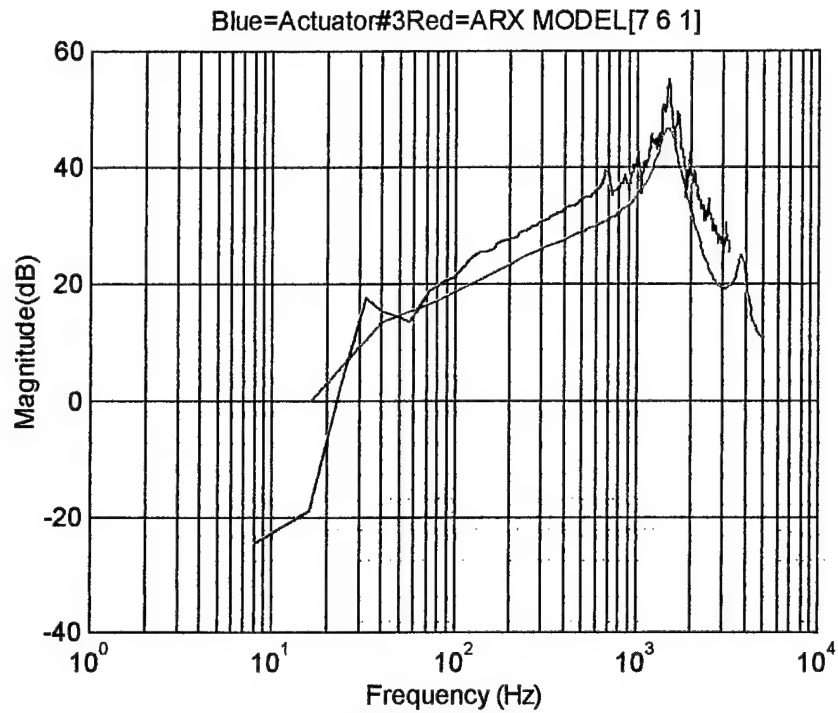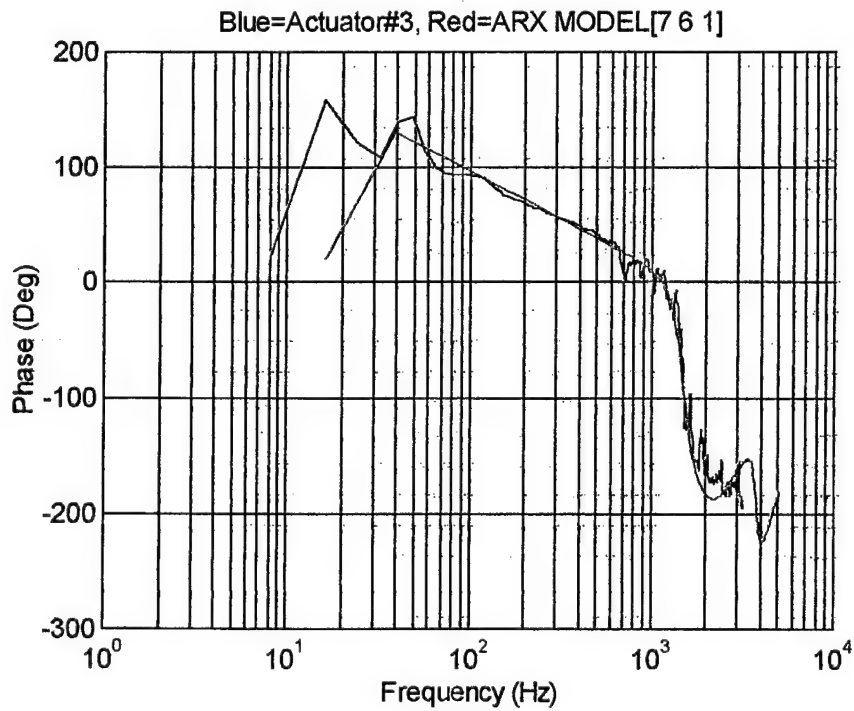
(b) Phase

Figure B.3
Frequency Response Comparison

118

Plot of ARX MODEL [7 6 1] Output vs. Actual output

Red=Model Output, Blue= Measured Output

Output Magnitude
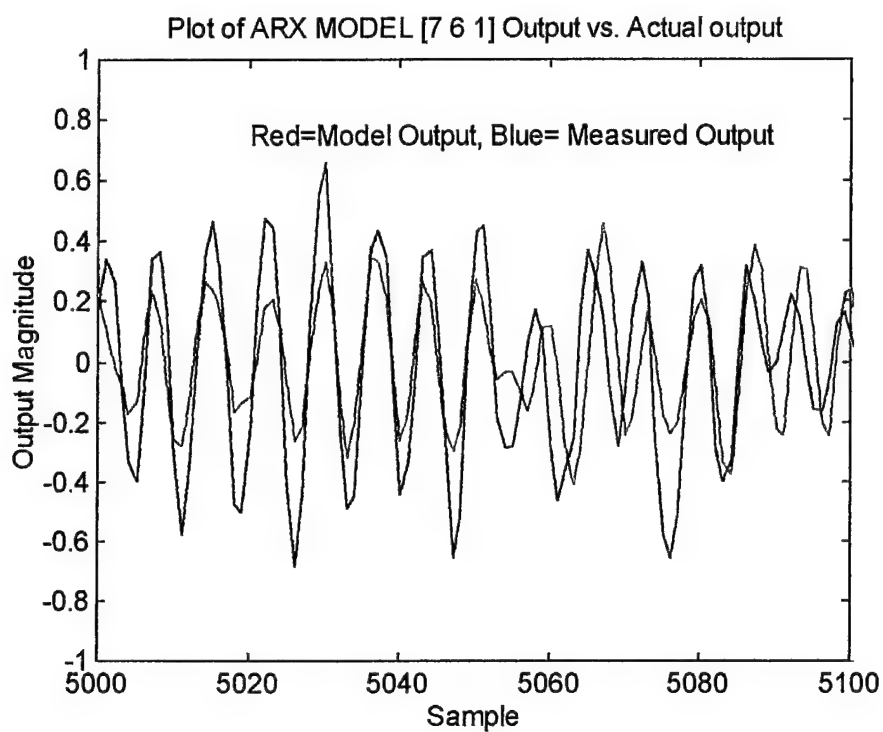
Sample

Figure B.4
Model Output Vs. Actual Output

Correlation function of residuals. Output # 1

Cross corr. function between input 1 and residuals from output 1

lag
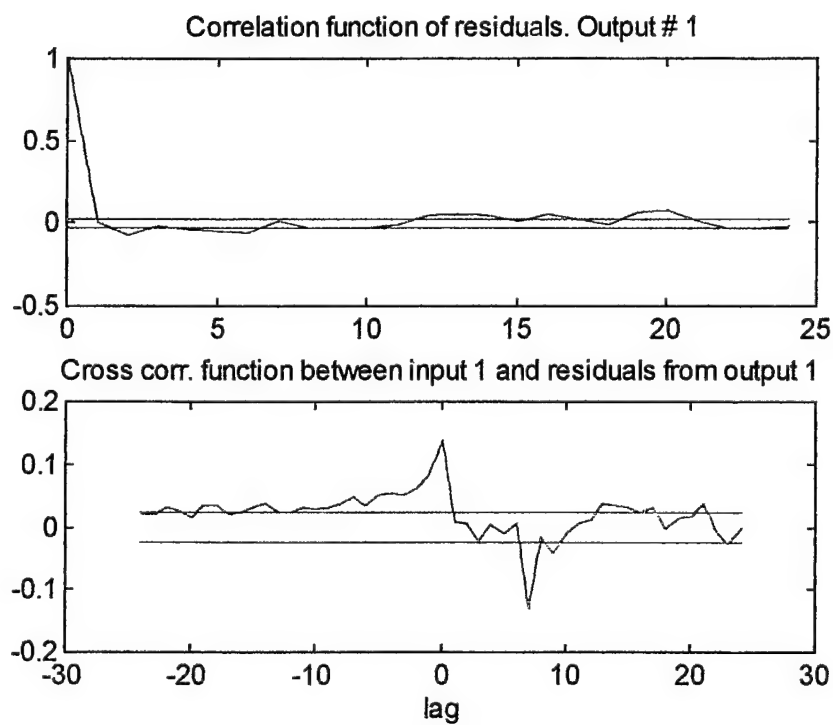
Figure B.5
Auto and Cross Correlation Functions

119
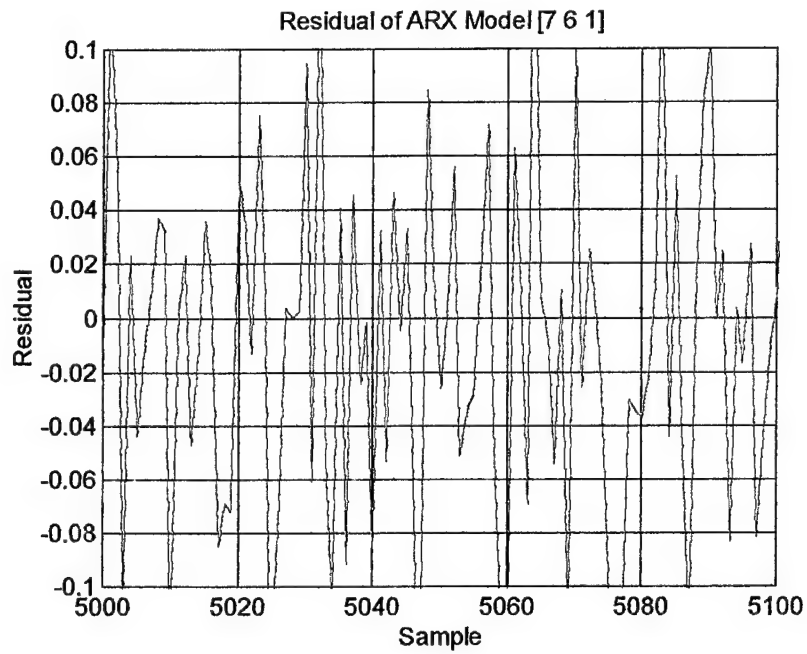
Figure B.6
Residual Vs. Sample
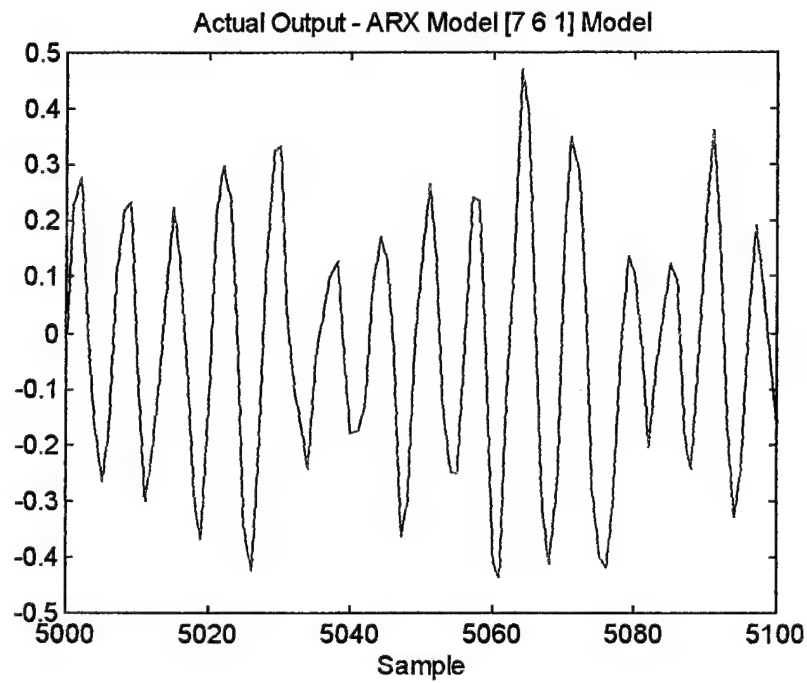
Figure B.7
Actual Output and Model Output Difference

120

C. Model Structure Acceptance for Actuator Four

The following plots were utilized in selecting the ARX structure [na=7 nb=7 nk=1] for actuator number four.
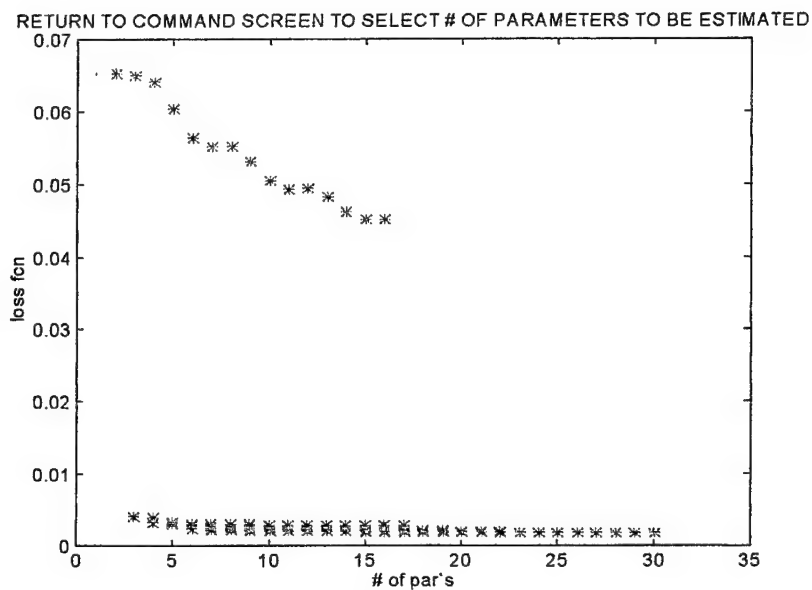
Figure C.1

Parameter Number Vs. Loss Function For *nk*=1

Figure C.2
Zero-Pole Plot

Blue=Actuator#4, Red=ARX MODEL[7 6 1] *Data Prefiltered*

(a) Magnitude

Blue=Actuator#4, Red=ARX MODEL[7 6 1] *Data Prefiltered*
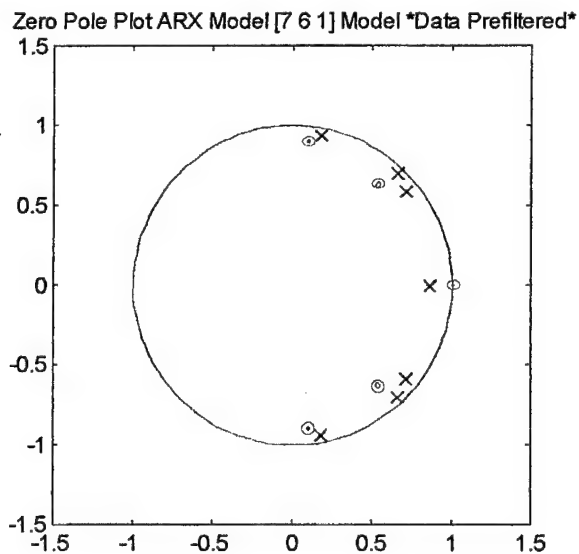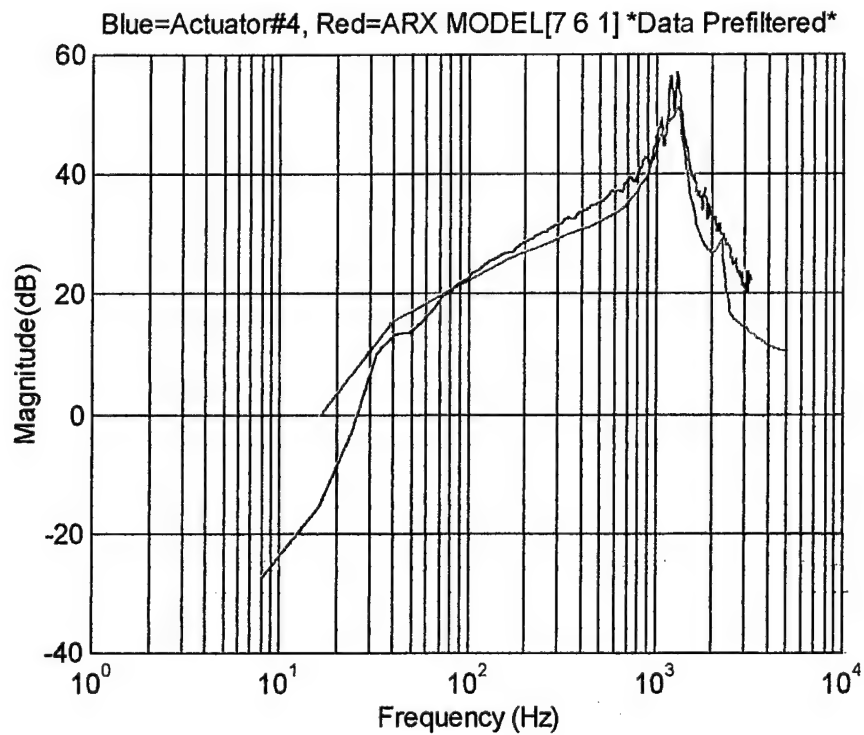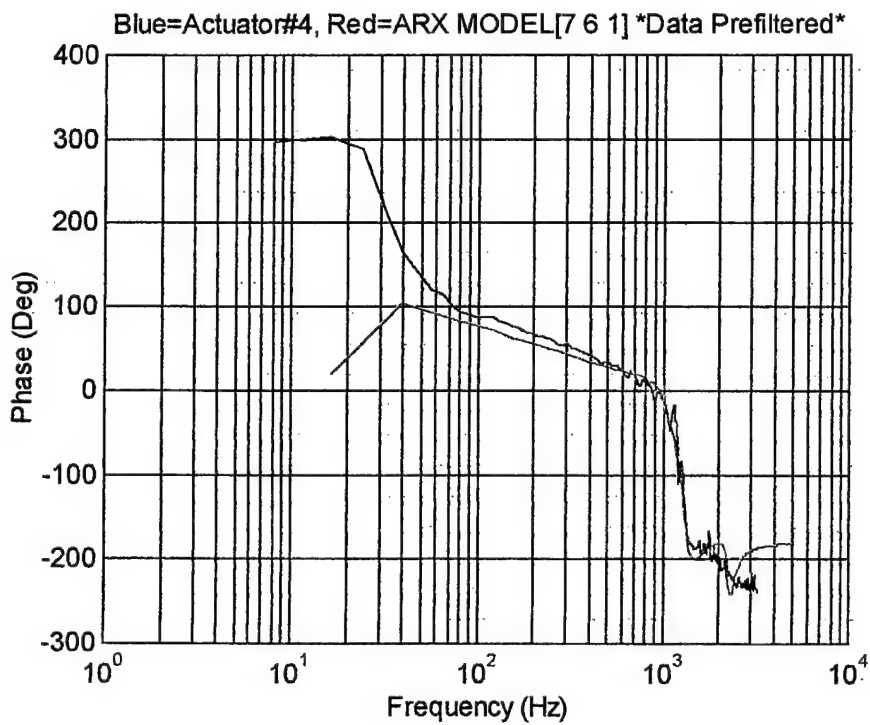
(b) Phase

Figure C.3
Frequency Response Comparison

122

Plot of ARX MODEL [7 6 1] Output vs. Actual output *Data Prefiltered*
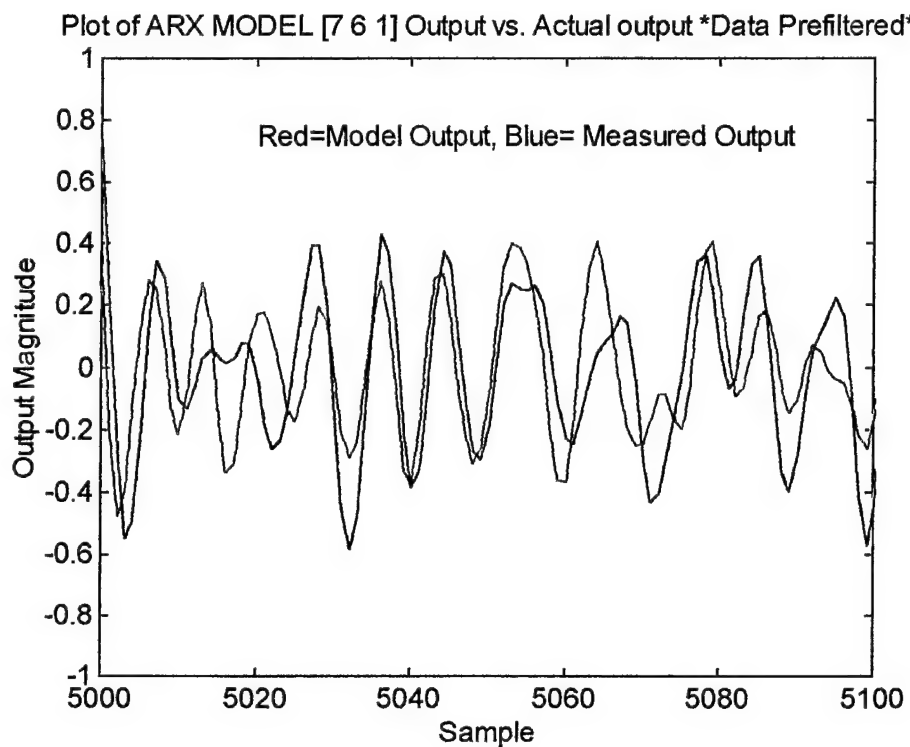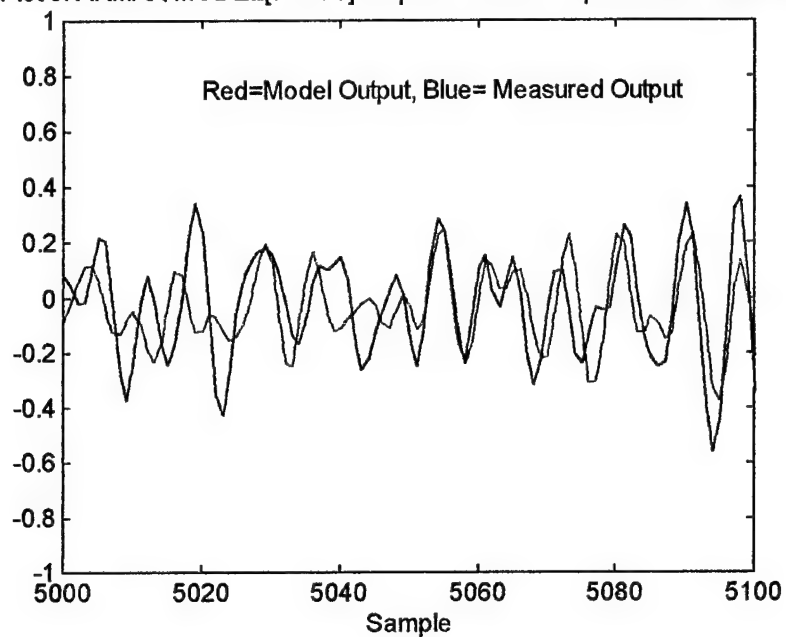

Figure C.4
Model output Vs. Actual Output
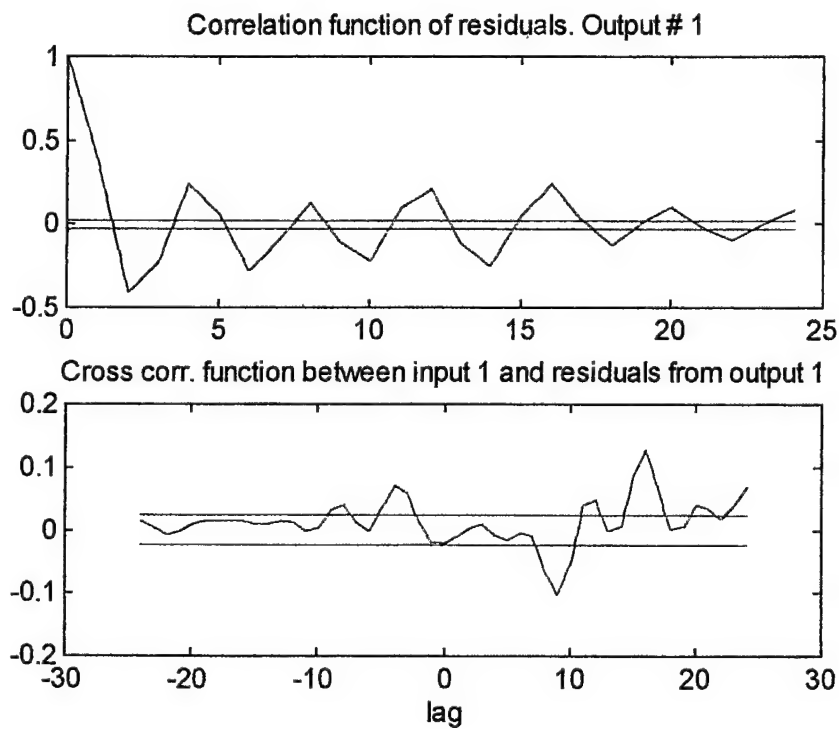
Figure C.5
Auto and Cross Correlation Functions
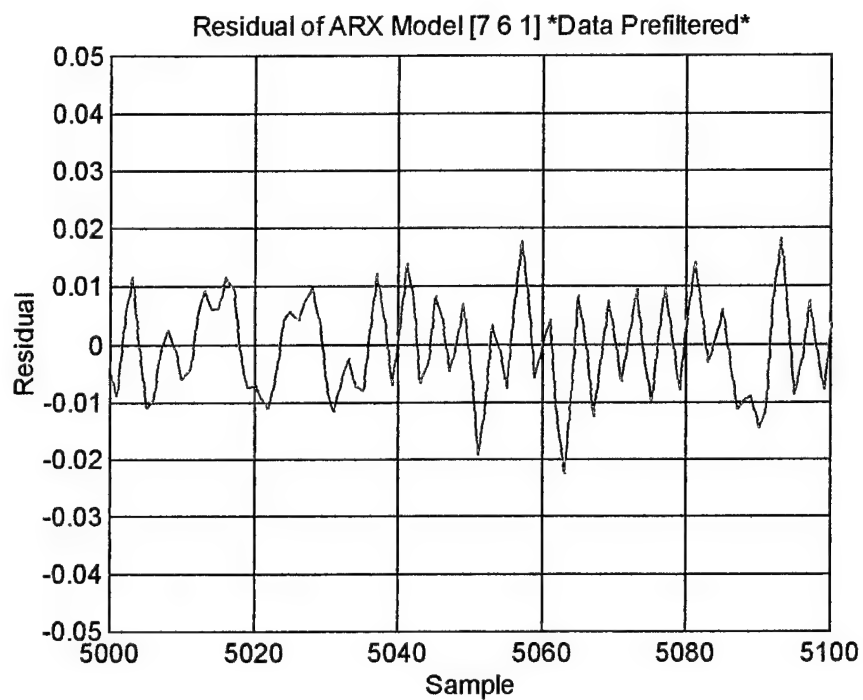
Figure C.6
Residual Vs. Sample
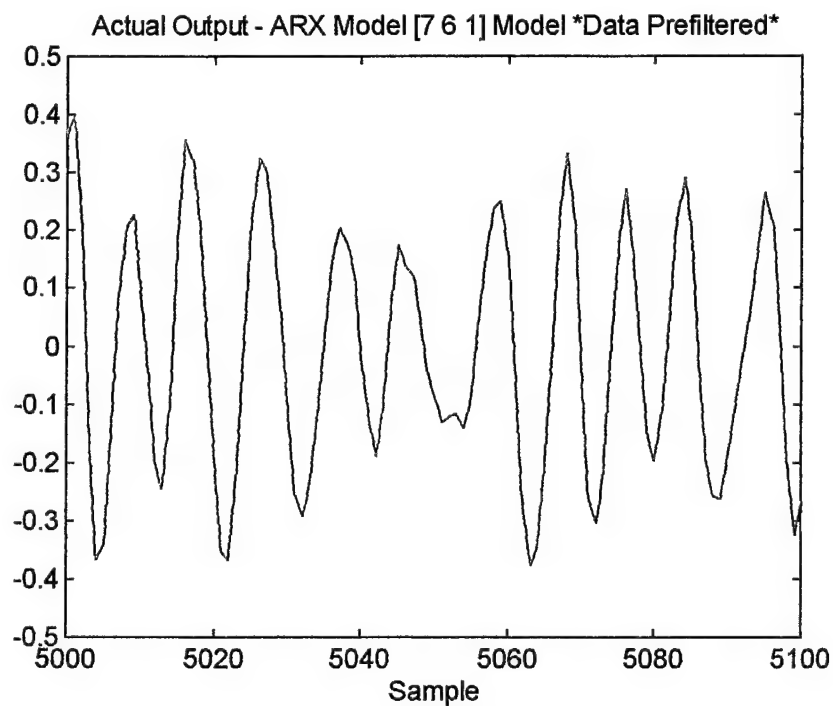
Figure C.7
Actual Output and Model Output Difference

124

D. Model Structure Acceptance for Actuator Five

The following plots were utilized in selecting the ARX structure [na=7 nb=7 nk=1] for actuator number five.
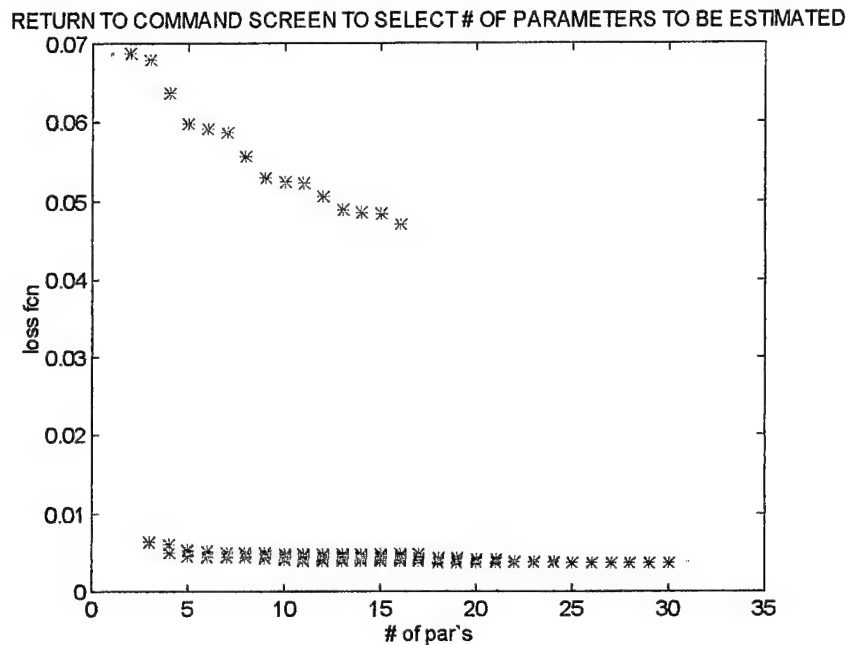
Figure D.1
Parameter Number Vs. Loss Function For *nk*=1)

Figure D.2
Zero-Pole Plot

125

Blue=Actuator#5, Red=ARX MODEL[7 6 1] *Data Prefiltered*

(a) Magnitude

Blue=Actuator#5, Red=ARX MODEL[7 6 1] *Data Prefiltered*
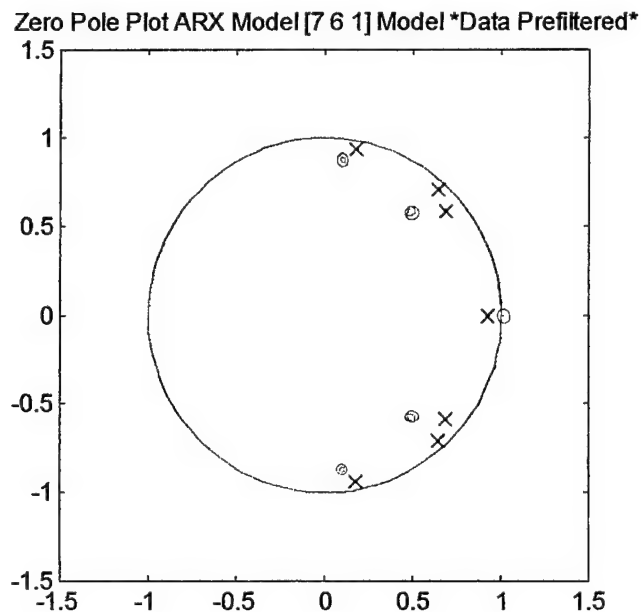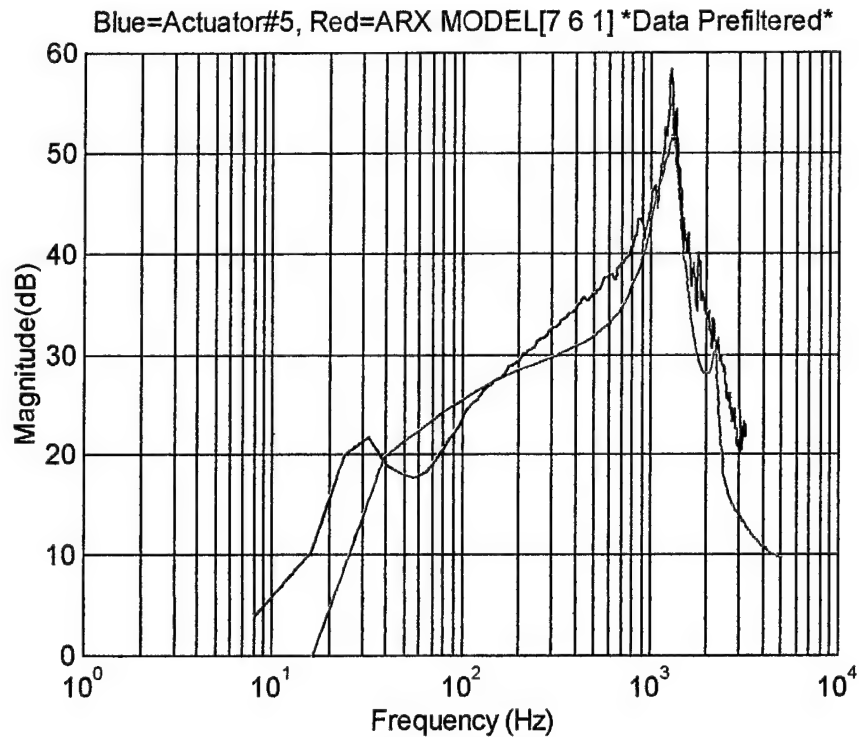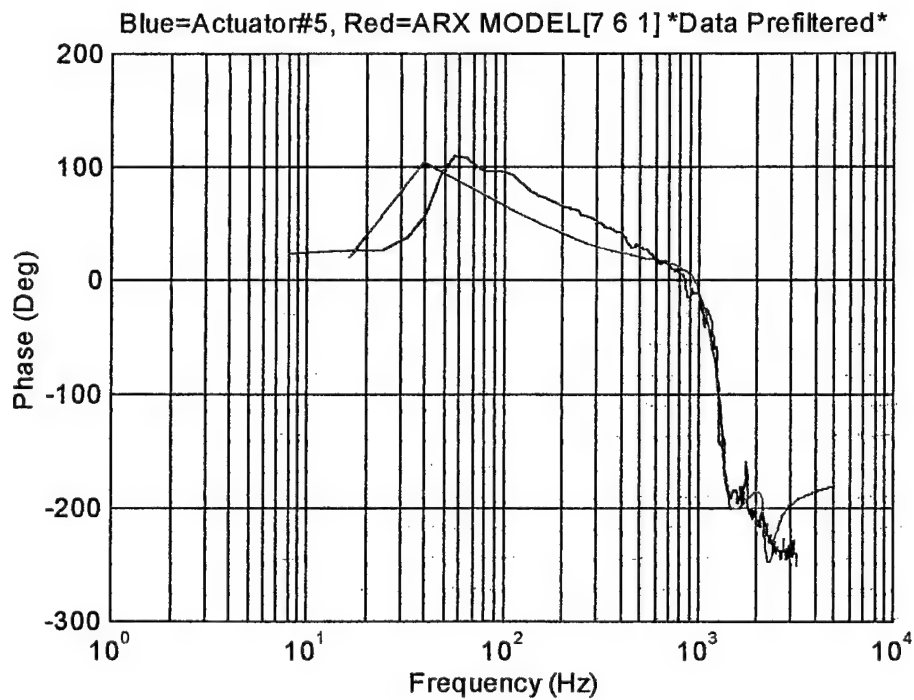
(b) Phase

Figure D.3
Frequency Response Comparison
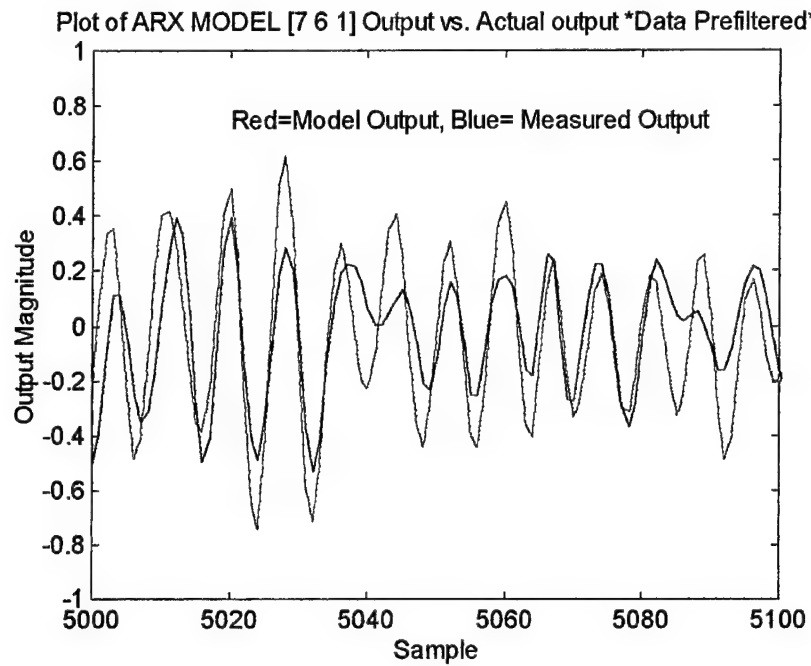
Figure D.4
Model Output Vs. Actual Output
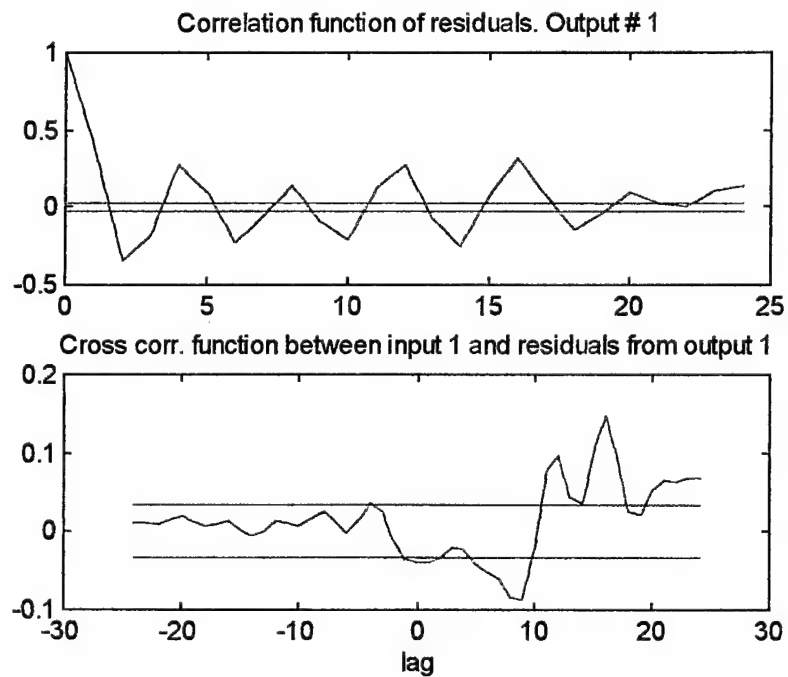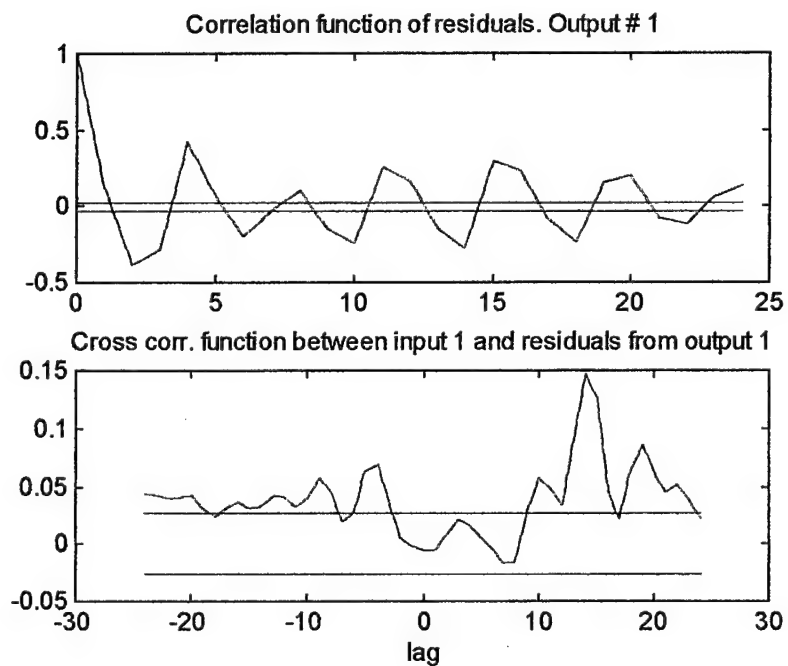

Figure D.5
Auto and Cross Correlation Functions
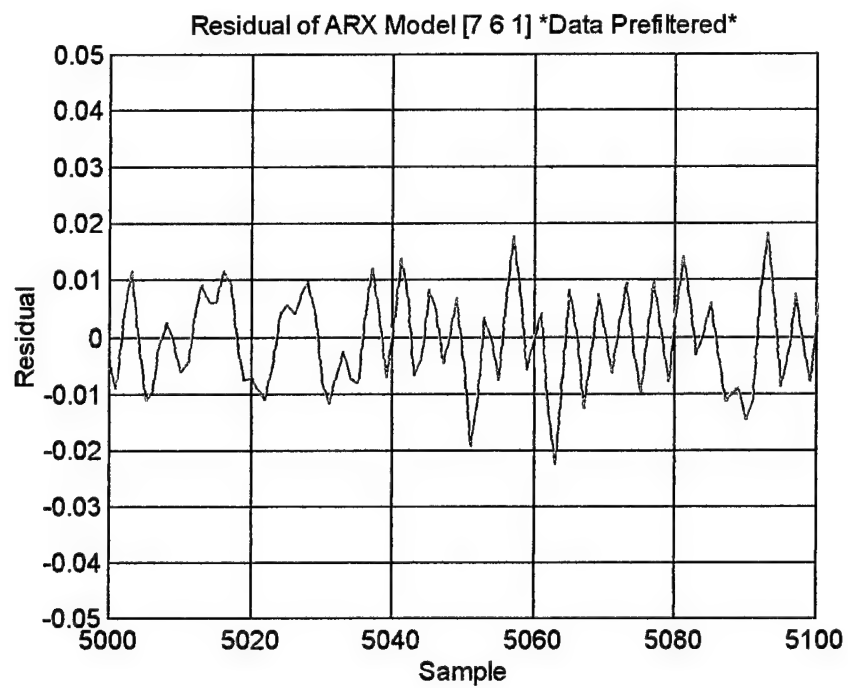
Figure D.6
Residual Vs. Sample
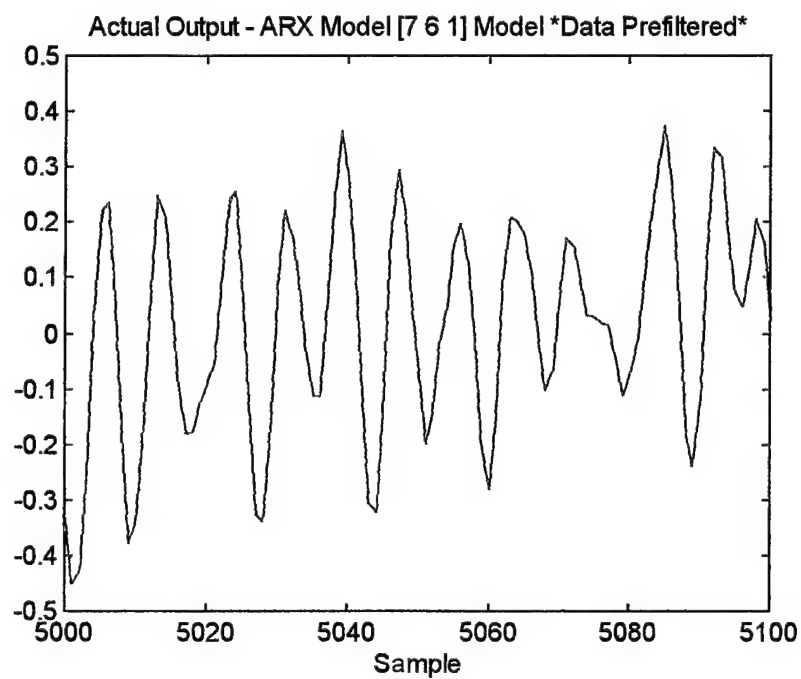
Figure D.7
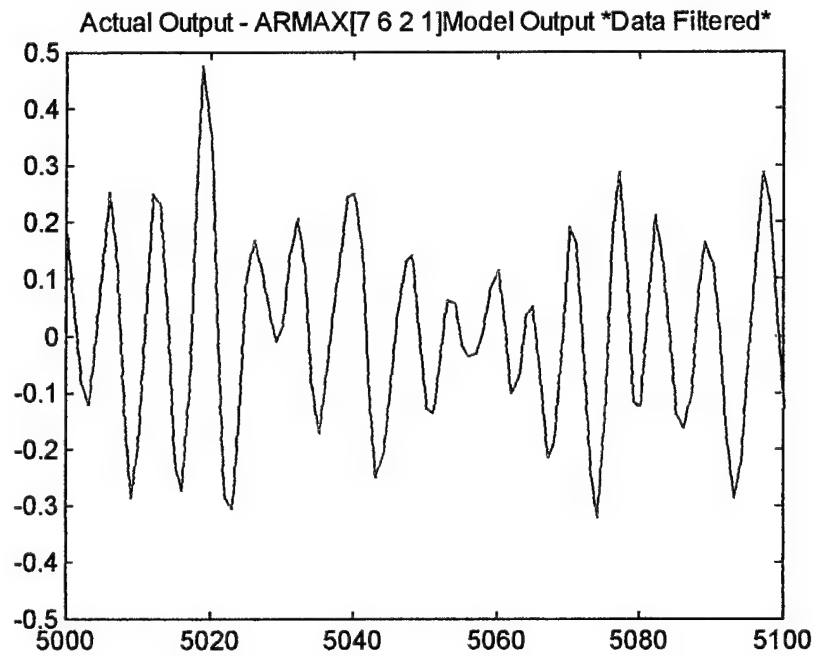Actual Output and Model Output Difference

128

E. Model Structure Acceptance for Actuator Six

The following plots were utilized in selecting the ARX structure [na=7 nb=7 nk=1] for actuator number six.

RETURN TO COMMAND SCREEN TO SELECT # OF PARAMETERS TO BE ESTIMATED
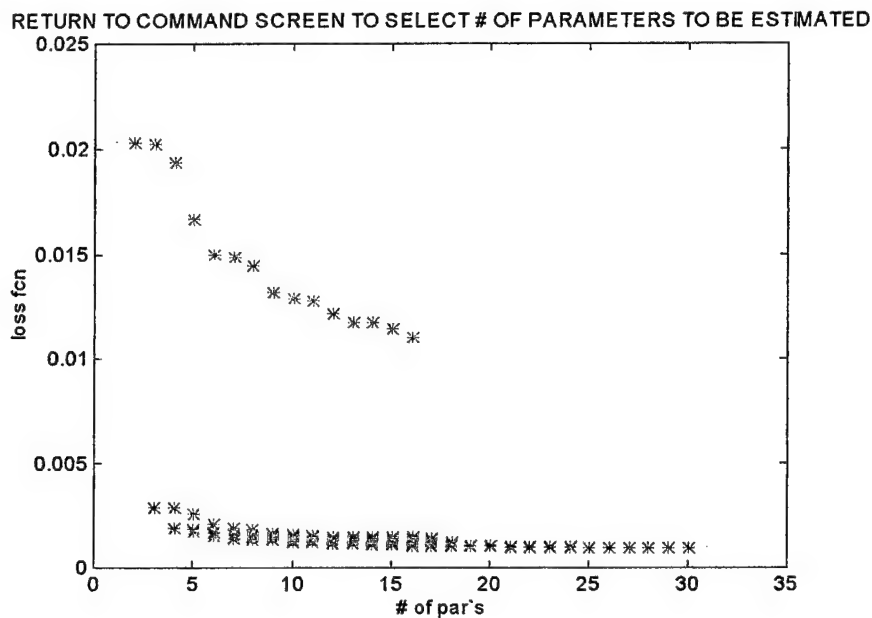
Figure E.1
Parameter Number Vs. Loss Function For *nk*=1
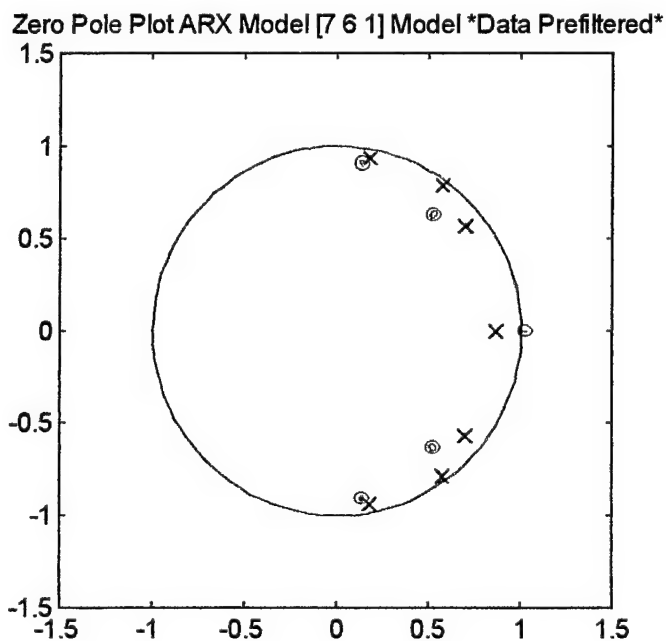
Figure E.2
Zero-Pole Plot

129
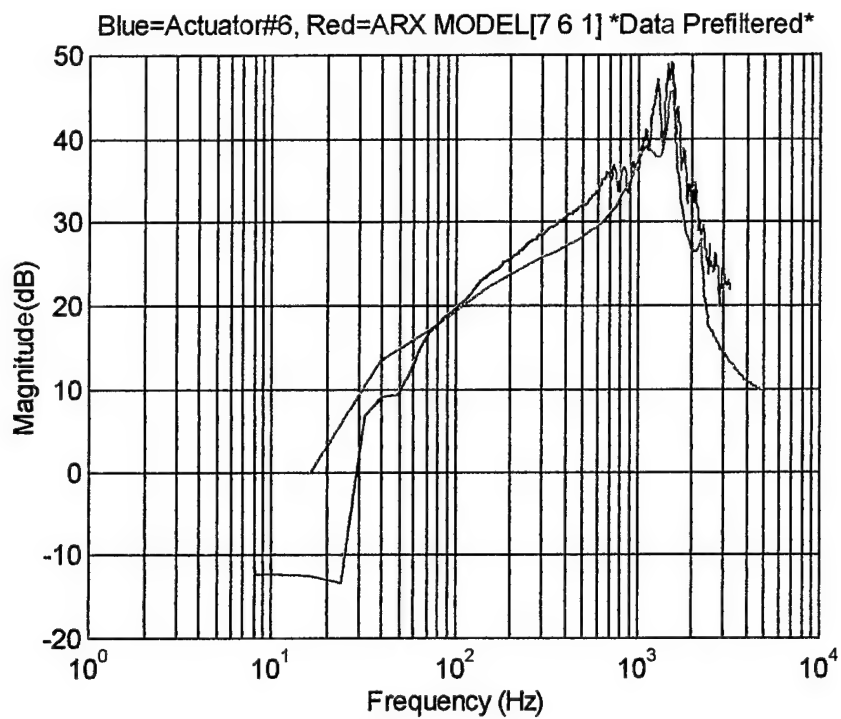
(a) Magnitude
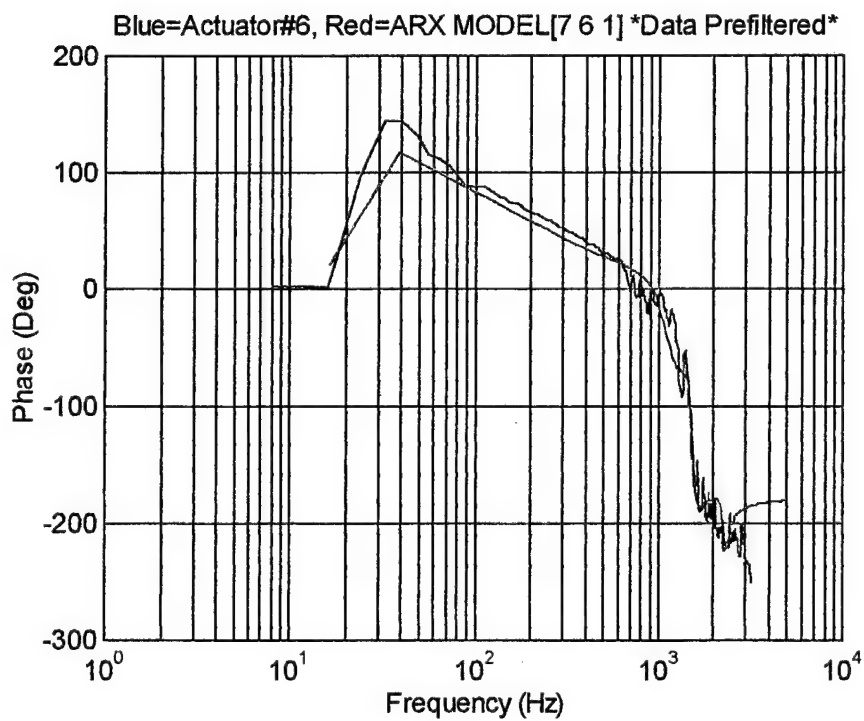
(b) Phase

Figure E.3
Frequency Response Comparison

130

Plot of ARX MODEL [7 6 1] Output vs. Actual output *Data Prefiltered*

Red=Model Output, Blue= Measured Output
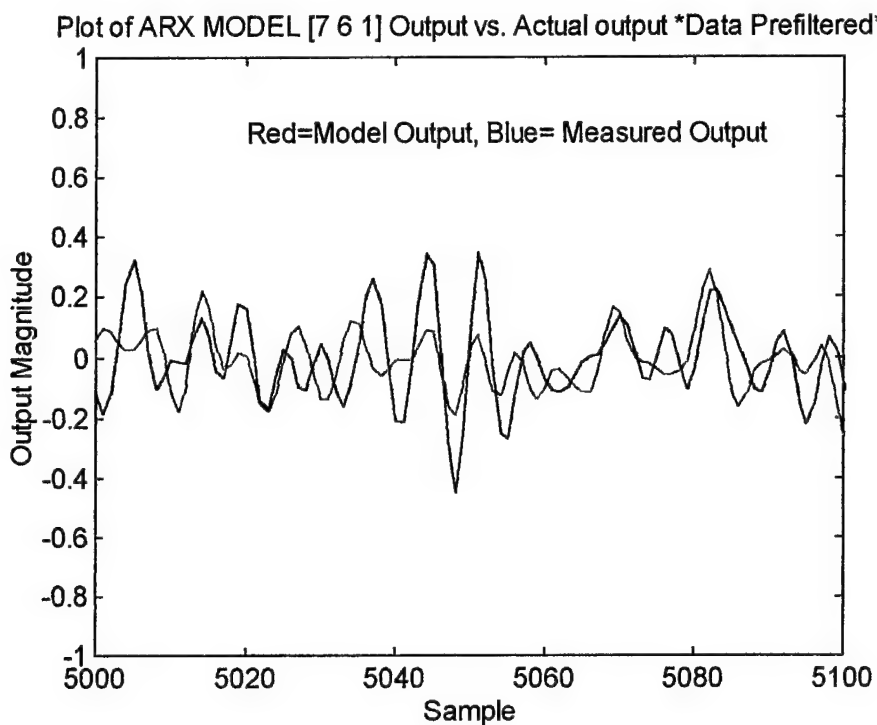
Figure E.4
Model Output Vs. Actual Output

Correlation function of residuals. Output # 1

Cross corr. function between input 1 and residuals from output 1
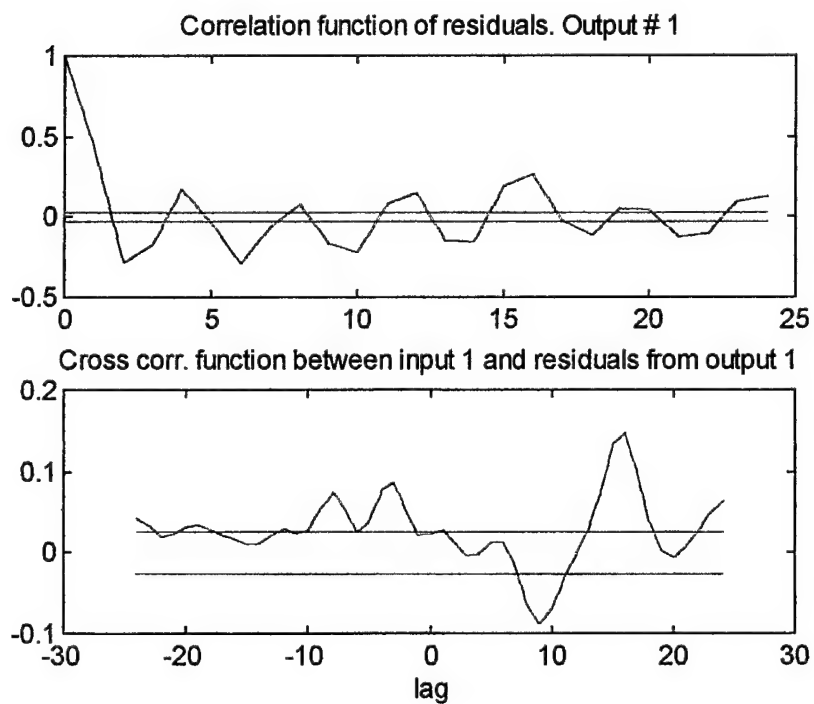
Figure E.5
Auto and Cross Correlation Functions
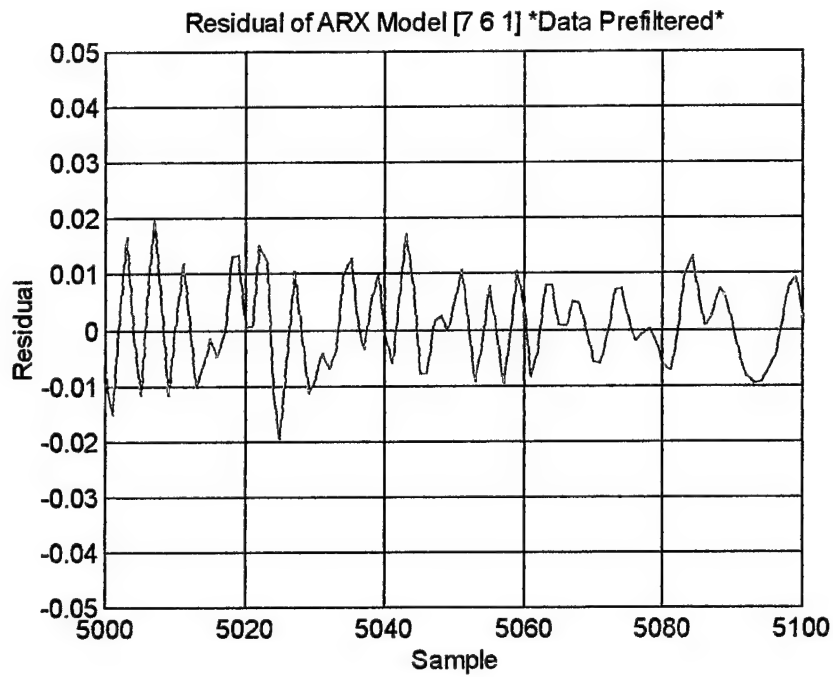
Figure E.6
Residual Vs. Sample
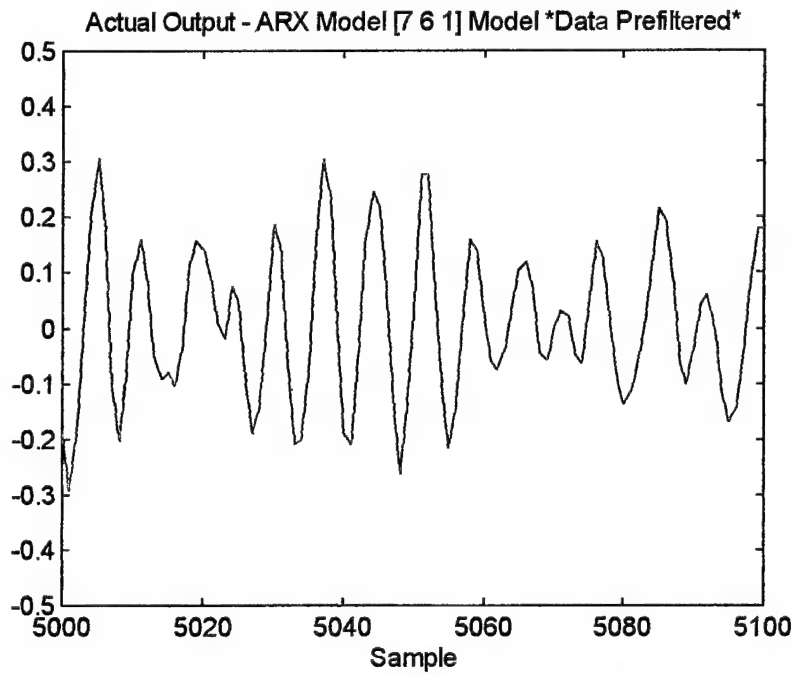
Figure E.7
Actual Output and Model Output Difference

132

APPENDIX C. MODEL VALIDATION PLOTS

A. Application of ARMAX Method to Actuator Number One.

The following plots were used in evaluating the application of the ARMAX and Box-Jenkins parameter estimation methods in modeling actuator number one. The structure [na=7 nb=6 nc=2 nk=1] was used.

Blue=Actuator#1Red=ARMAX MODEL[7 6 2 1] *Data Prefiltered*

(a) Magnitude

Blue=Actuator#1Red=ARMAX MODEL[7 6 2 1] *Data Prefiltered*

(b) Phase
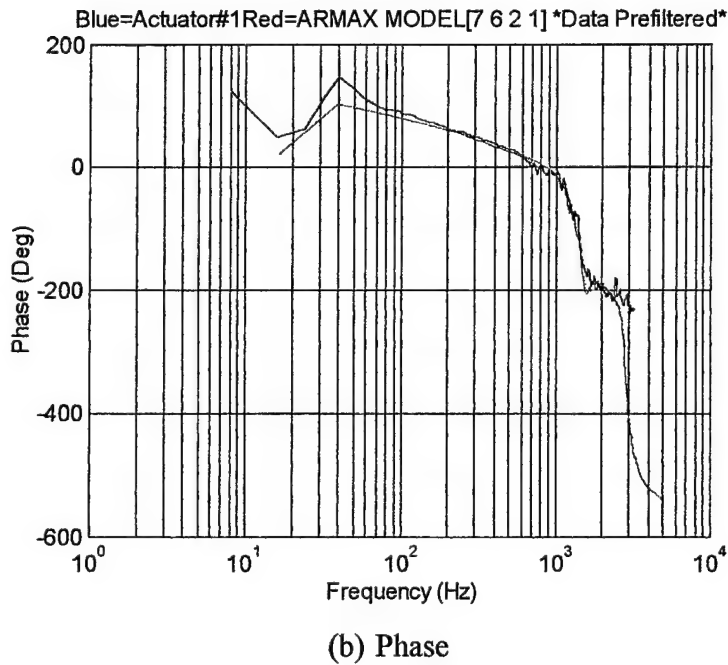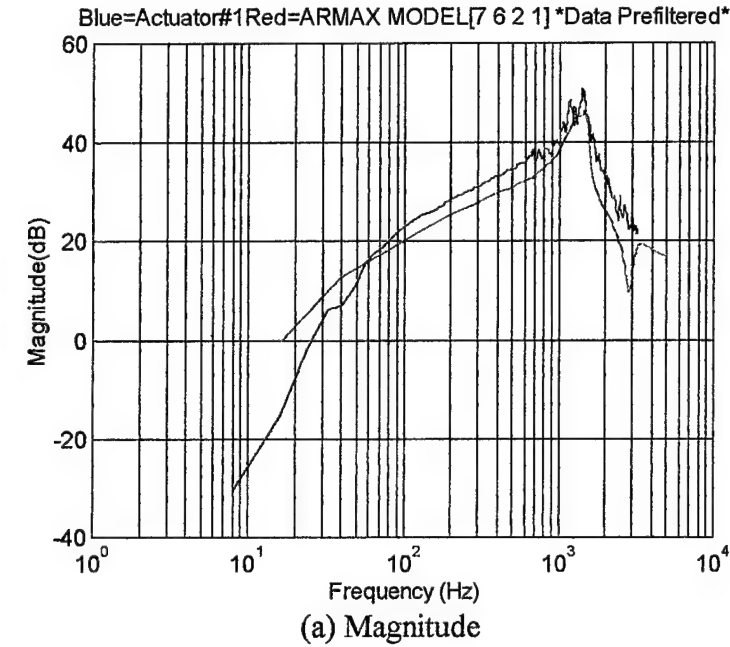
Figure A.1

Frequency Response Comparison
Plot of ARMAX MODEL[7 6 2 1] Output vs. Actual output *Data Prefiltered*

Red=Model Output, Blue= Measured Output

Sample

Figure A.2
Model Output Vs. Actual Output

Correlation function of residuals. Output # 1

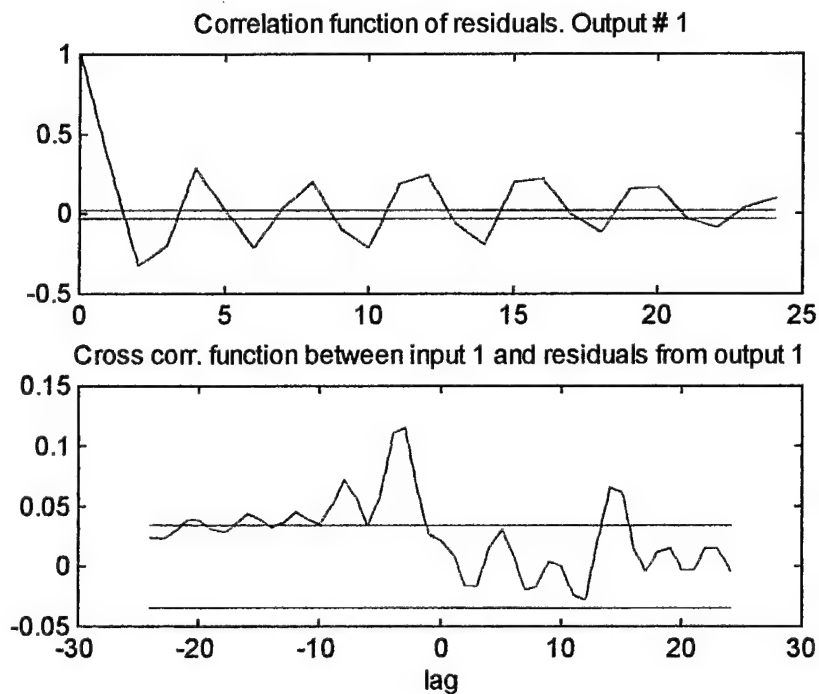Cross corr. function between input 1 and residuals from output 1

lag

Figure A.3.
Auto and Cross-Correlation Functions
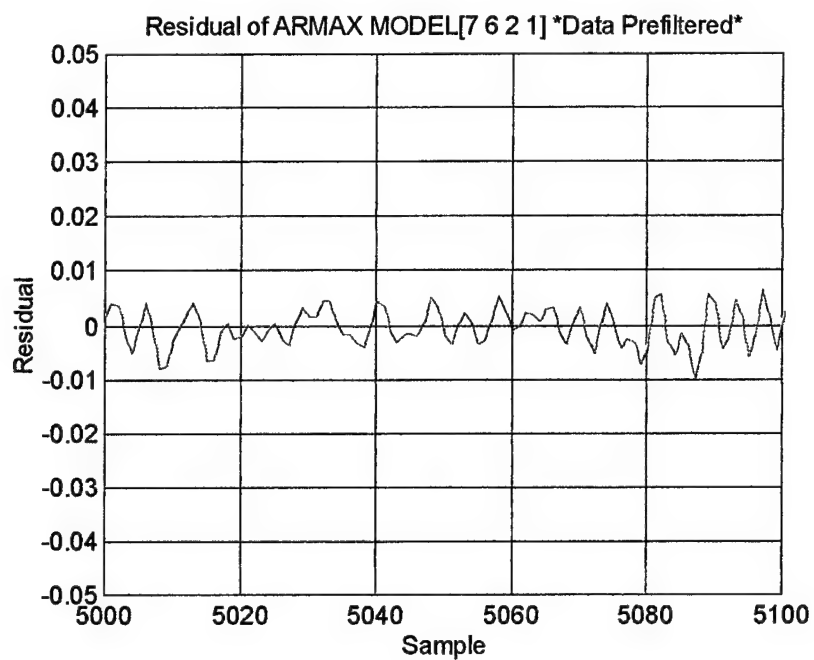
Figure A.4
Residual Vs. Sample
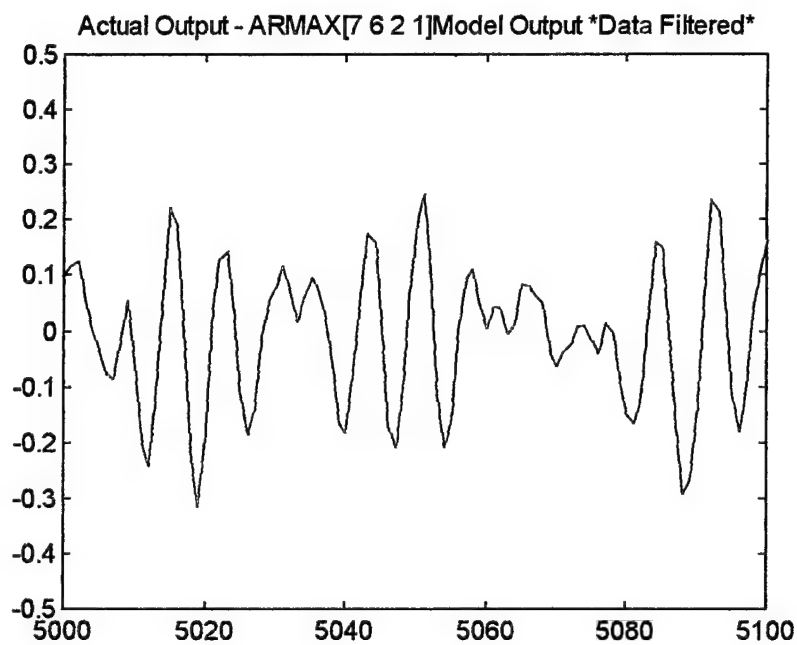
Figure A.5
Actual Output and Model Output Difference

135
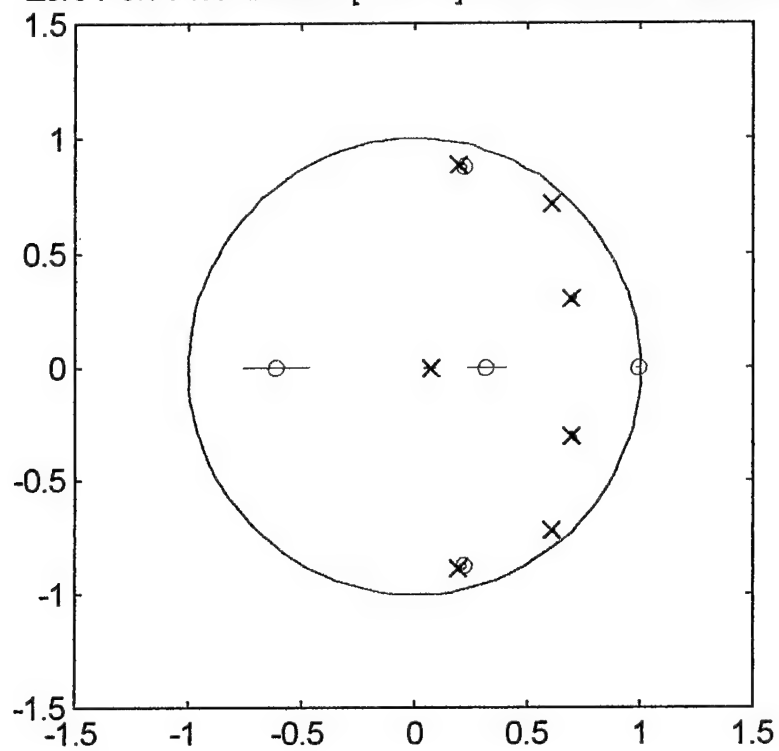
Figure A.6
Zero-Pole Plot

B. Application of ARMAX Method to Actuator Number Two.

The following plots were used in evaluating the application of the ARMAX parameter estimation method in modeling actuator number two. The structure [na=7 nb=6 nc=2 nk=1] was used. Two additional plots from the Box-Jenkins [*nb*=6 *nc*=2 *nc*=2 *na*=7 *nk*=1] model are included for comparison.

Blue=Actuator#2Red=ARMAX MODEL[7 6 2 1] *Data Prefiltered*

(a) Magnitude

Blue=Actuator#2Red=ARMAX MODEL[7 6 2 1] *Data Prefiltered*

(b) Phase

137
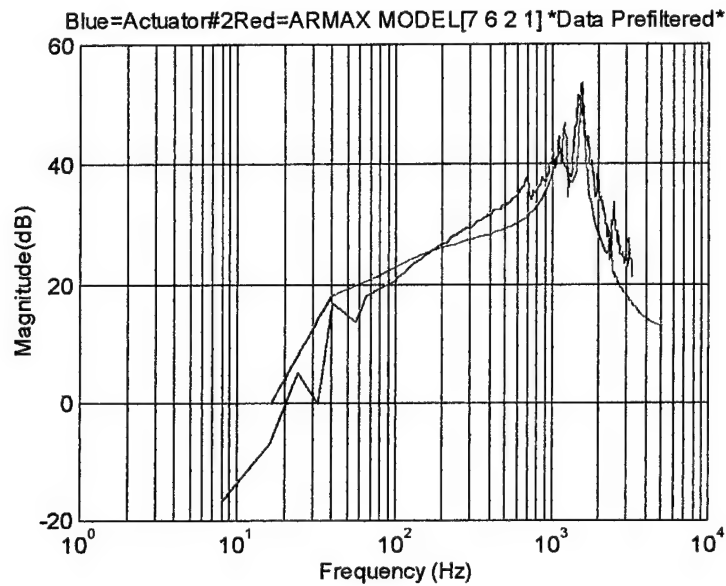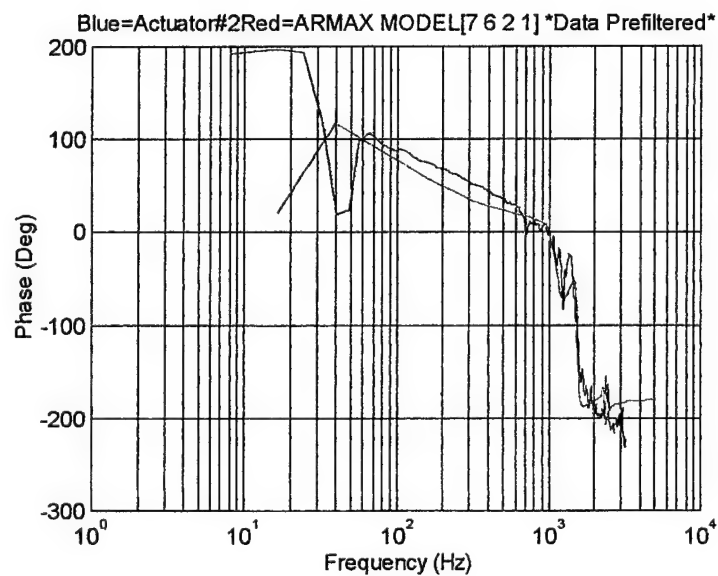
Figure B.1
Frequency Response Comparison

Plot of ARMAX MODEL[7 6 2 1] Output vs. Actual output *Data Prefiltered*

Figure B.2
Model Output Vs. Actual Output

Figure B.3
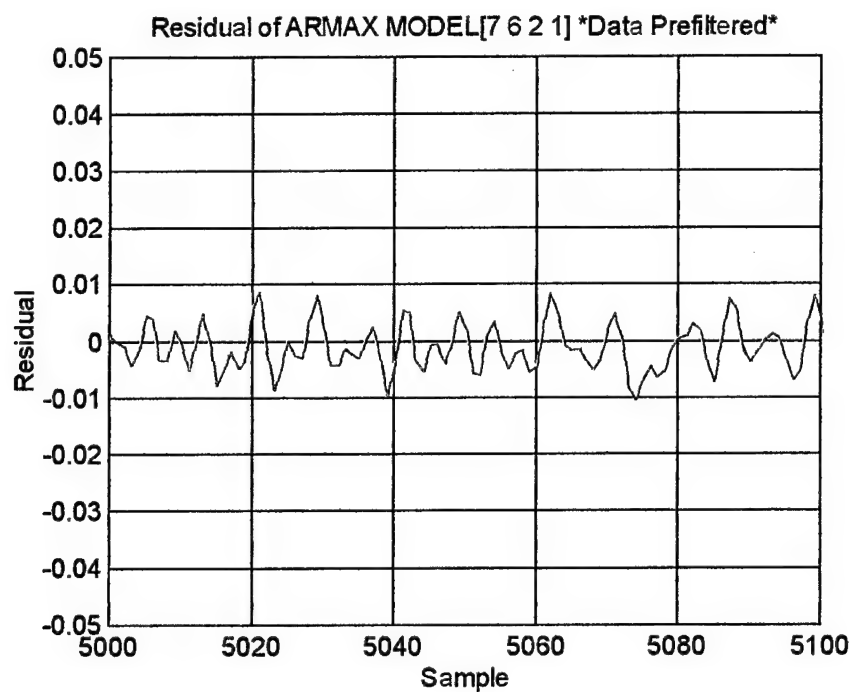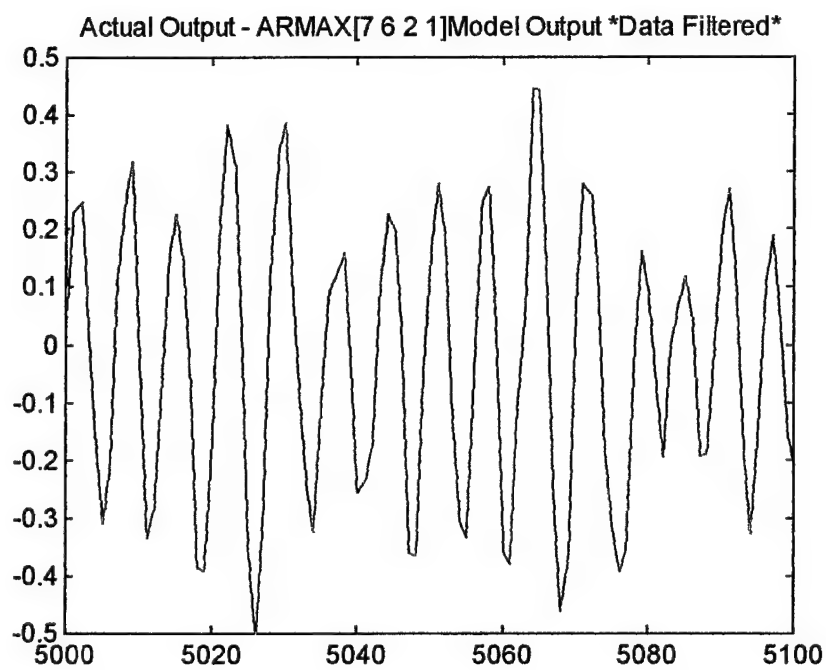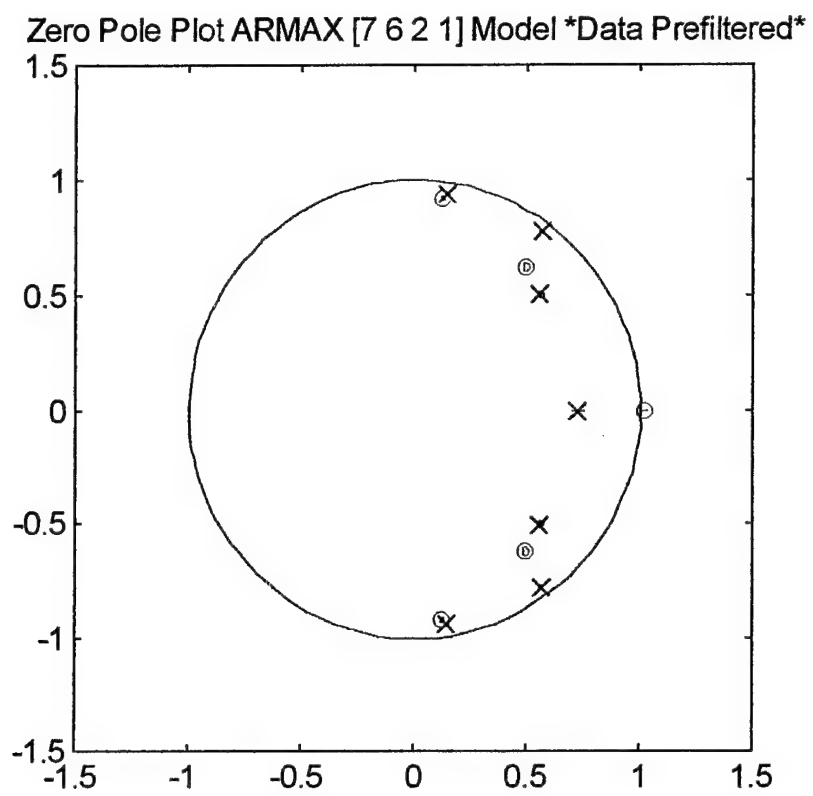Auto and Cross Correlation Functions
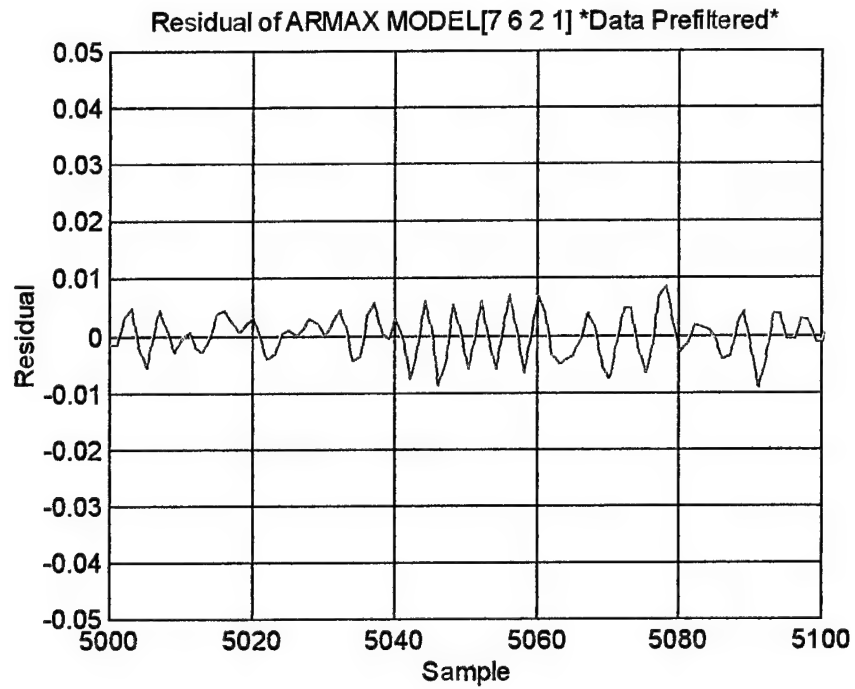
Figure B.4
Residual Vs. Sample

Figure B.5
Actual Output and Model Output Difference

139

Zero Pole Plot ARMAX [7 6 2 1] Model *Data Prefiltered*
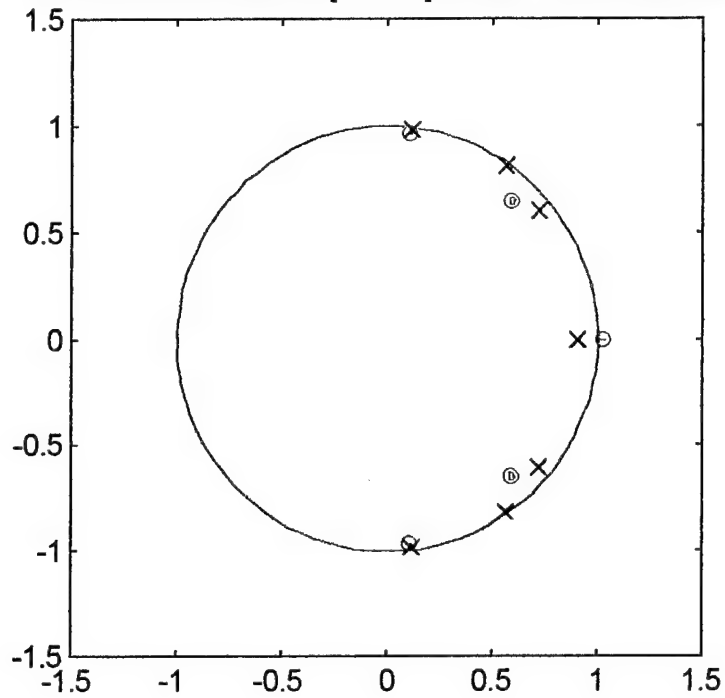
Figure B.6
Zero-Pole Plot

Zero Pole Plot Box-Jenkins Model [6 2 2 7 1] *Data Prefiltered*
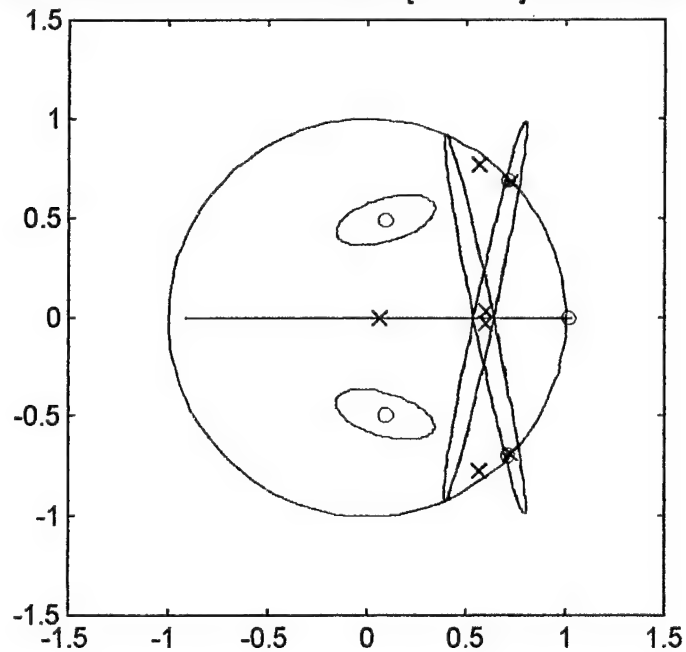
Figure B.7
Zero-Pole Plot for Box-Jenkins Model

140
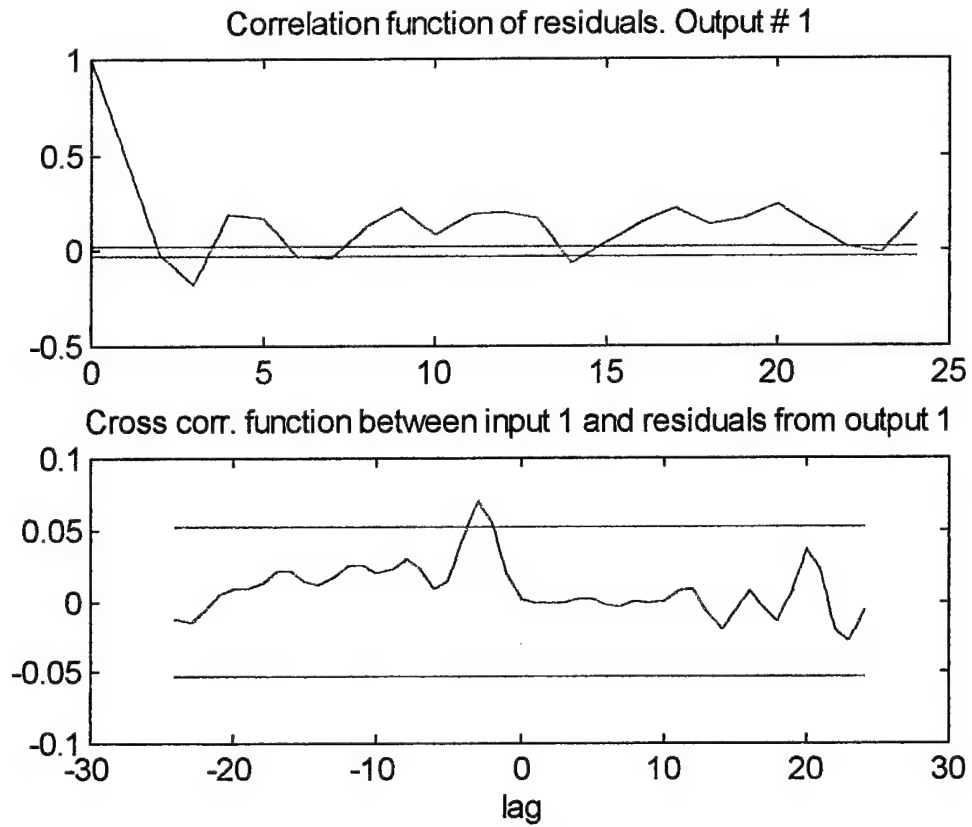
Figure B.8
Auto and Cross Correlation Functions for Box-Jenkins Model

C. Application of ARMAX Method to Actuator Number Three.

The following plots were used in evaluating the application of the ARMAX parameter estimation method in modeling actuator number three. The ARX based structure [na=7 nb=6 nc=2 nk=1] was used.
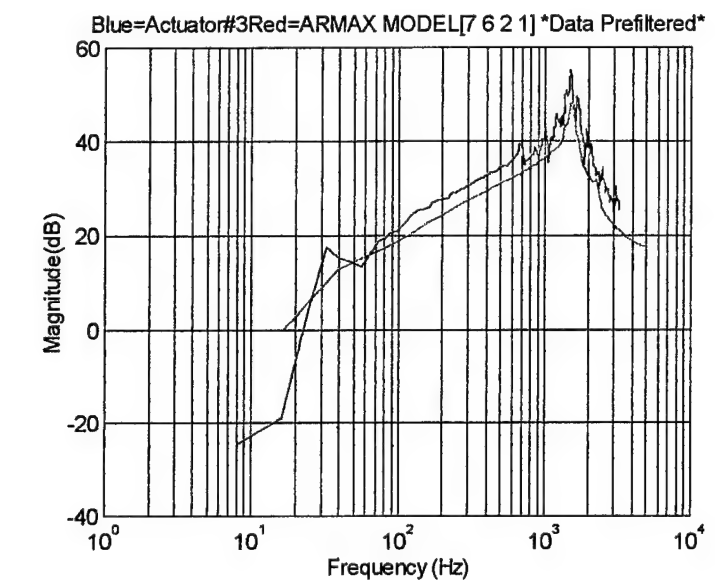
(a) Magnitude
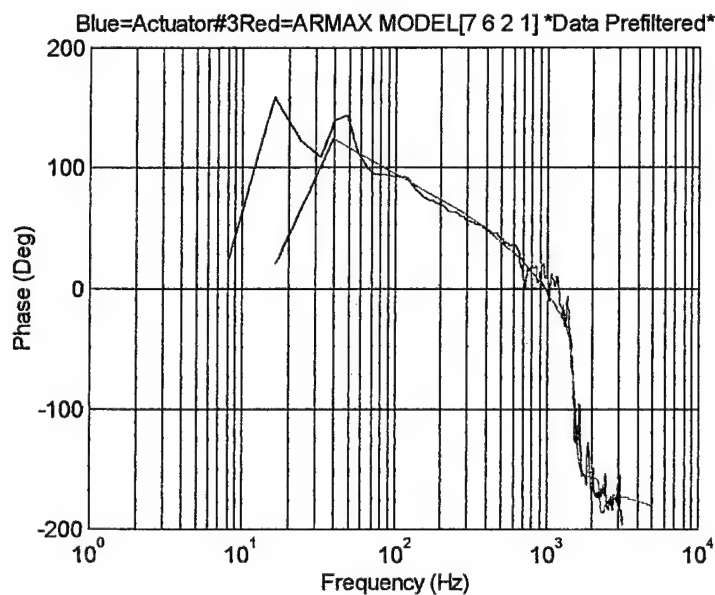
(b) Phase

Figure C.1
Frequency Response Comparison
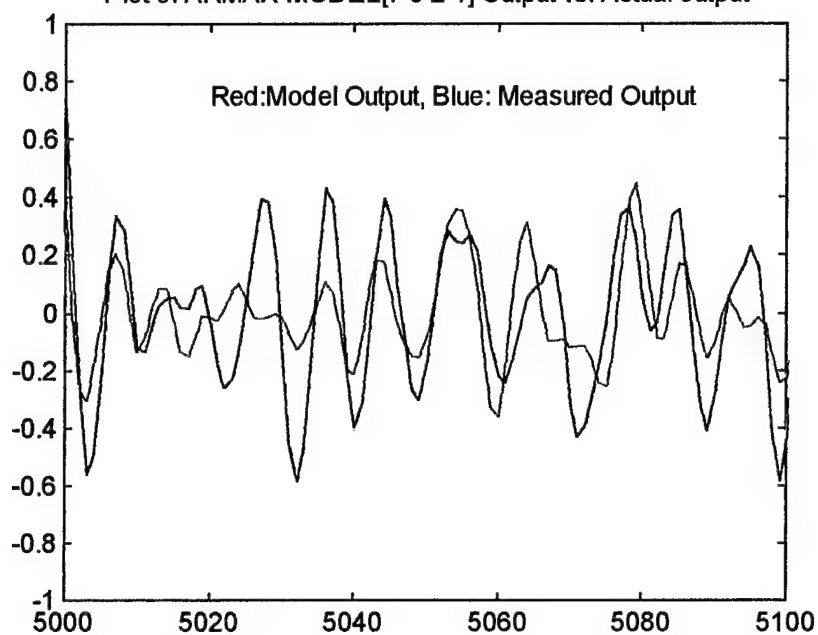
Plot of ARMAX MODEL[7 6 2 1] Output vs. Actual output *Data Prefiltered*
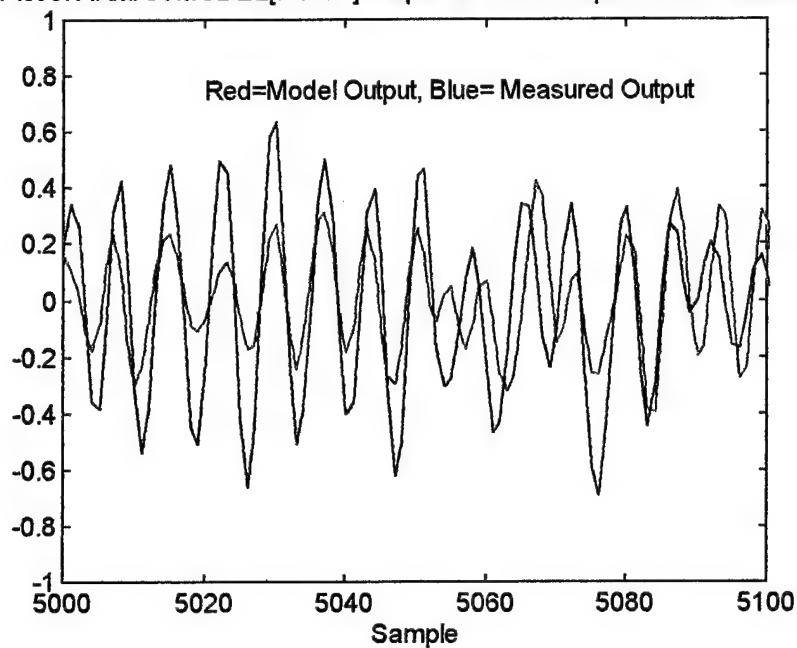
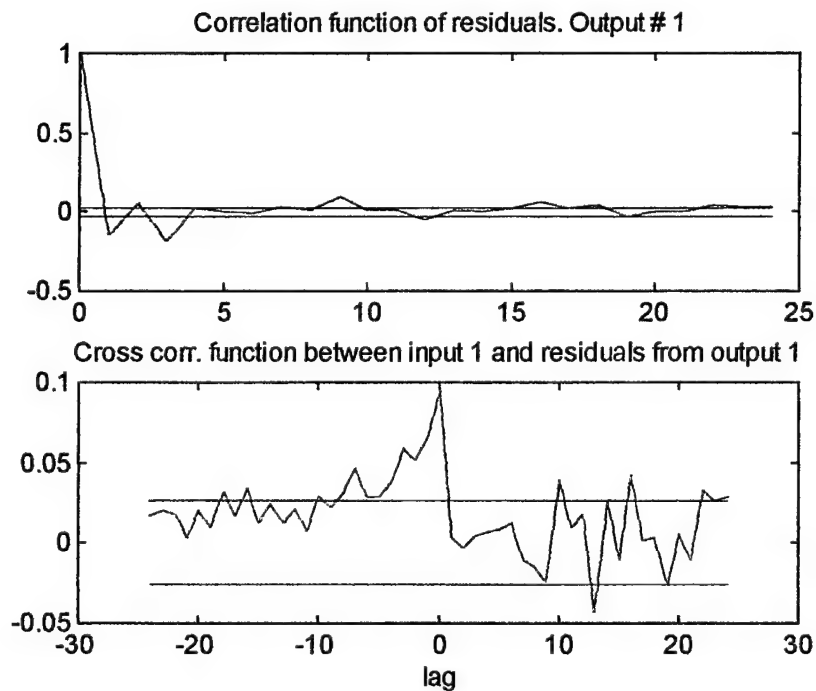Figure C.2
Model Output Vs. Actual Output
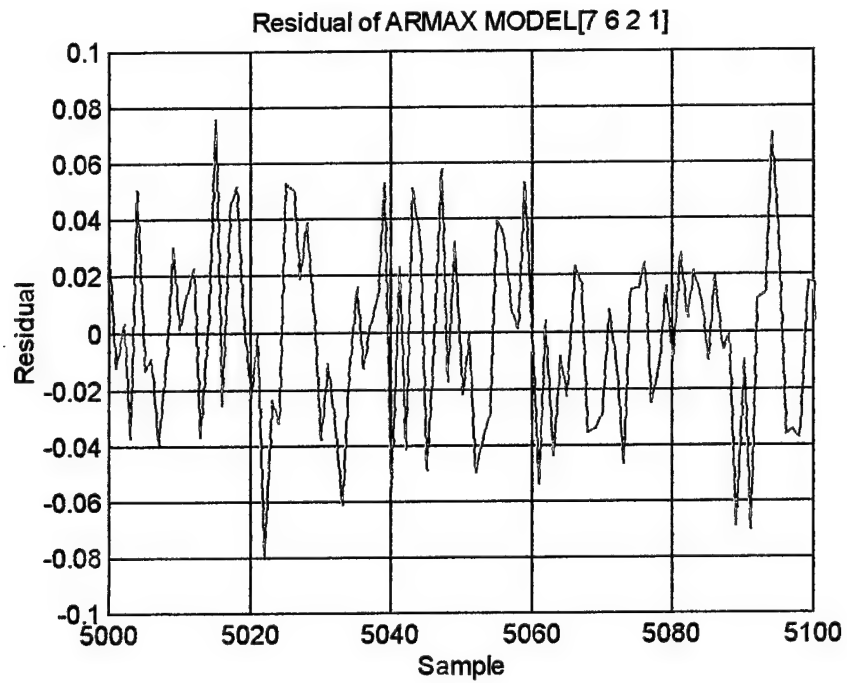

Figure C.3
Auto and Cross Correlation Functions
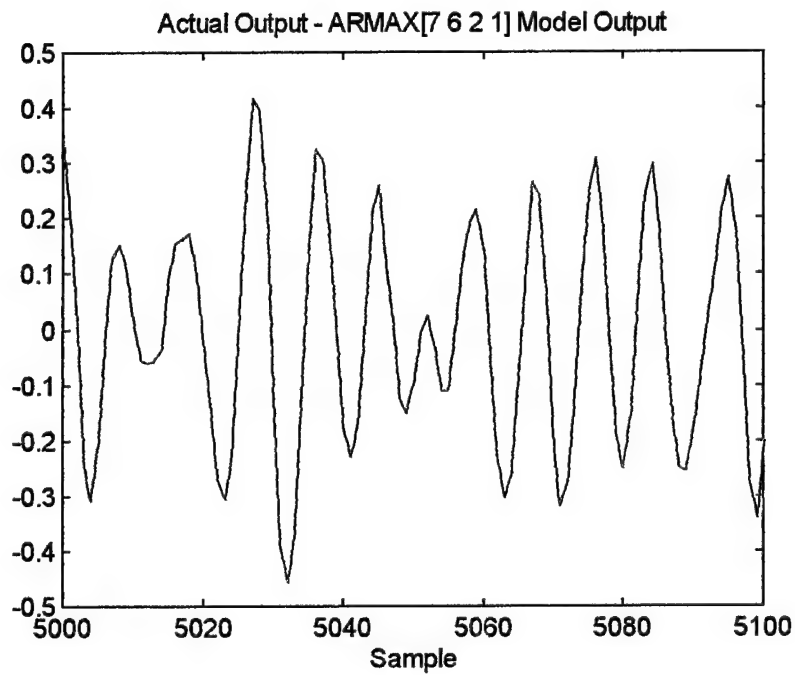
143

Figure C.4
Residual Vs. Sample

Figure C.5
Actual Output and Model Output Difference

144

Figure C.6
Zero-Pole Plot

D. Application of ARMAX Method to Actuator Number Four.

The following plots were used in evaluating the application of the ARMAX parameter estimation method in modeling actuator number four. The structure [na=7 nb=6 nc=2 nk=1] was used.
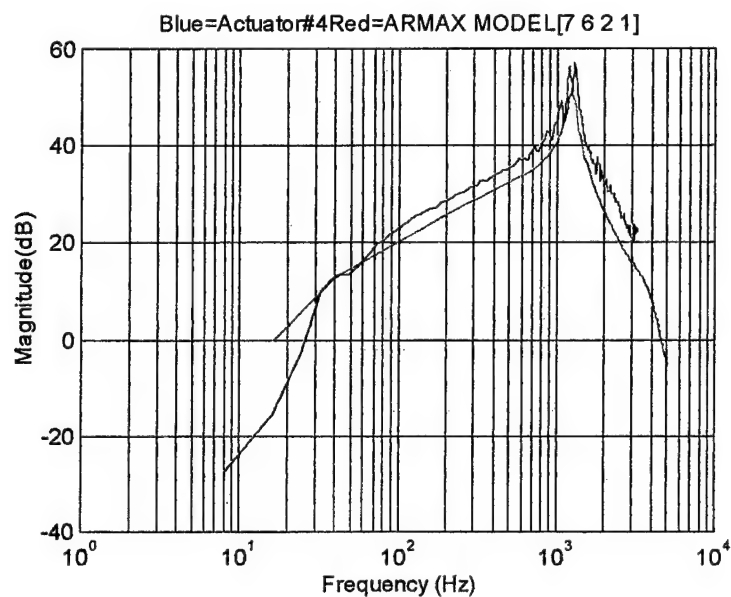
(a) Magnitude
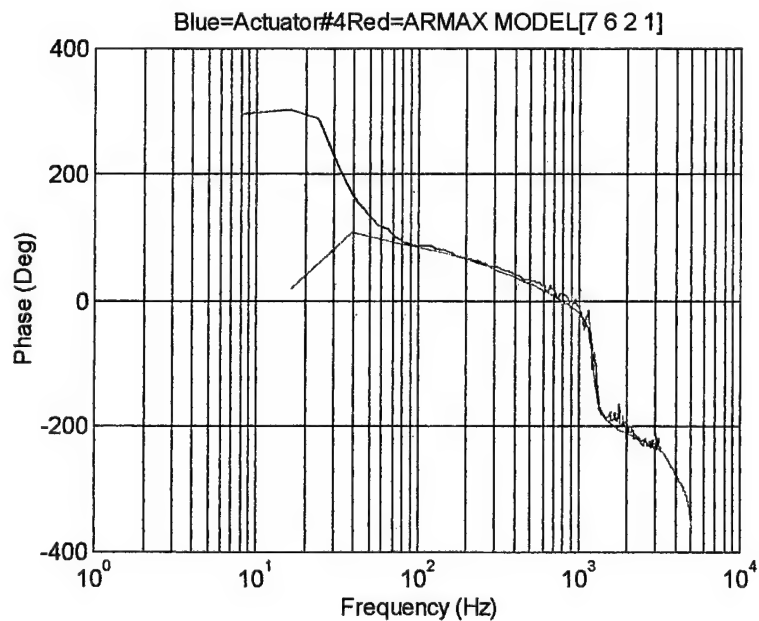
(b) Phase

Figure D.1

Frequency Response Comparison
Plot of ARMAX MODEL[7 6 2 1] Output vs. Actual output

Figure D.2
Model Output Vs. Actual Output

Figure D.3
Auto and Cross Correlation Functions

Figure D.4
Residual Vs. Sample

Figure D.5
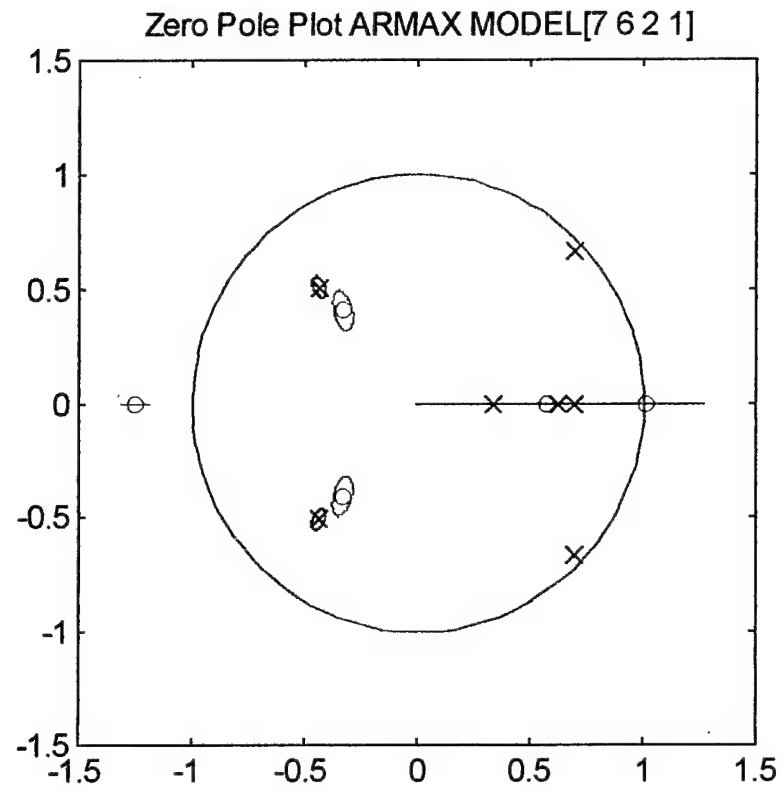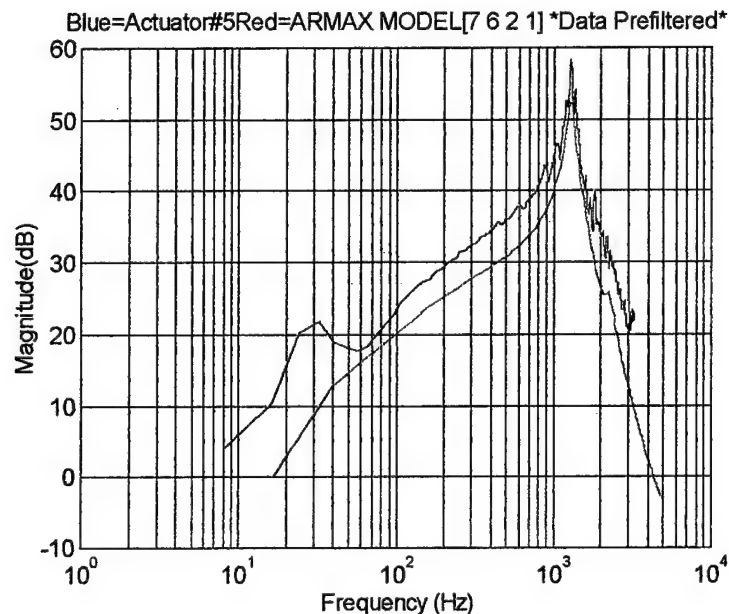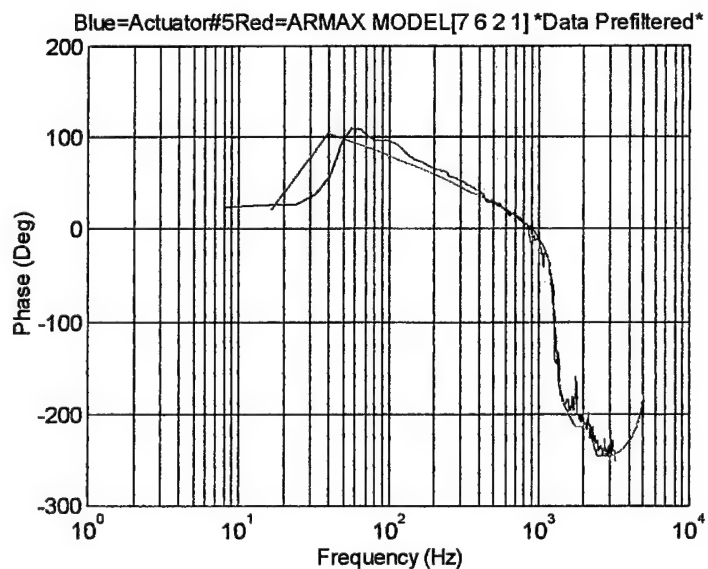Actual Output and Model Output Difference

148

Figure D.6
Zero-Pole Plot

149

E. Application of ARMAX Method to Actuator Number Five.

The following plots were used in evaluating the application of the ARMAX parameter estimation method in modeling actuator number five. The structure [na=7 nb=6 nc=2 nk=1] was used.

Blue=Actuator#5Red=ARMAX MODEL[7 6 2 1] *Data Prefiltered*

(a) Magnitude

Blue=Actuator#5Red=ARMAX MODEL[7 6 2 1] *Data Prefiltered*

(b) Phase

Figure E.1
Frequency Response Comparison

150

Plot of ARMAX MODEL[7 6 2 1] Output vs. Actual output *Data Prefiltered*
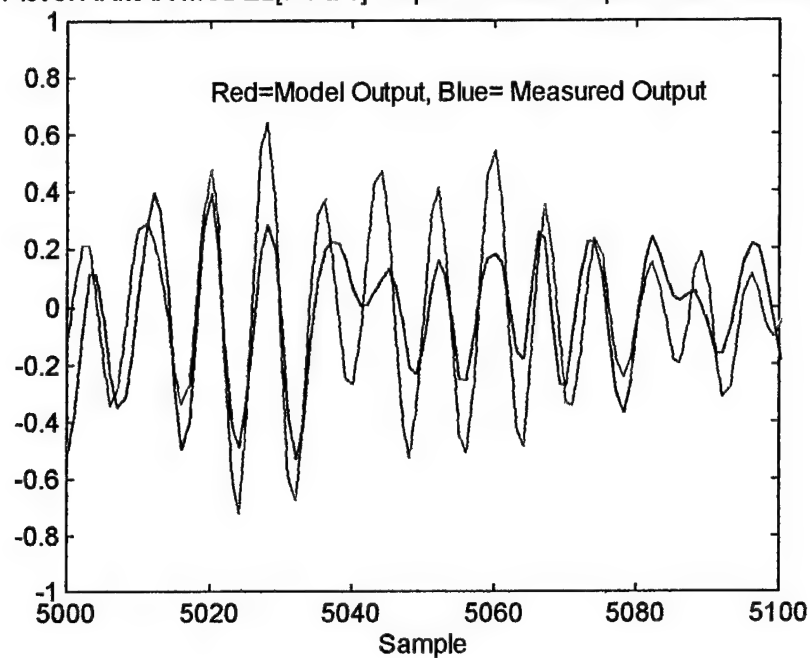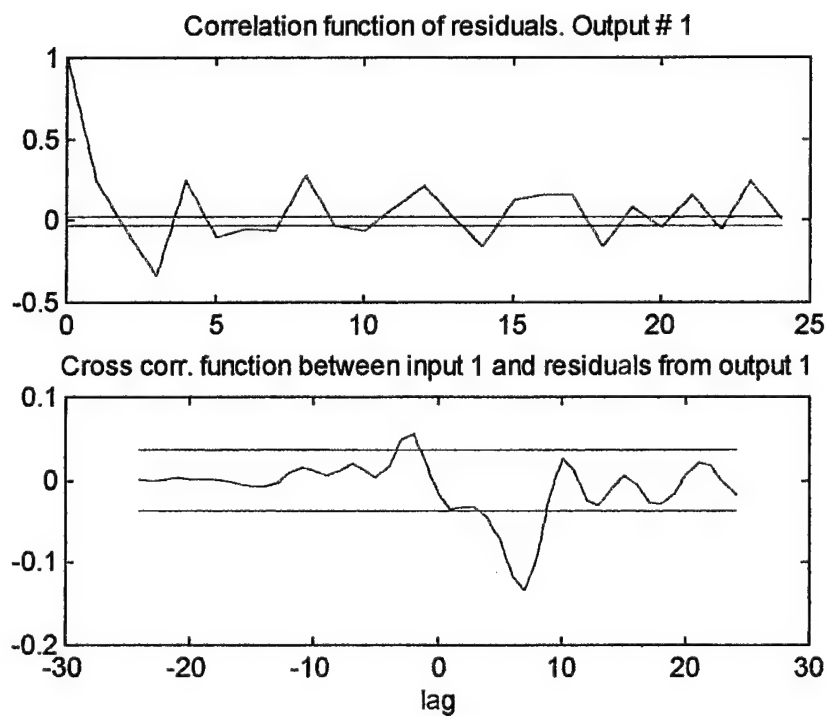

Figure E.2
Model Output Vs. Actual Output

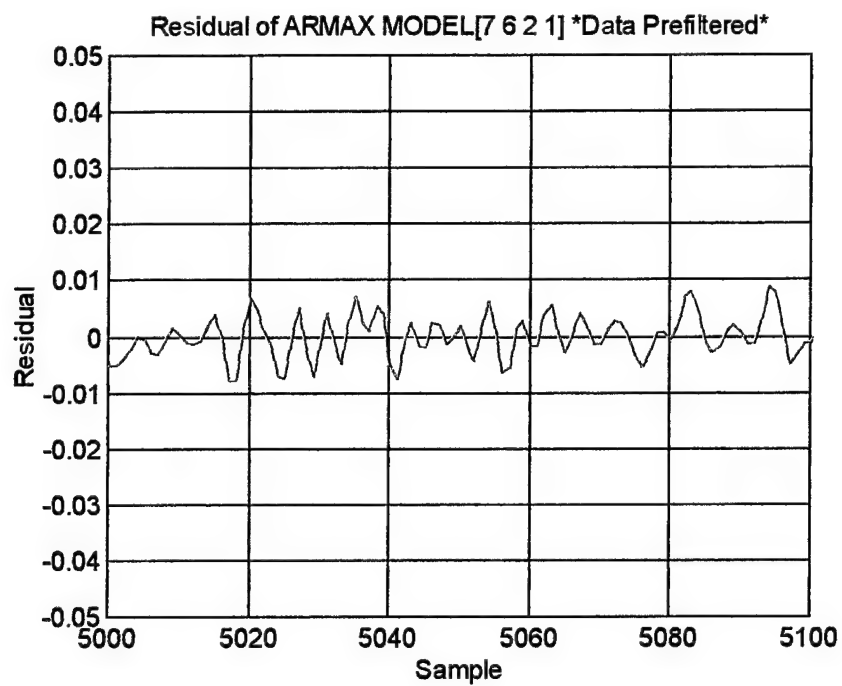
Figure E.3
Auto and Cross Correlation Functions

Residual of ARMAX MODEL[7 6 2 1] *Data Prefiltered*

Figure E.4
Residual Vs. Sample

Actual Output - ARMAX[7 6 2 1]Model Output *Data Filtered*
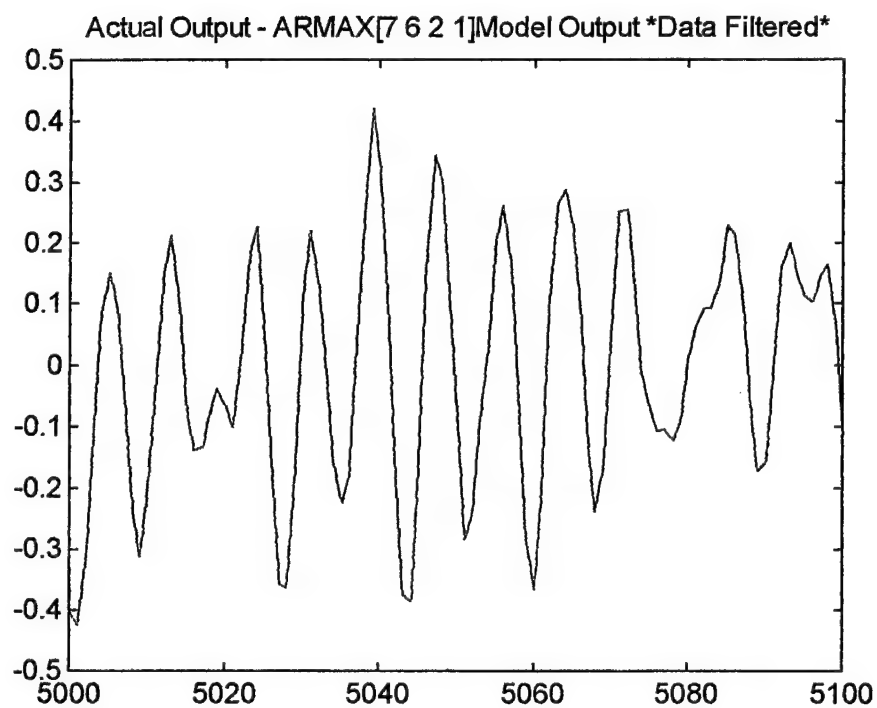
Figure E.5
Actual Output and Model Output Difference

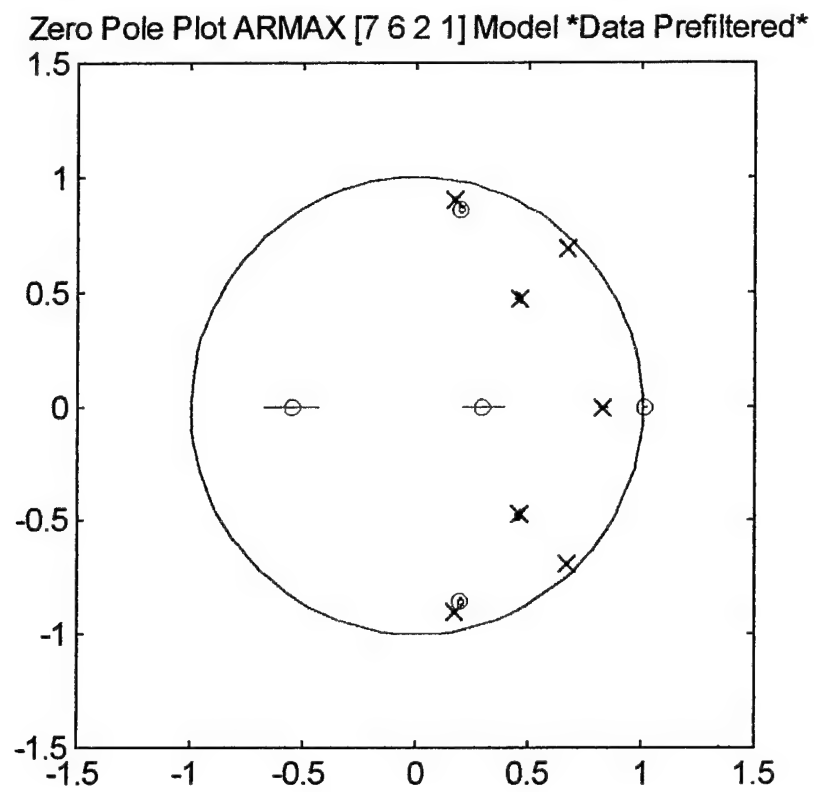Zero Pole Plot ARMAX [7 6 2 1] Model *Data Prefiltered*

Figure E.6
Zero-Pole Plot

F. Application of ARMAX Method to Actuator Number Six.

The following plots were used in evaluating the application of the ARMAX parameter estimation method in modeling actuator number six. The structure[na=7 nb=6 nc=2 nk=1] was used.

(a) Magnitude

(b) Phase

Figure F.1

154

Figure F.4
Residual Vs. Sample
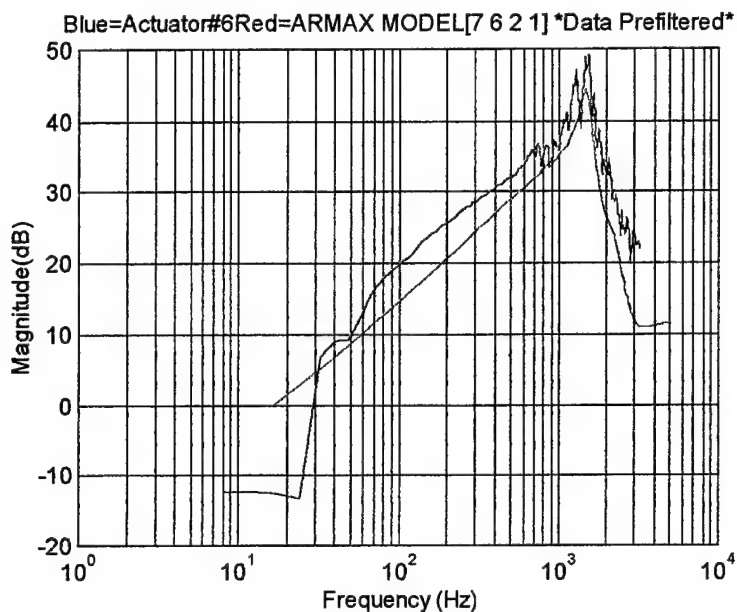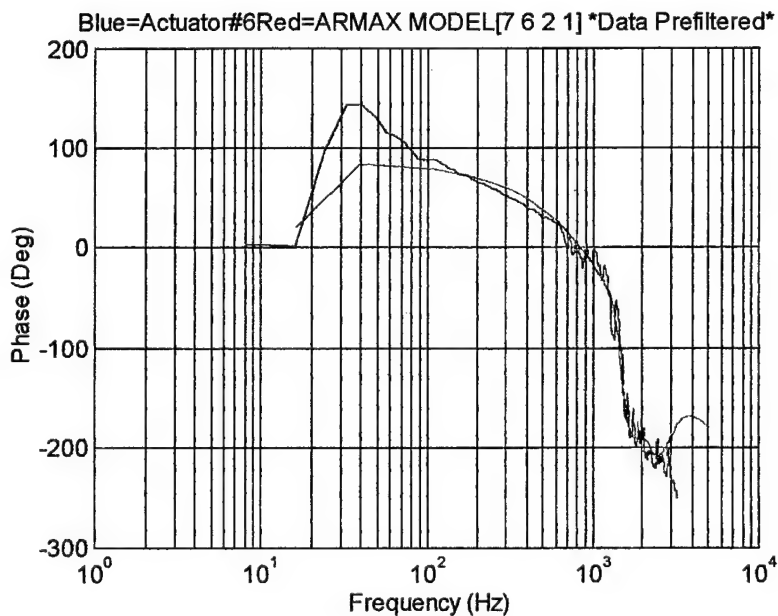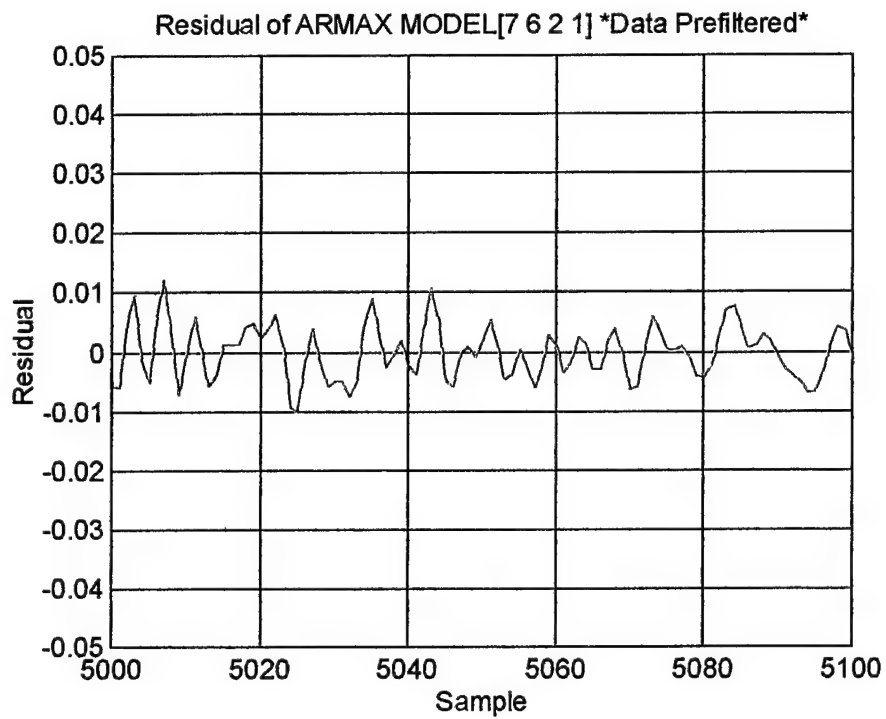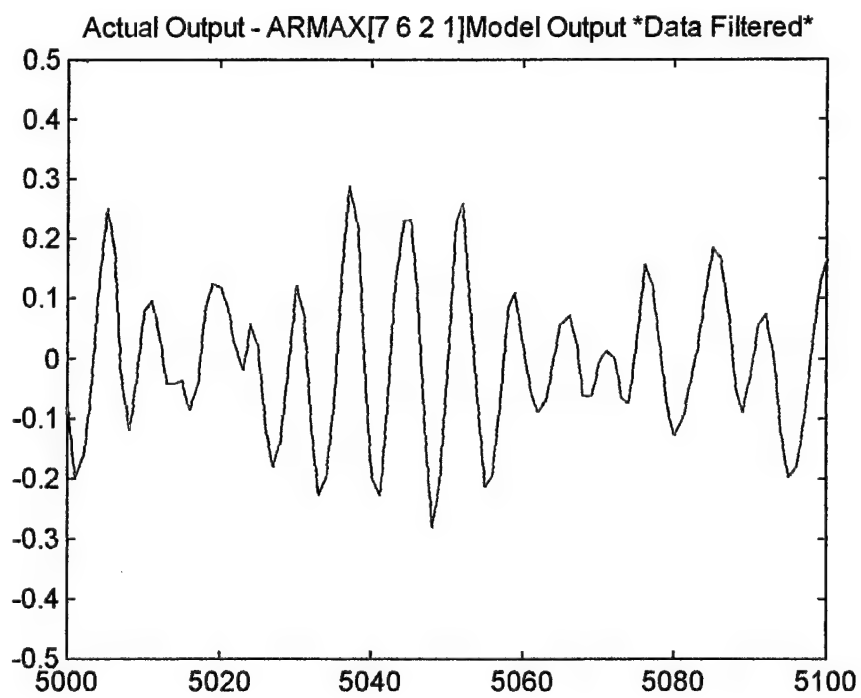

Figure F.5
Actual Output and Model Output Difference

156

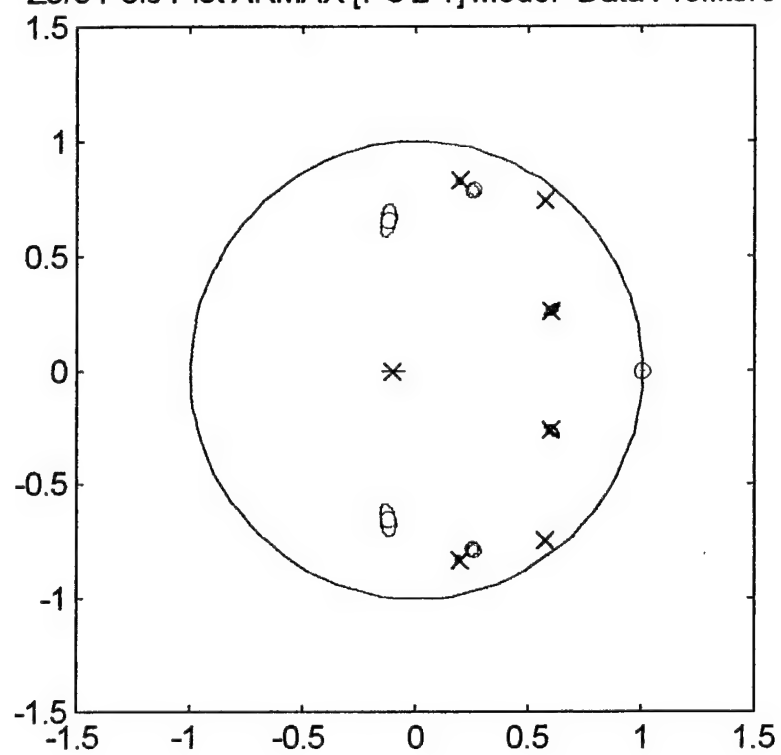Zero Pole Plot ARMAX [7 6 2 1] Model *Data Prefiltered*

Figure F.6
Zero Pole Plot

LIST OF REFERENCES

1. Stewart, D. "A Platform with Six Degrees of Freedom" Proceedings of the Institute of Mechanical Engineering, London, 1965-1966,Volume 180, Part I, pp. 371-386.

2. Gough, V.E. "Communication to Article by D. Stewart" Proceedings of the Institute of Mechanical Engineering, London, 1965-1966,Volume 180, Part I, pp. 379-381.

3. Nanua, P., Waldron, K.J. and Murthy, V. "Direct Kinematic Solution of a Stewart Platform" IEEE Transactions on Robotics and Automation, Volume 6, No. 4, August 1990, pp. 438-443.

4. Geng, Z. J. and Haynes, L. S. "Six Degree of Freedom Active Vibration Control Using the Stewart Platforms," IEEE Transactions on Control Systems Technology, Vol. 2, No. 1, pp. 45-53, March 1994.

5. Spanos, J. , Rahman, Z. and Blackwood, G., "A Soft 6-Axis Active Vibration Isolator" Proceedings, American Control Conference, Seattle, June 21-23, 1995.

6. Shubert, Dale W. " Characteristics of an Active Vibration Isolation System Using Absolute Velocity Feedback and Force Actuation" Proceedings of the Conference on Recent Advances In Active Control of Sound and Vibration, Virginia Polytechnic Institute and State University, Blacksburg VA 15-17 April 1991 pp 448-463.

7. Franklin, Gene F. , Powell, David J. & Emami-Naeini, Abbas, " Feedback Control of Dynamic Systems" Third Ed. Addison-Wesley, Reading MA, 1994.

8. Agrawal, B.N. , Bang, H. and Jones, E., " Application of Piezoelectric Actuators and Sensors in Vibration Control of Flexible Spacecraft Structures" 43rd Congress of the International Astronautical Federation, August 28 - September 5 1992, Washington D.C.

9. Ljung, Lennart, "System Identification Theory for the User", Prentice Hall, Englewood Cliffs NJ, 1987.

10. Ljung, Lennart and Glad, Torkel, "Modeling of Dynamic Systems", PTR Prentice Hall, Englewood Cliffs, New Jersey, 1994.

11. Ljung, Lennart, "System Identification Toolbox for use with MATLAB User's Guide, The Math Works, Inc., Natick MA, 1991

INITIAL DISTRIBUTION LIST

1. Defense Technical Information Center 2
   8725 John J. Kingman Road., Ste 0944
   Ft. Belvoir, VA 22060-6218

2. Dudley Knox Library.. 2
   Naval Postgraduate School
   411 Dyer Road
   Monterey, CA 93943-5150

3. Chairman, Code AA.. 1
   Department of Aeronautics and Astronautics
   Naval Postgraduate School
   Monterey, CA 93943

4. Professor Brij N. Agrawal, Code AA/Ag.. 2
   Department of Aeronautics and Astronautics
   Naval Postgraduate School
   Monterey, CA 93943

5. Dr. Gangbing Song, Code AA/Sb 2
   Department of Aeronautics and Astronautics
   Naval Postgraduate School
   Monterey, CA 93943

6. Dr. Albert Bosse... 1
   Naval Research Laboratory Code 8220
   4555 Overlook Ave. SW
   Washington, DC 20375-5355

7. Dr. Eric Anderson 1
   CSA Engineering INC.
   2850 W. Bayshore Road
   Palo Alto, CA 94303-3843

8. LCDR George D. Beavers.. 2
   c/o 516 22nd St.
   Dunbar, WV 25064